

Cross Section Measurements of Deuteron Electro-Disintegration at Very High Recoil Momenta and Large 4-Momentum Transfers (Q^2)

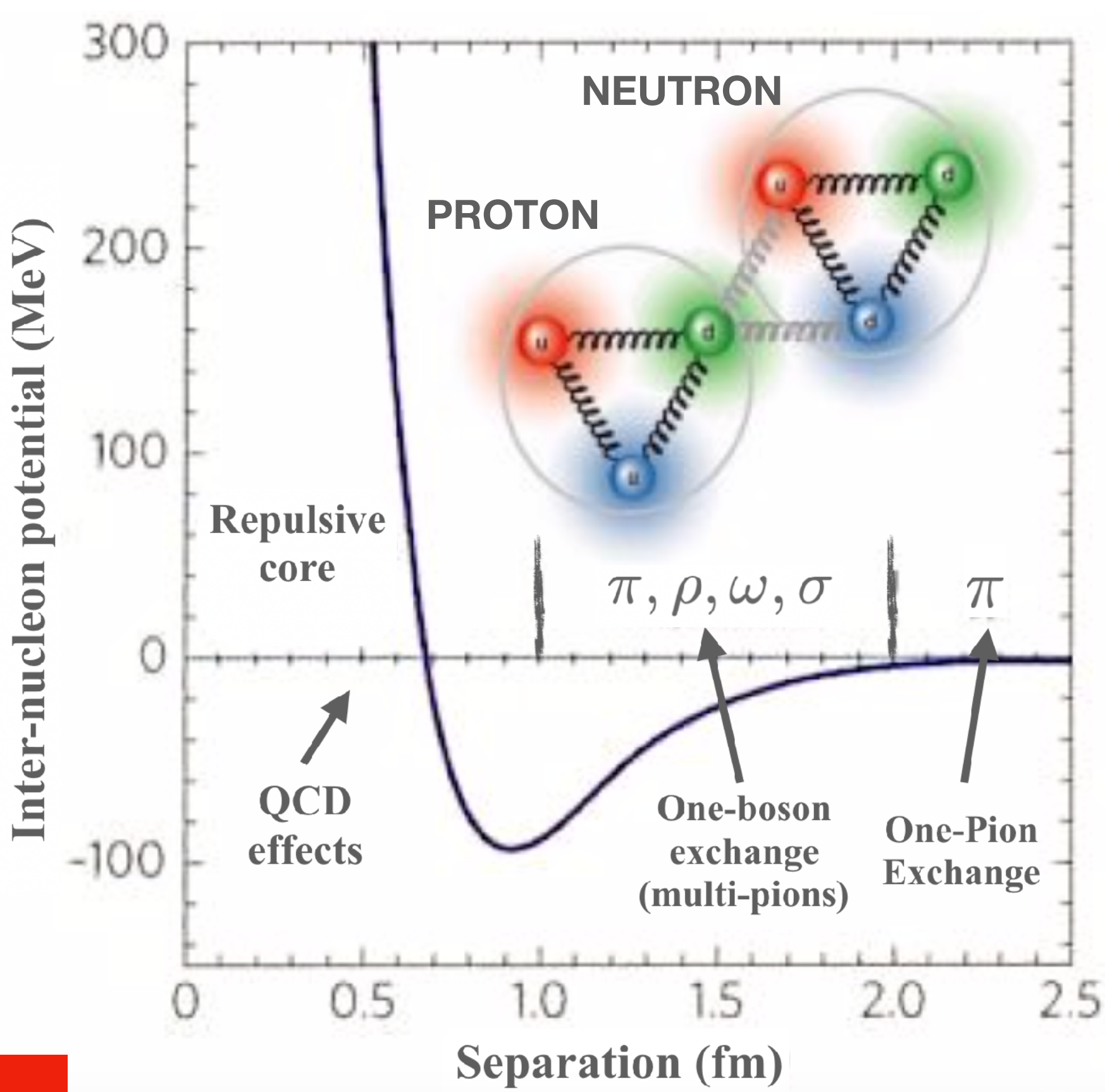
Joint Halls A/C Summer Meeting
July 16, 2020

Carlos Yero
Spokespeople: Drs. Werner Boeglin and Mark Jones



Motivation

- Deuteron is the simplest np bound state: starting point to study nuclear force (or NN potential)
- Understand the short range structure by probing high momentum tails of the deuteron
- At short ranges, np start overlap: overlap is directly related to SRCs in $A > 2$ nuclei
- Extract momentum distributions beyond 500 MeV/c recoil momenta at PWIA kinematics

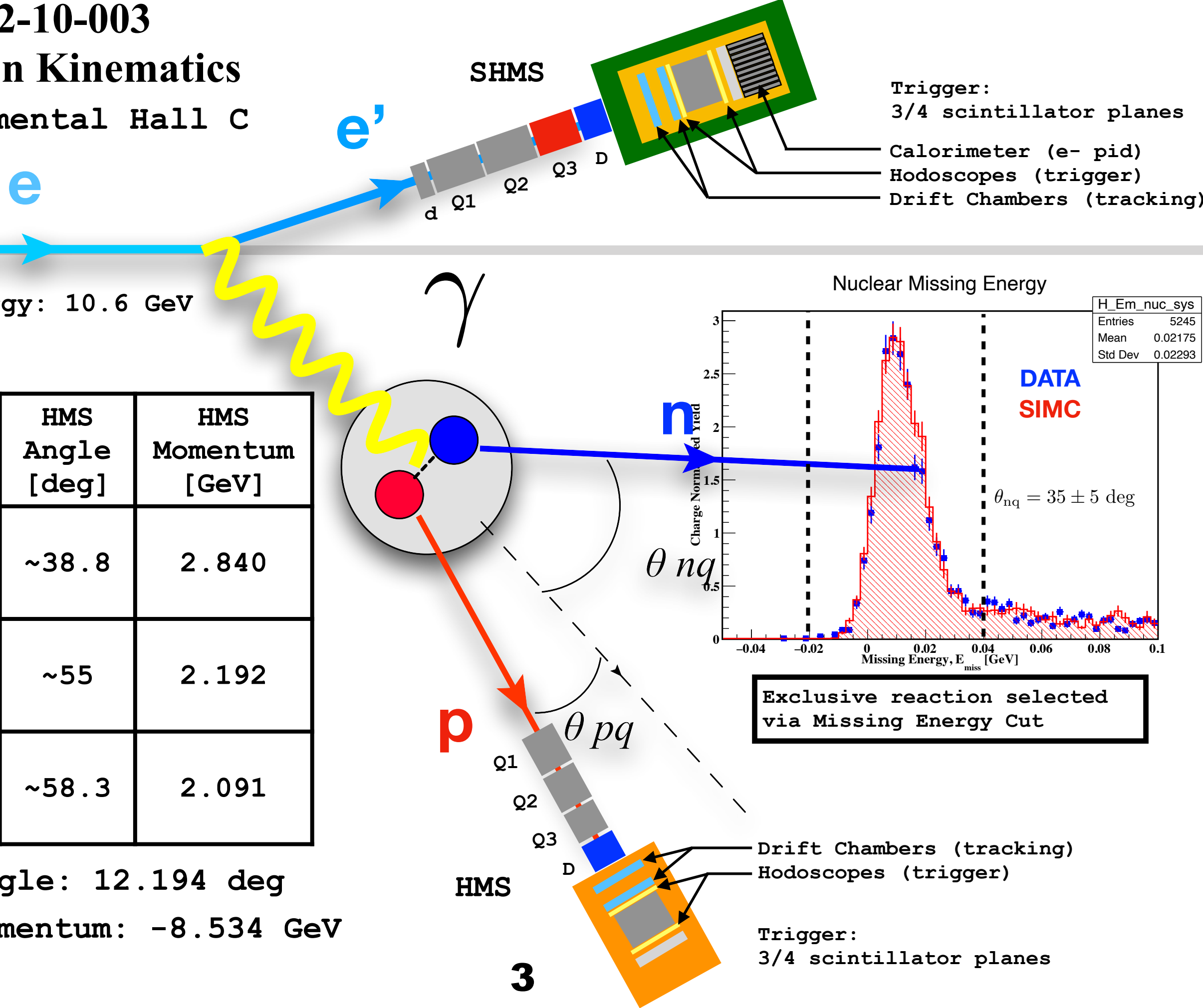


For historical overview of the nuclear force: [SEE BACKUP SLIDES](#)

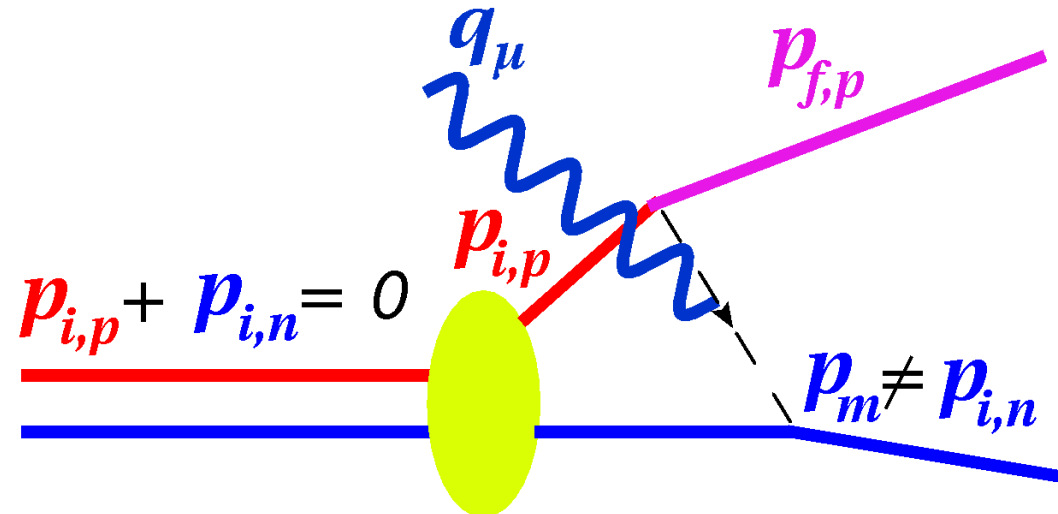
E12-10-003

D($e, e' p$)n Kinematics

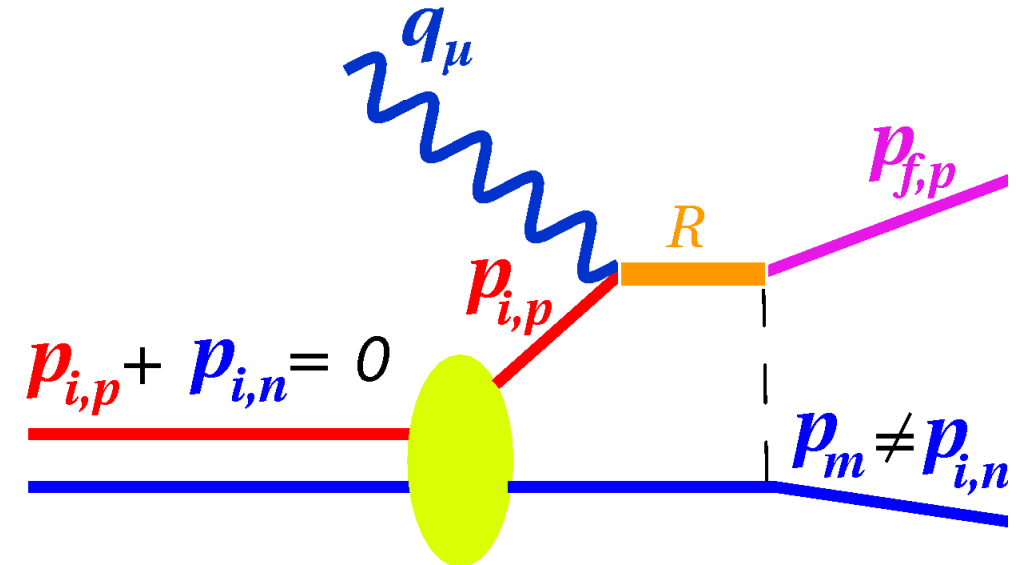
Experimental Hall C



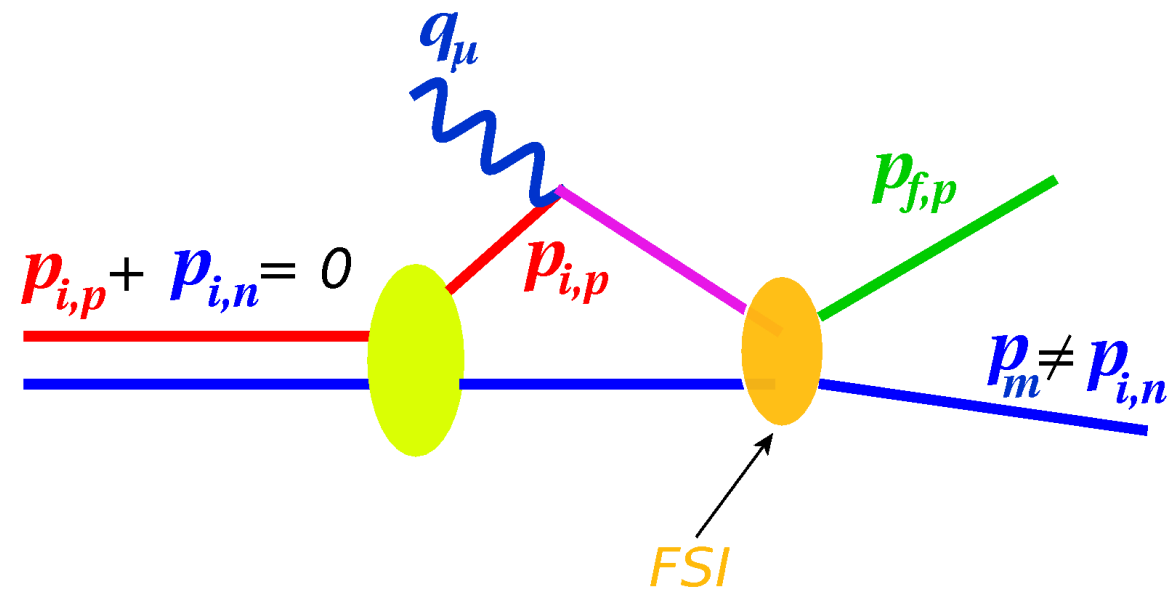
D(e,e'p)n Feynman Diagrams



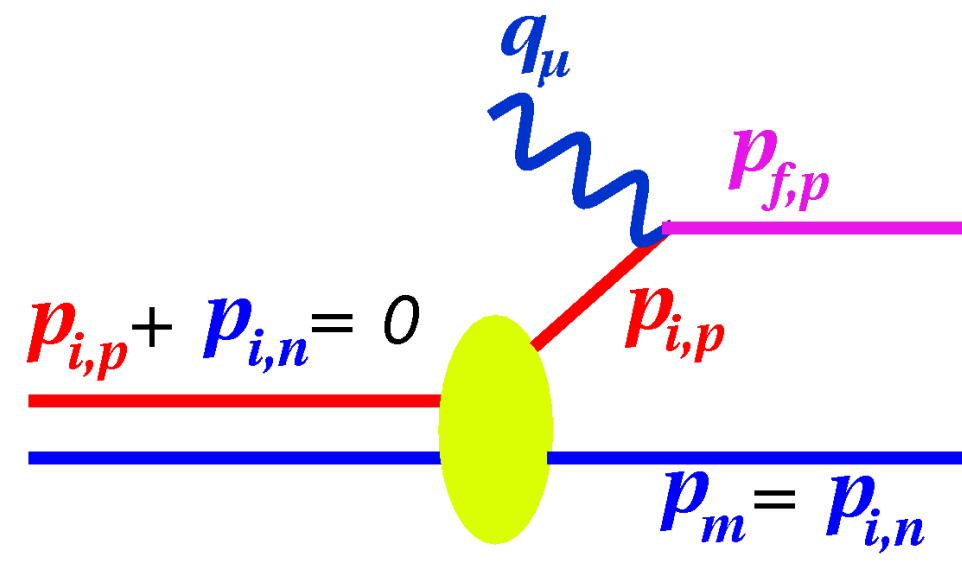
(a) Meson-Exchange Currents (MEC)



(b) Isobar Configurations (IC)



(c) Final State Interactions (FSI)



(d) Plane Wave Impulse Approximation (PWIA)

Deuteron Momentum Distribution

Experiment

$$\sigma_{exp} \equiv \frac{d^5\sigma}{d\omega d\Omega_e d\Omega_p}$$

Theory

$$\approx K \cdot \sigma_{ep} \cdot S(p_m)$$

$$S(p_m) \approx \sigma_{red} \equiv \frac{\sigma_{exp}}{K \sigma_{ep}}$$

Factorization **ONLY**
possible in PWIA

ep off-shell cross section

electron scatters off a bound proton within the nucleus; usually,
de Forest σ_{cc1} or σ_{cc2} is prescribed

Spectral Function, $S(p_m)$

the momentum distribution inside the deuteron is interpreted as
the probability density of finding a bound proton with
momentum p_i

First D(e,e'p)n Experiments at: $Q^2 > 1 \text{ GeV}^2$

JLab Hall A (2011)

JLab Hall B (2007)

CD-Bonn FSI (MS)

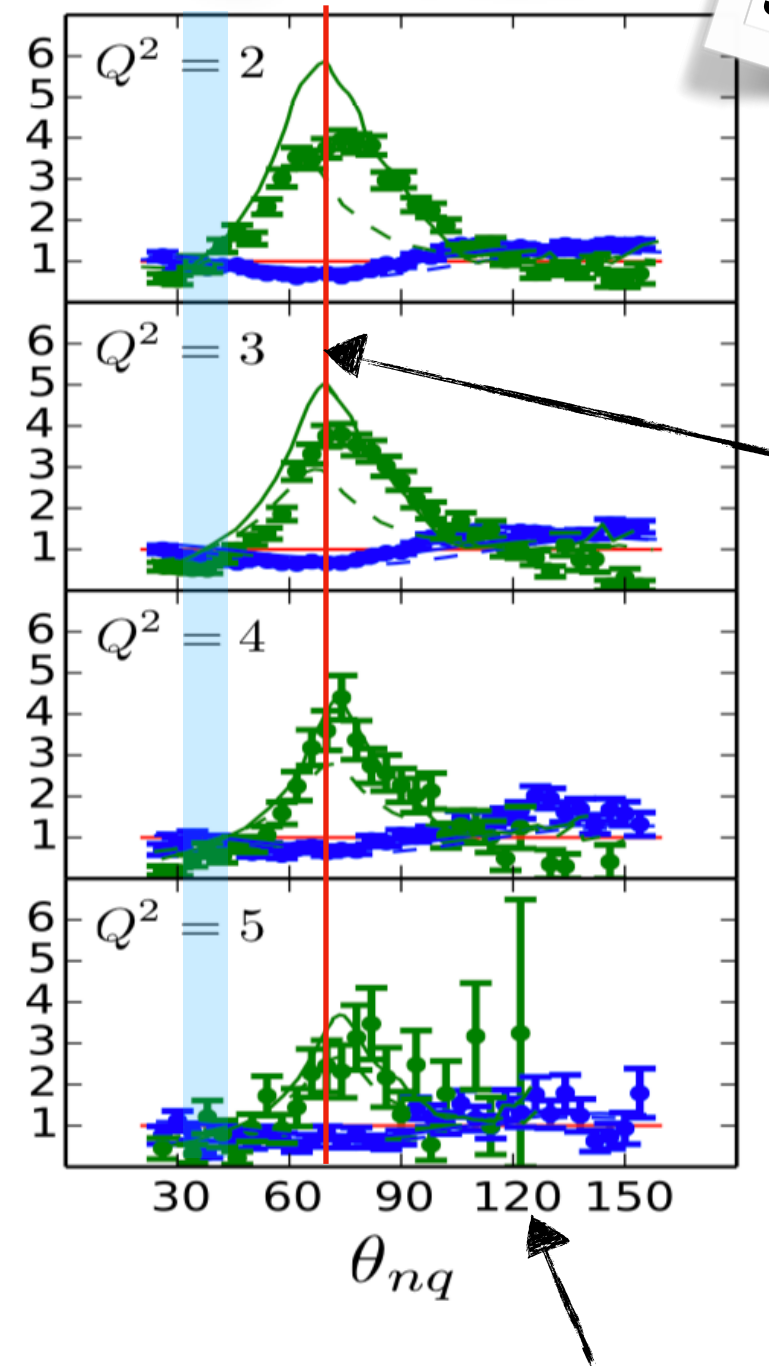
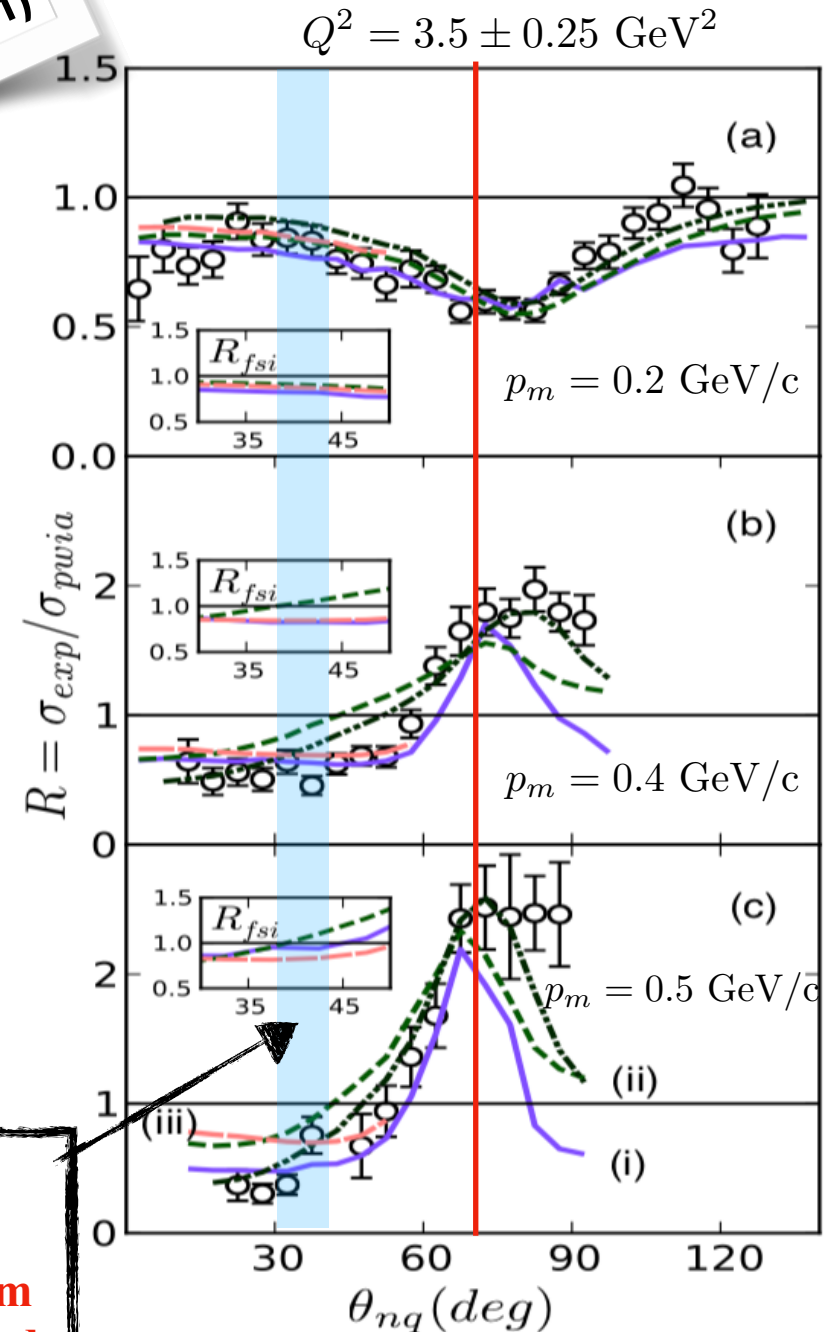
JVO Model
(J.W. Van Orden)

Paris FSI
(J.M. Laget)

Paris FSI+MEC+IC
(J.M. Laget)

DATA

Reduced FSIs at
~40 deg ($R \sim 1$)
genuine momentum
distributions probed



FSI peaks
at ~70 deg
(predicted
by GEA)

● $0.2 \leq p_m \leq 0.3 \text{ GeV}/c$

◆ $0.4 \leq p_m \leq 0.6 \text{ GeV}/c$

Paris FSI
(J.M. Laget)

CD-Bonn FSI (MS)

Reduced FSIs
at ~120 deg
($R \sim 1$),
But ICs are significant

- Data shows FSI peaks at ~70 deg (predicted by GEA and J.M Laget)
- FSI greatly reduced at ~40 and ~120 deg

Plots Reference:

W.U.Boeglin and M. Sargsian Int.J.Mod.Phys. E24 (2015) no.03, 1530003

Data Analysis of the E12-10-003 Commissioning Experiment at Hall C

- ➊ The E12-10-003 experiment was carried out on April 3-9
(only 6 out of 21 days of the requested beam time for full experiment)

See Backup Slides for first steps in general analysis:

1. Set reference times cuts
2. Set detector time window cuts
3. Perform detector calibrations
4. Optics Optimization
5. Data-to-Simulation Comparison

$D(e,e'p)n$

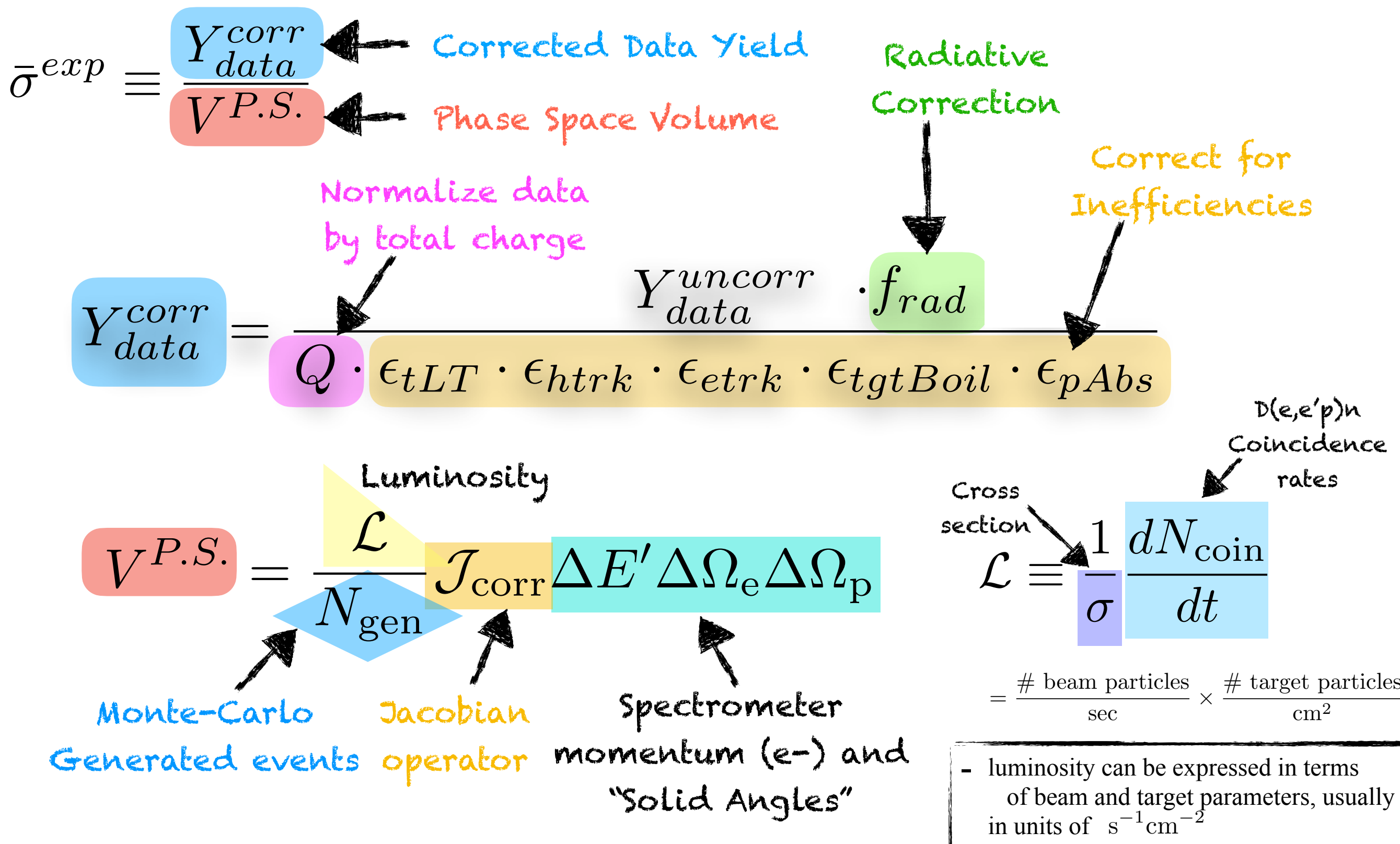
Data Analysis Cuts

- ➊ These cuts are used to select a clean sample of e- in the SHMS coincident with protons in the HMS that correspond to $D(e,e'p)n$
- ➋ Exact cuts are also applied to simulation (except for PID cuts)
- ➌ All plots shown have been integrated over all neutron recoil angles

SEE BACKUP SLIDES
for plots of data analysis cuts
(shown only for 80 MeV setting but are
also applied to high missing momentum data)

Extraction of D($e,e'p$)n Coincidence Cross Sections at Hall C

Extraction of the D(e,e'p)n Cross Section

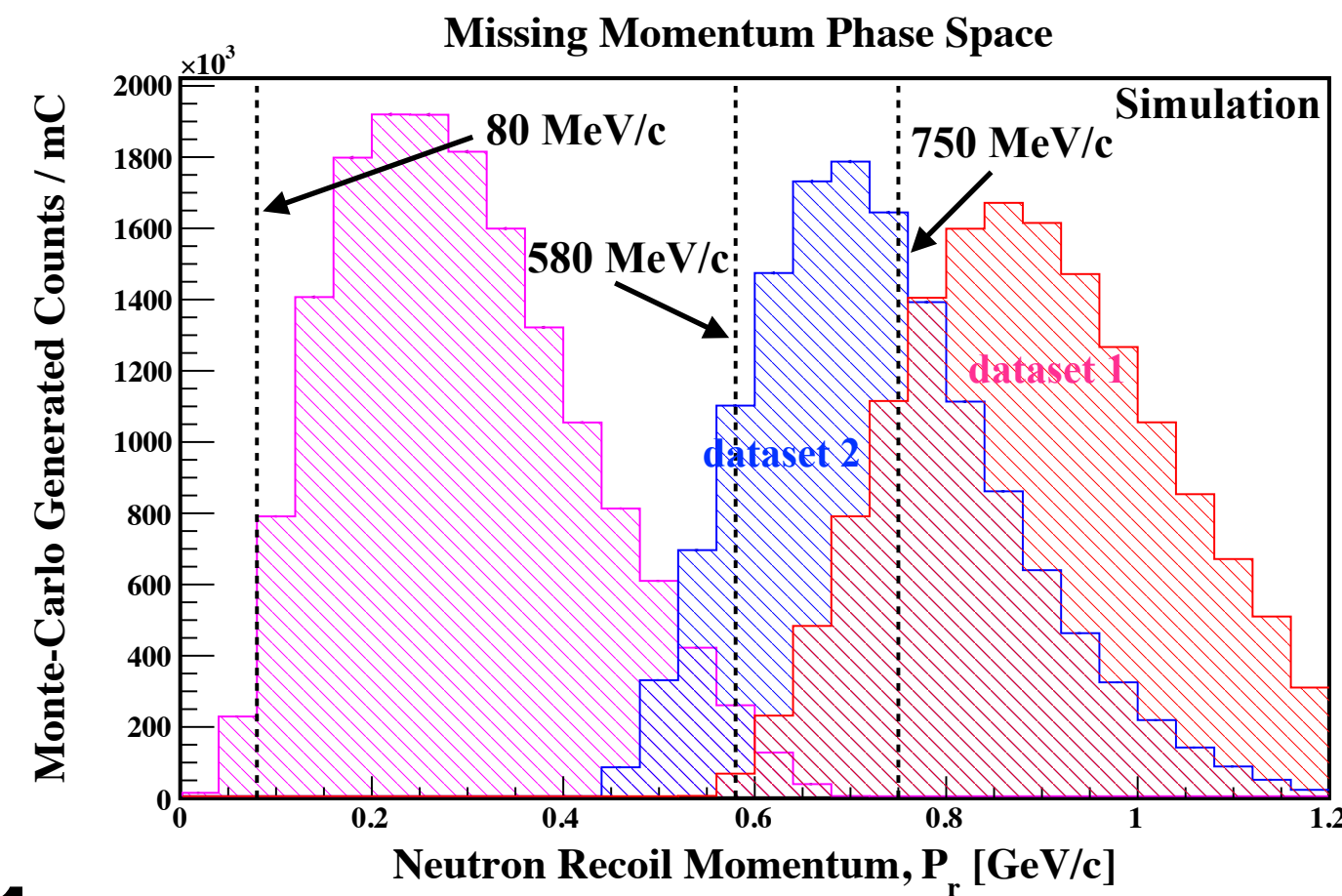
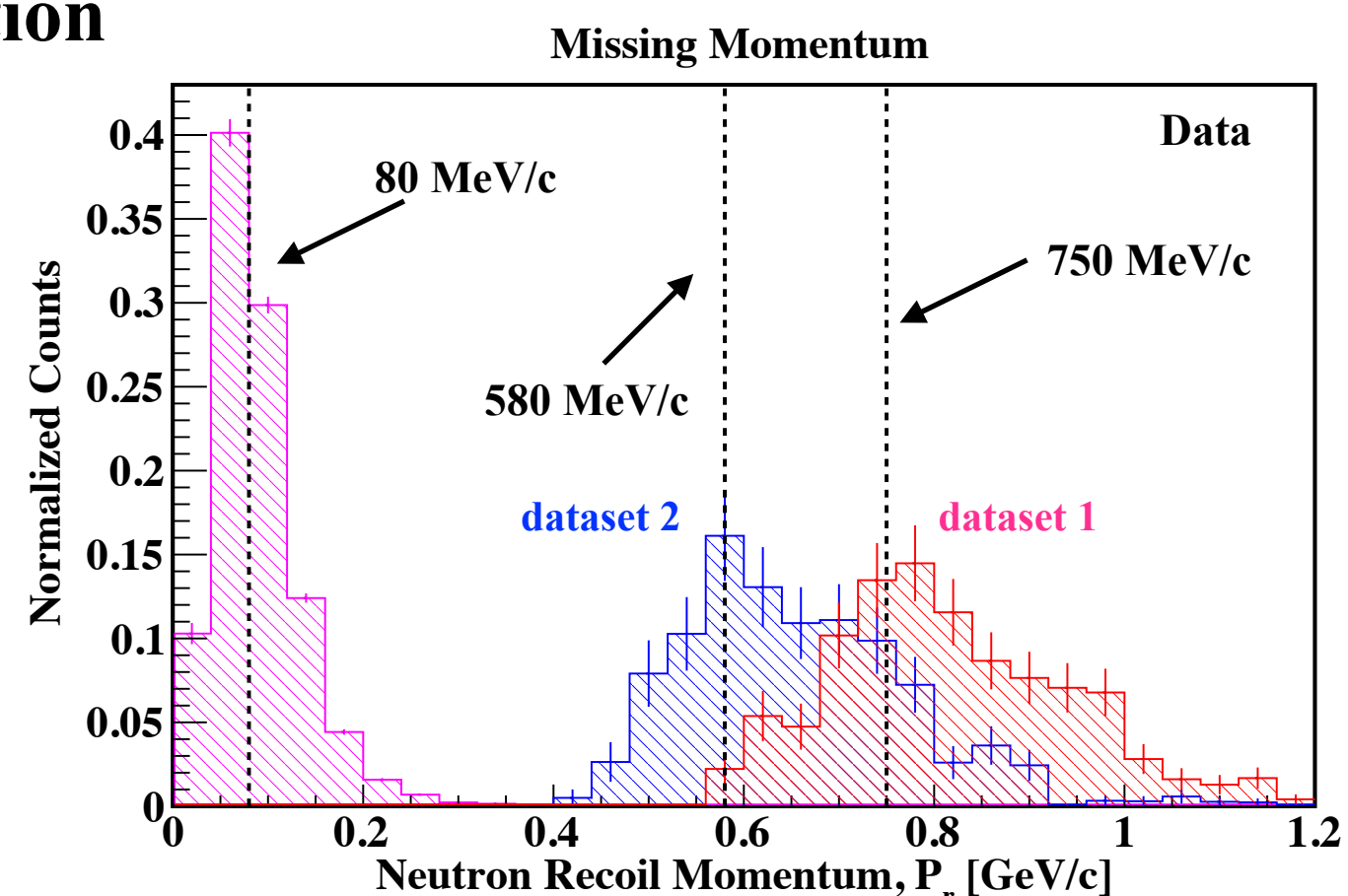


Extraction of the D(e,e'p)n Cross Section

Corrected Data Yield

$$\bar{\sigma}^{exp} \equiv \frac{Y_{data}^{corr}}{V P.S.}$$

Phase Space Volume



D(e,e'p) Momentum Distributions

Reduced cross section
(theoretical momentum distributions within PWIA)

$$\sigma_{red}^{(p_r, \theta_{nq})}$$

$$K \equiv k \cdot f_{rec} \sim P_f, P_m, q$$

kinematic factor

final proton momentum

neutron recoil momentum

3-momentum transfer

$$\frac{\sigma_{bc}^{exp}}{K \sigma_{cc1}}$$

Bin-center Corrected Experimental cross sections

Kinematic Factor times deForest ep cross section

$$\sigma_{cc1} \sim G_{Ep}(Q^2), G_{Mp}(Q^2)$$

deForest Off-shell ep cross-section

(Proton form factor parametrization)

J. Arrington, Implications of the discrepancy between proton form factor measurements, [Phys. Rev. C69, 022201 \(2004\)](#)

- ➊ Division by deForest cross section and kinematic factor removes kinematical dependencies on reduced cross section

Error Analysis of D(e,e'p)n Coincidence Cross Sections at Hall C

$\delta\theta_e [mr]$	+/- 0.17	Uncertainty in SHMS angle
$\delta\theta_p [mr]$	+/- 0.24	Uncertainty in HMS angle
$\delta E_f/E_f$	+/- 9.1E-04	Uncertainty in SHMS momentum
$\delta E_b/E_b$	+/- 7.5E-04	Uncertainty in Beam Energy
$d\sigma_{exp}^{kin}$	6.5%	← Maximum Kinematic Systematic Error on Cross Section
$d\sigma_{exp}^{norm}$	3.6 - 8.4 %	← Normalization Systematic Error on Cross Section
$d\sigma_{exp}^{stats}$	20 - 30 %	← Statistical Error on Cross Section on average (at 580/750 MeV/c settings)

- ⌚ $(d\sigma_{exp}^{syst})^2 = (d\sigma_{exp}^{kin})^2 + (d\sigma_{exp}^{norm})^2$: total systematic error is quadrature sum of kin. and norm errors
- ⌚ $(d\sigma_{exp}^{tot})^2 = (d\sigma_{exp}^{stats})^2 + (d\sigma_{exp}^{syst})^2$: total error is quadrature sum of statistical and systematic errors
- ⌚ Total cross section error is dominated by statistical error

See Backup Slides
 for detailed Tables and Plots of
 Statistical/Systematic Errors

Summary of Theoretical Calculations for E12-10-003

Theoretical Calculation	Final State Interactions (np parametrization)	Nucleon Form Factors (parametrization)	Deuteron Wave Function
J.M. Laget	SAID	Galster: GEn Hall A Exp: GEp	Paris
M.M. Sargsian	SAID	JJK	CD-Bonn AV18
S. Jeschonnek & J.W.V. Orden	SAID/Regge	GKex05 AMT	WJC2 CD-Bonn AV18

S. Galster, et al., Nucl. Phys. B32 (1971) 221 (**Galster, neutron electric form factor, GEn**)

O. Gayou, et al., Phys. Rev. Lett. 88 (2002) 092301 (**Hall A Exp. proton electric form factor, GEp**)

J.J. Kelly, Phys. Rev. C70, 068202 (2004) (**JJK**)

E.L. Lomon, Phys. Rev. C66, 045501 (2002) (**GKex05**)

J. Arrington, W. Melnitchouk, and J.A. Tjon, Phys. Rev. C76, 035205 (2007) (**AMT**)

R.A. Arndt, W.J. Briscoe, I.I. Strakovsky, and R.L. Workman, Phys. Rev. C76, 025209 (2007) (**SAID**)

W.P. Ford, S. Jeschonnek, and J.W.V. Orden, Phys. Rev. C 87, 054006 (2013) (**Regge**)

M. Lacombe, B. Loiseau, J. M. Richard, R. Vinh Mau, J. Côté, P. Pirès, and R. de Tourreil
Phys. Rec. C21, 861 (1980) (**Paris Potential**)

R.B. Wiringa, V.G.J. Stoks, and R. Schiavilla, Phys. Rev. C51, 38 (1995) (**AV18**)

R. Machleidt, Phys. Rev. C63, 024001 (2001) (**CD-Bonn**)

F. Gross and A. Stadler, Few Body Syst. 44, 295 (2008) (**WJC2**)

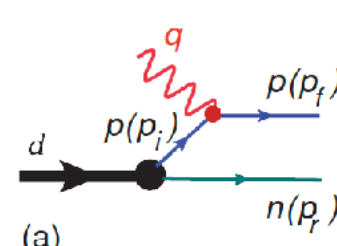
**See Backup Slides: Overview of
Theoretical Potentials to
Theoretical Cross Sections**

❖ Effective Feynman Diagrammatic Approach (calculate scattering amplitudes)

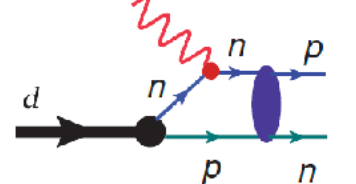
- Scattering amplitudes are calculated using the Generalized Eikonal Approximation (GEA) at high Q^2 ($> 1 \text{ (GeV/c)}^2$) under the assumptions of the Virtual Nucleon Approximation

Feynman diagrams under GEA

PWIA



Charge-Exchange FSI



Charge-Exchange FSI

$$\frac{d^5\sigma}{dE'd\Omega_e d\Omega_p} \propto | \langle s_f, s_r | A^\mu | s_d \rangle |^2$$

Effects included in the amplitude calculations

- Non-factorization effects
- Off-shell FSI re-scattering effects
- Charge-exchange re-scattering effects
- Off-shell electromagnetic interaction effects

total transition amplitude

$$\langle s_f, s_r | A^\mu | s_d \rangle$$

Initial (d) and final (np) spin projections of deuteron

$$\langle s_f, s_r | A_0^\mu | s_d \rangle = \sqrt{2}\sqrt{(2\pi)^3 2E_r} \sum_{s_i} J_N^\mu(s_f, p_f; s_i, p_i)$$

$$\times \Psi_d^{s_d}(s_i, p_i, s_r, p_r),$$

Total E.M. current operator
(on-shell + off-shell components)

$$\Psi_d^{s_d}(s_1, p_1, s_2, p_2) = -\frac{\bar{u}(p_1, s_1)\bar{u}(p_2, s_2)\Gamma_{DNN}^{s_d}\chi_{s_d}}{(p_1^2 - m^2)\sqrt{2}\sqrt{(2\pi)^3 2(p_2^2 + m^2)^{\frac{1}{2}}}},$$

General Solution to
Bethe-Salpeter
Equation

Wave function used for numerical estimates

$$\Psi_d(p) = \Psi_d^{\text{NR}}(p) \frac{M_d}{2(M_d - \sqrt{m^2 + p^2})}$$

Ref: M. Sargsian and M. Strikman, Phys. Lett. B 639, 223 (2006).

❖ Laget Diagrammatic Approach (calculate scattering amplitudes)

- Scattering amplitudes are calculated using the Laget diagrammatic approach which takes into account the full kinematics from the beginning of the calculations

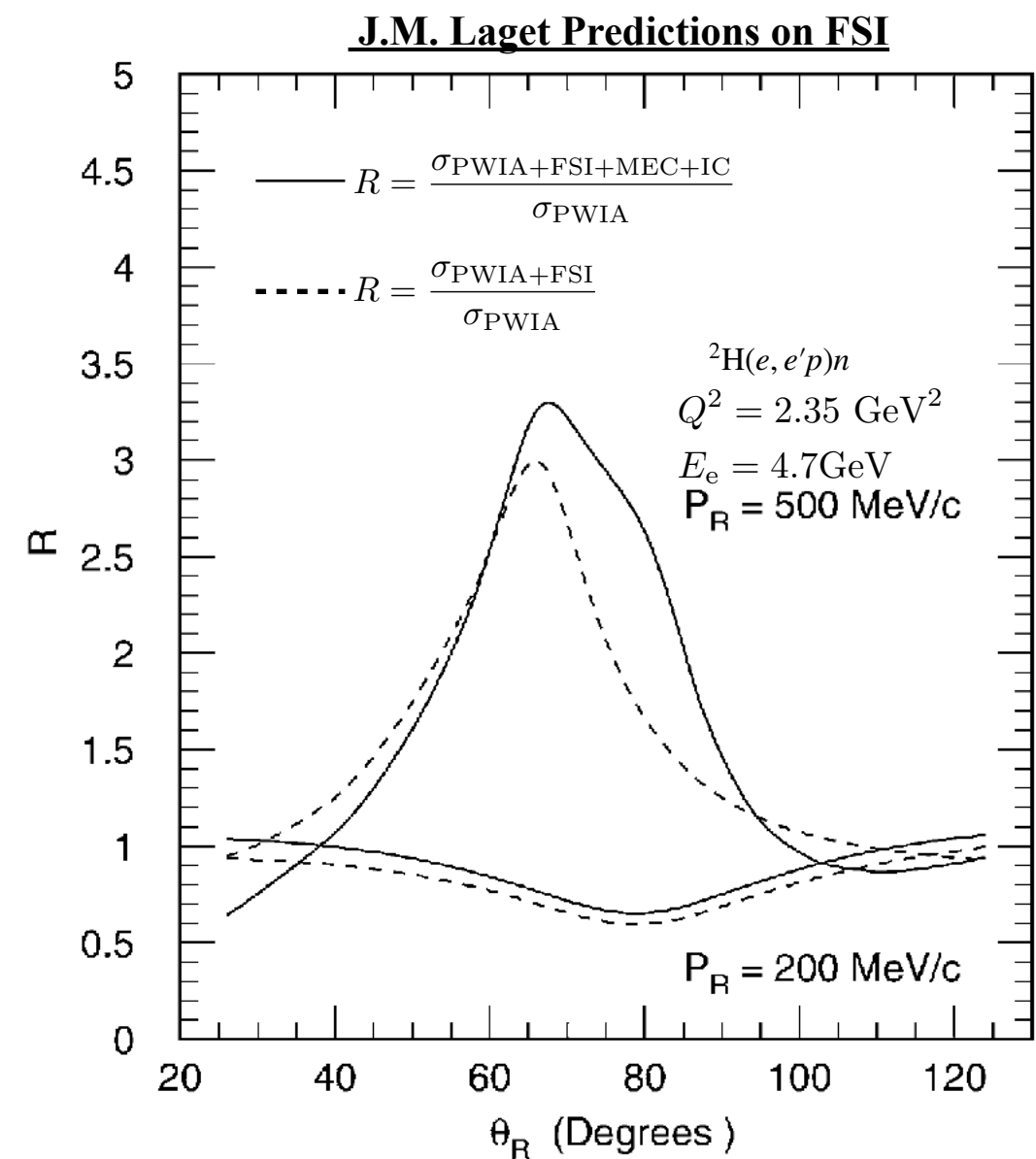
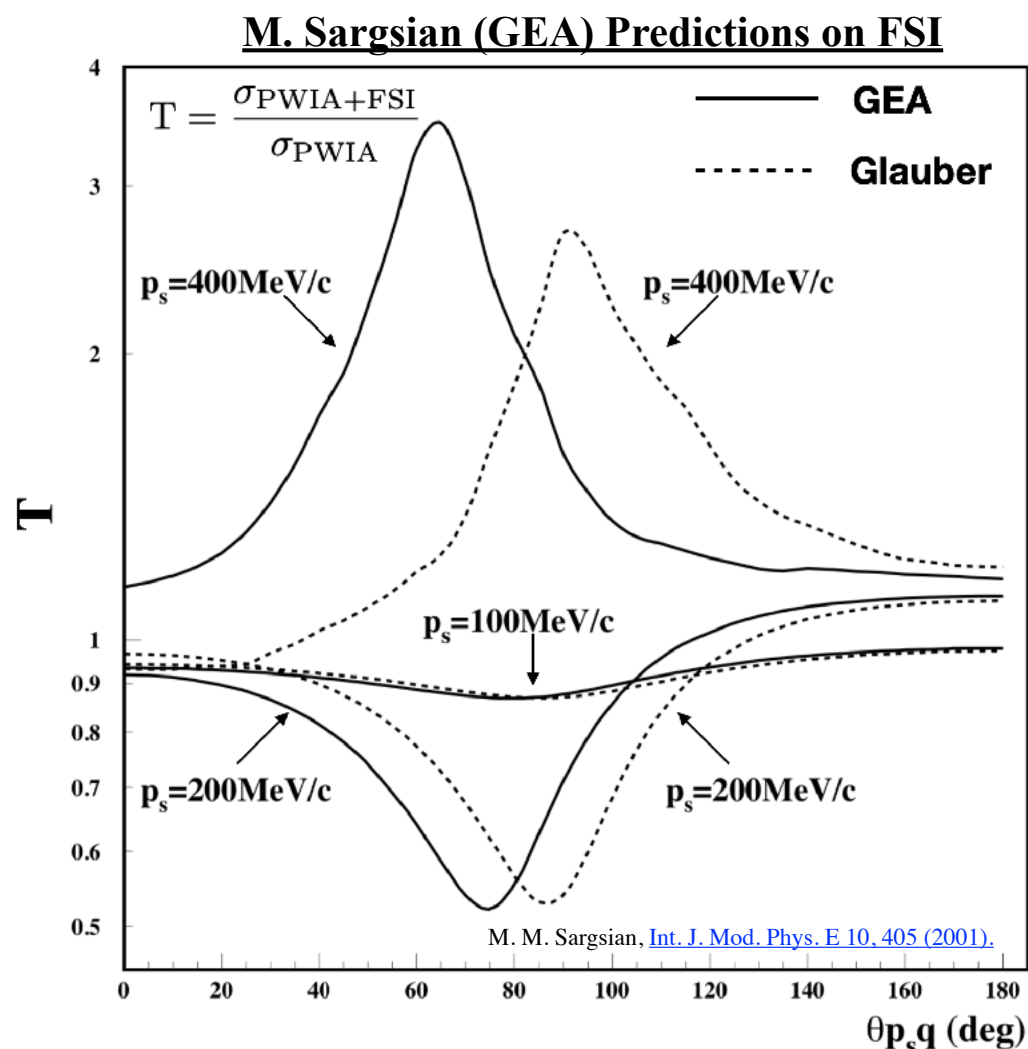
See Ref. [J.M. Laget, Phys. Rep. 69 (1981) 1]

Scattering Amplitude from Laget Diagrammatic Approach

$$\langle \psi_p, \psi_n | A_{\text{tot}} | \psi_D \rangle = \langle \psi_p, \psi_n | A_{\text{PWIA}} | \psi_D \rangle + \langle \psi_p, \psi_n | A_{\text{FSI}} | \psi_D \rangle + \\ \langle \psi_p, \psi_n | A_{\text{MEC}} | \psi_D \rangle + \langle \psi_p, \psi_n | A_{\text{IC}} | \psi_D \rangle$$

- Laget calculations accounts for relativistic effects of the bound nucleons from the beginning of the calculations

► Laget FSI calculations agree with GEA prediction of re-scattering peak at ~70 deg



Glauber Eikonal Approximation: recoil effects are neglected (stationary bound nucleon) and FSI peak stays at neutron recoil angles ~90 deg

Generalized Eikonal Approximation: Accounts for the relativistic effects of bound nucleons and predicts FSI peak at neutron recoil angles of ~ 70 deg.

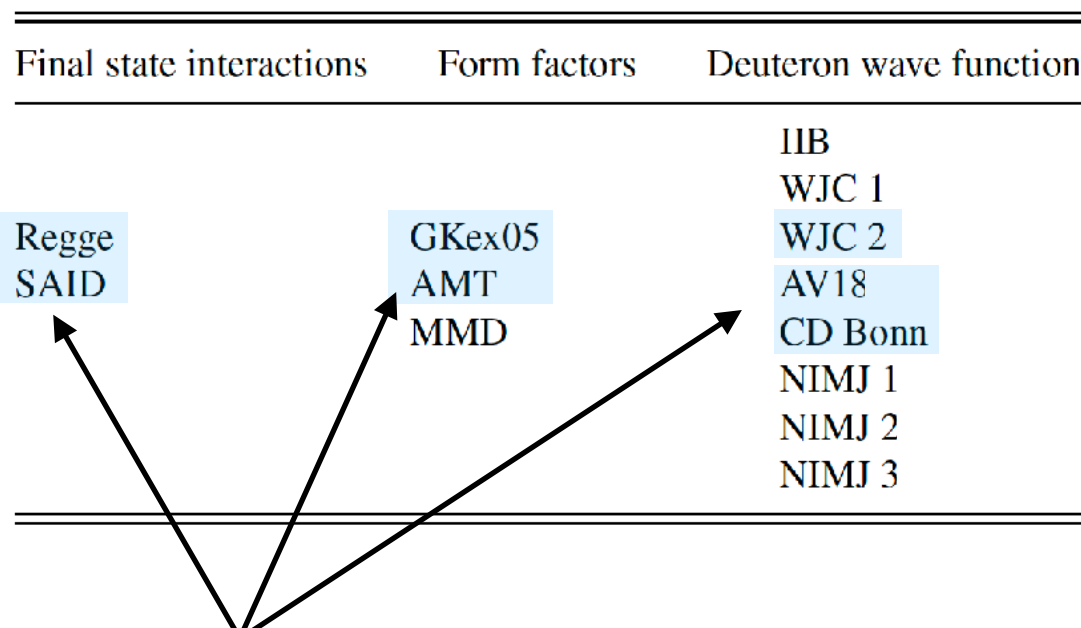
Theoretical Calculations by S. Jeschonnek & J.W.V. Orden

[W.P. Ford, S. Jeschonnek and J.W.V. Orden, Phys. Rev. C90, 064006 (2014)]

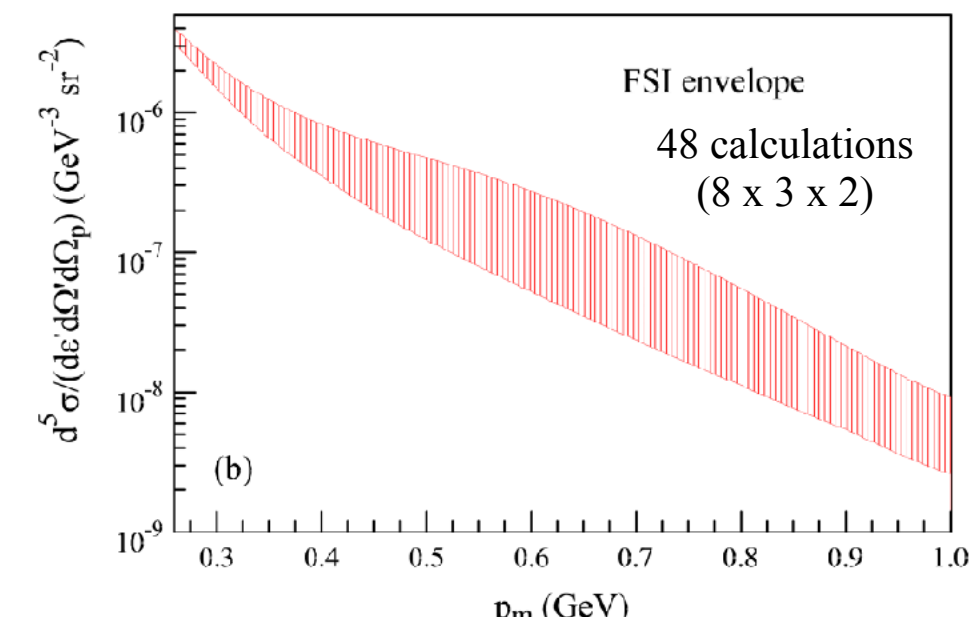
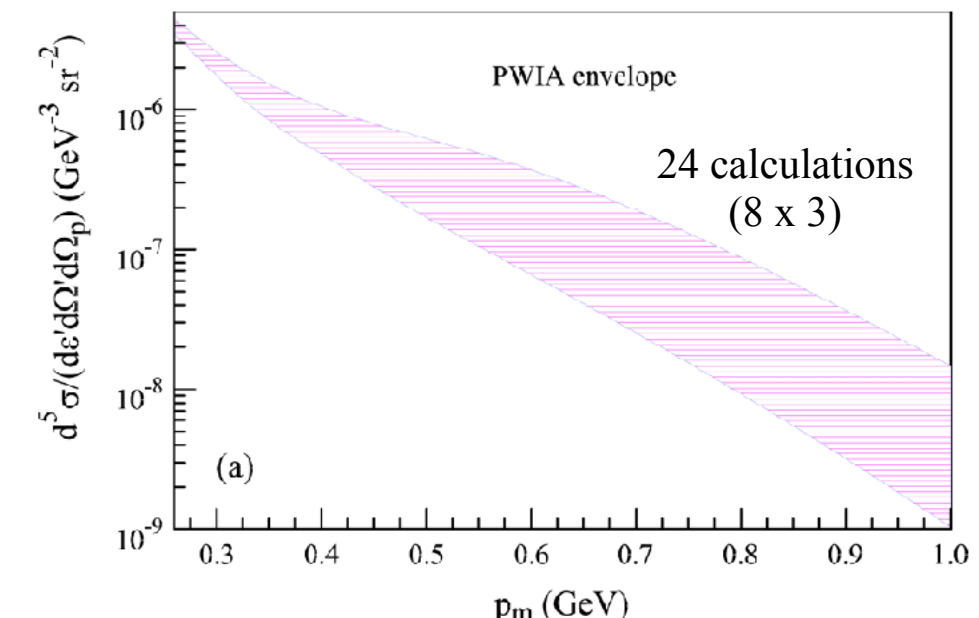
❖ Bethe-Salpeter formalism used in the calculations of wave functions

- ➊ The new method of extracting the momentum distributions takes into account a variety of model inputs providing a theoretical uncertainty
- ➋ A wide variety of bound-state wave functions, nucleon form factors and final state interactions are used as input in the cross section calculations (band of cross section calculations)

- ➌ The E12-10-003 kinematics from the original proposal were used in the calculations

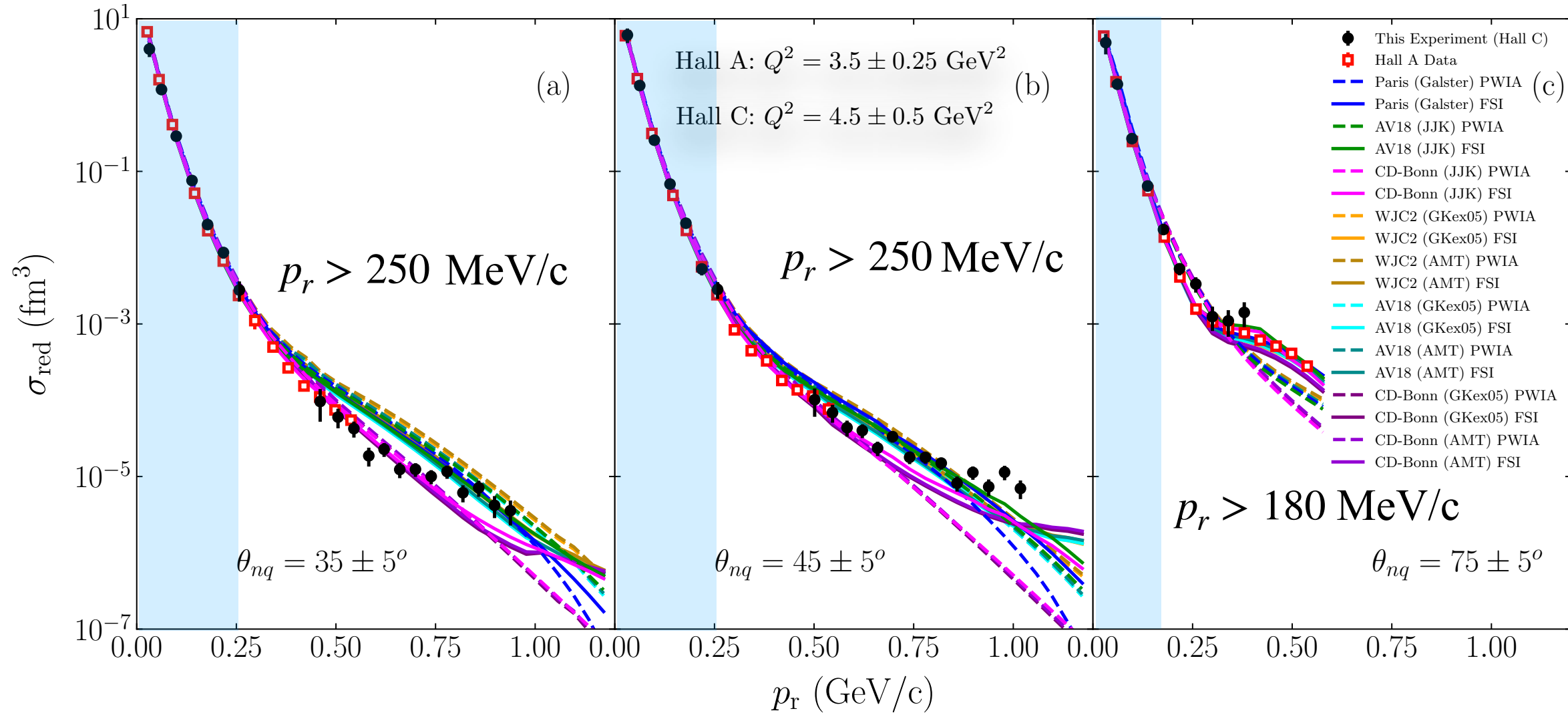


Cross section calculations using combinations of these parametrizations and wave functions were provided by S. Jeschonnek and J.W.V. Orden using the actual kinematics for this experiment.



D(e,e'p)n Cross Section Experiment Results

D(e,e'p)n Momentum Distributions



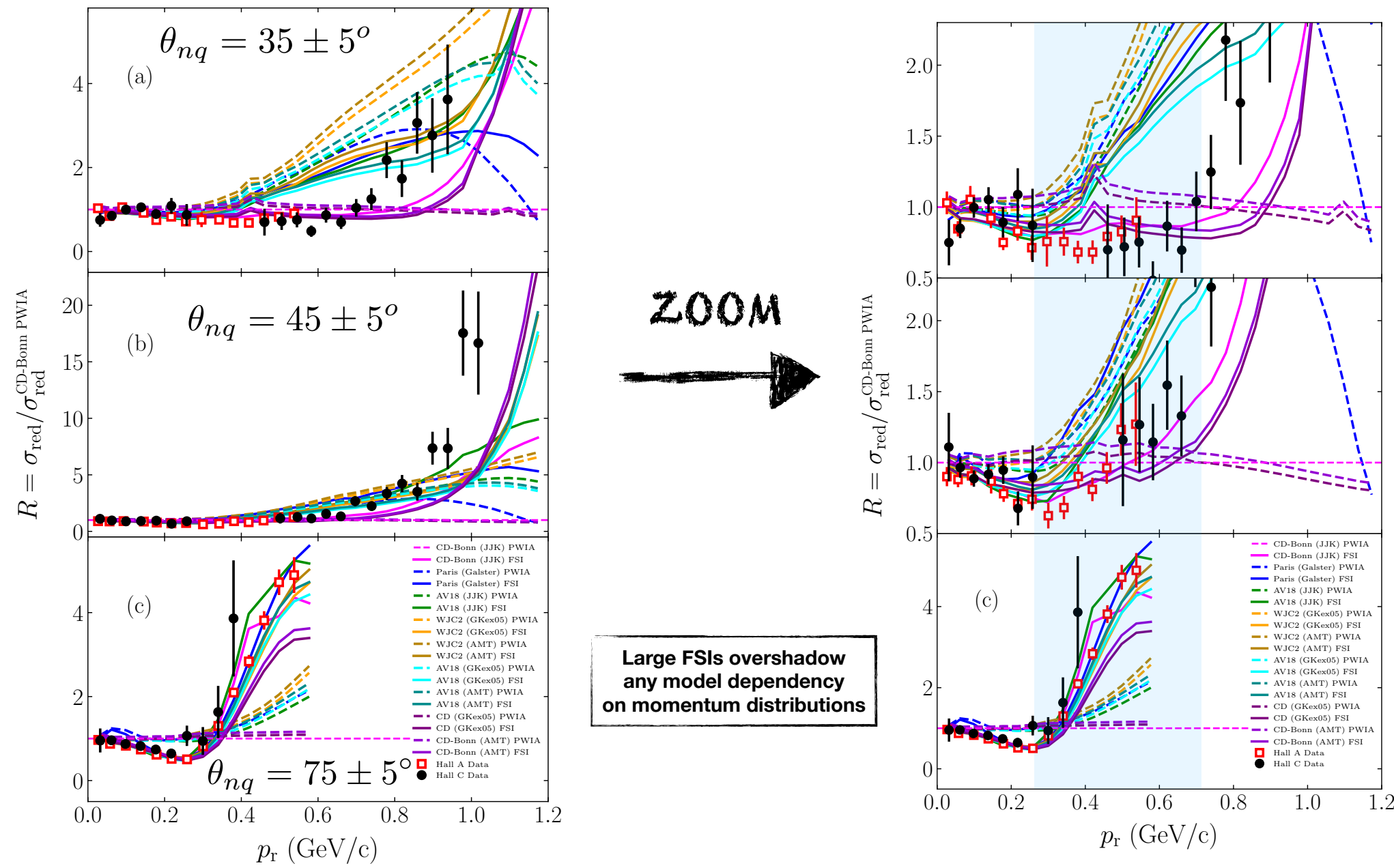
- $p_r < 250 \text{ MeV}/c$, FSIs small and NN dominated by OPEP (for 35 and 45 deg)
- $p_r > 250 \text{ MeV}/c$, CD-Bonn differs from Paris/AV18 models (for 35 and 45 deg)
- Hall C data reproduces previous Hall A data very well

J.M. Laget, Phys. Lett. B609, 49 (2005) (Paris: Galster)

M.M. Sargsian, Phys. Rev. C82, 014612 (2010) (CD-Bonn/AV18: JJK parametrization)

W.P. Ford, S. Jeschonnek and J.W.V. Orden, Phys. Rev. C90, 064006 (2014) (CD-Bonn, AV18, WJC2: GKex05, AMT parametrizations)

D(e,e'p)n Ratio to CD-Bonn (JJK) PWIA



- Data agrees with CD-Bonn FSI up to $p_r \sim 700 \text{ MeV}/c$ at 35 and 45 deg
- At $p_r \sim 300 - 700 \text{ MeV}/c$, $R \sim 0.5 - 1 \rightarrow 35, 45 \text{ deg}$ compared to $R \sim 2 - 5 \rightarrow 75 \text{ deg}$ (FSIs largely reduced at smaller angles)
- $p_r > 700 \text{ MeV}/c$ data is NOT described by any model

$$\sigma \sim |A_{\text{PWIA}} + iA_{\text{FSI}}|^2 \sim A_{\text{PWIA}}^2 - 2A_{\text{PWIA}}A_{\text{FSI}} + A_{\text{FSI}}^2$$

where $A_{\text{FSI}} \sim i|A_{\text{FSI}}|$

Approximate cancellation of amplitudes leads to reduction in FSI at specific kinematics

$$\frac{\sigma}{\sigma_{\text{PWIA}}} \sim 1 - 2 \frac{A_{\text{FSI}}}{A_{\text{PWIA}}} + \frac{A_{\text{FSI}}^2}{A_{\text{PWIA}}^2}$$

Statistical Significance Test on Reduced Cross Sections

- The fall-off observed in the reduced cross sections is smaller (less steep) for data compared to theory at higher recoil momenta

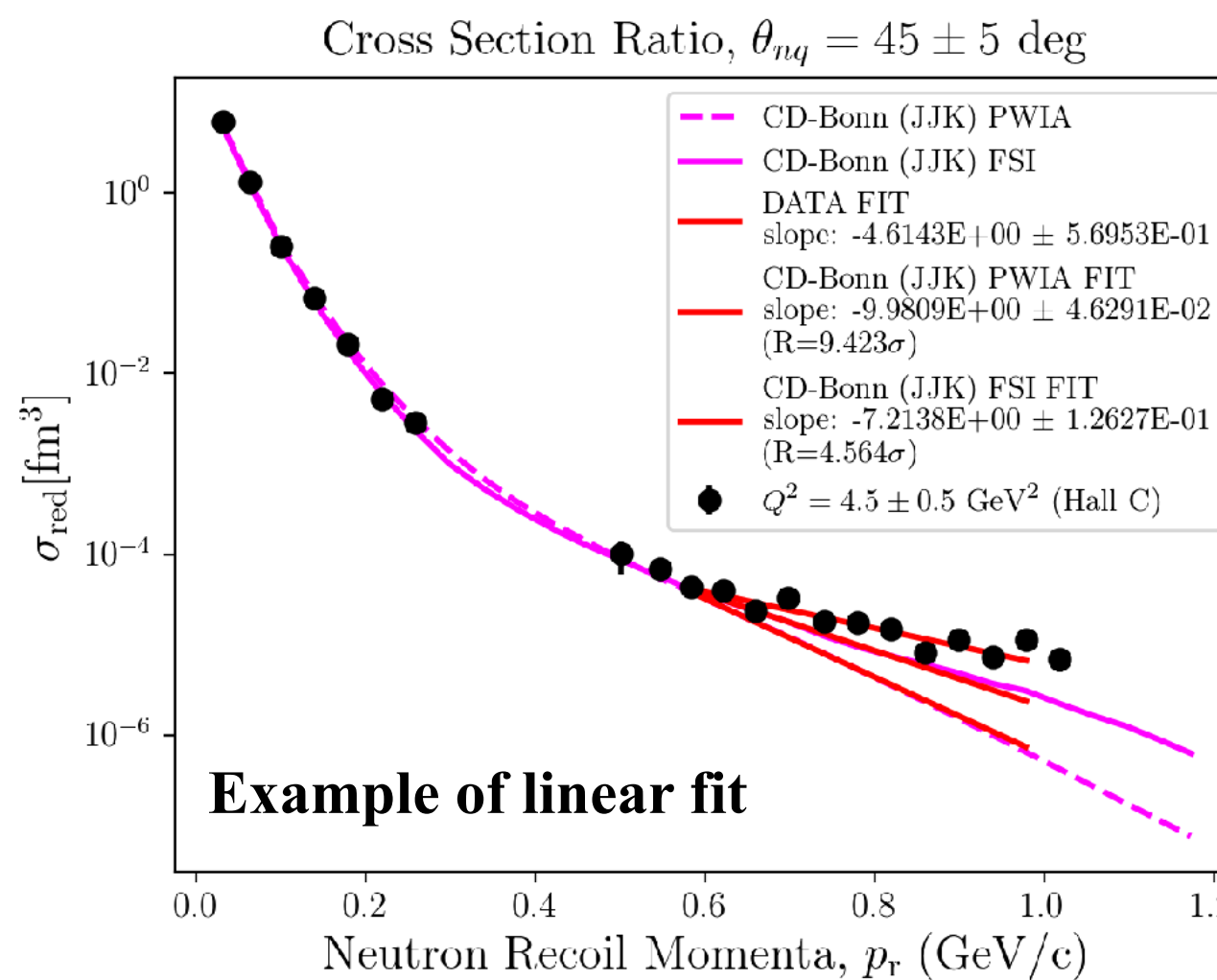
Is the discrepancy between data and theory slopes statistically significant ?

- Compare the slopes of the theoretical and experimental reduced cross sections at neutron recoil momenta between 0.55 - 1.0 GeV/c

- Calculate the Z-score to determine number of standard deviations between slopes of the the data and theory linear fits.

$$Z = \frac{\mu_{\text{data}} - \mu_{\text{theory}}}{\sigma_{\mu_{\text{data}}}}$$

data slope **theory slope**
data slope error



**See Backup Slides for
all the plots with linear fits**

Statistical Significance Test: Fit Slopes and Chi2

- Slopes are dependent on the NN potential and approximately independent of different parametrizations within the same potential
- The data differs from the CD-Bonn slopes by $\sim 4 - 9$ standard deviations (statistical fluctuations extremely unlikely) [[See Slides 78,79](#)]

Theoretical Model	PWIA (35 deg) SLOPE	PWIA (45 deg) SLOPE	FSI (35 deg) SLOPE	FSI (45 deg) SLOPE
Paris (Galster)	-8.3	-8.3	-8.2	-7.7
AV18 (JJK)	-7.9	-7.8	-8.4	-7.3
AV18 (GKex05)	-8.1	-8.1	-8.8	-8.0
AV18 (AMT)	-8.1	-8.1	-8.8	-8.0
CD-Bonn (JJK)	-10.1	-10.0	-9.6	-7.2
CD-Bonn (GKex05)	-10.3	-10.3	-10.2	-7.7
CD-Bonn (AMT)	-10.3	-10.2	-10.2	-7.6
WJC2 (GKex05)	-7.8	-7.8	-8.5	-7.8
WJC2 (AMT)	-7.8	-7.8	-8.4	-7.8

DATA	35 deg slope: -4.7 χ^2_{red} : 0.66	45 deg slope: -4.6 χ^2_{red} : 1.4
------	--	---

SUMMARY

- The experiment measured cross sections for the exclusive $D(e,e'p)n$ reaction at $Q^2 = 4.5 \text{ (GeV/c)}^2$ for neutron recoil momentum up to 1.0 GeV/c and neutron recoil angles between 35 to 75 deg
- At large angles ~75 deg, FSIs dominate above 300 MeV/c, and there is virtually no difference between the models due to large FSIs which overshadow the true momentum distributions
- DATA was best described by CD-Bonn models at smaller recoil angles (35 deg) and recoil momenta up to ~700 MeV/c
- Above 700 MeV/c, NO calculation describes the data

Overall, given that this was a 6-day commissioning and statistically limited experiment, it has very interesting results, as no model seems to describe the data above recoil momenta of 700 MeV/c. In addition, the data exhibits a significantly smaller fall-off (slope) beyond $p_r=550 \text{ MeV/c}$ compared to all models. This discrepancy is worth exploring further in the full experiment.

ACKNOWLEDGMENTS

I would like to thank my advisor and co-advisor, Drs. Werner Boeglin and Mark Jones for their constant support and useful discussions on this topic.

In addition, I would like to acknowledge the entire Accelerator Division and Hall C staff and technicians and all graduate students, users and staff who took shifts or contributed to the equipment for the Hall C upgrade making all four commissioning experiments possible.

Last (but not least) thanks to Misak Sargsian, J.M. Laget, Sabine Jeschonnek and J.W. Van Orden for providing the theoretical calculations for this experiment.

This work was in part supported by:

- the Nuclear Regulatory Commission (NRC) Fellowship grant No: NRC-HQ-84-14-G-0040 to Carlos Yero
- the Doctoral Evidence Acquisition (DEA) Fellowship to Carlos Yero
- the DOE grant No: DE-SC0013620 to FIU



THANK YOU !

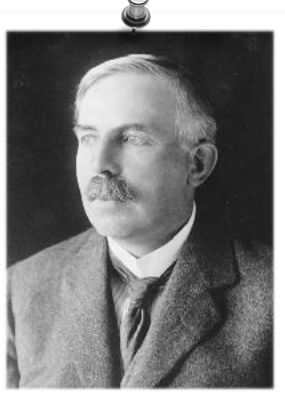


BACK-UP SLIDES

A Brief History of the Nuclear Force: From Meson Theory to Phenomenology

1911:

E. Rutherford discovers the atomic nucleus by “scattering alpha particles from Au foil.” In 1917, he proved the 1H nucleus is present in the nuclei of all other atoms



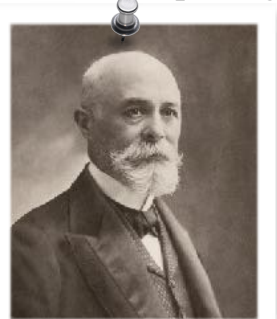
1932:

J. Chadwick discovers the neutron in a scattering experiment



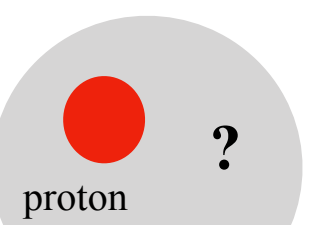
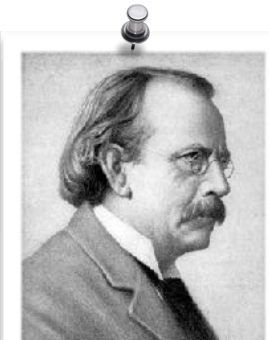
1896:

H. Becquerel discovers radioactivity from Uranium salt on photographic plates



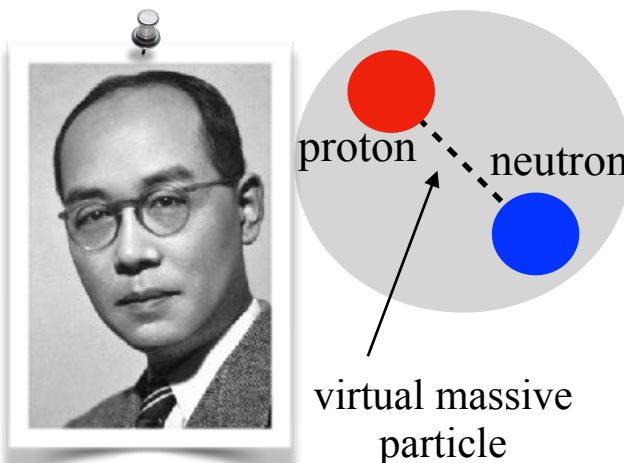
1897:

- J.J. Thompson discovers the electron (beta rays deflected by an electric field),
- the electron indicated the atom had internal structure



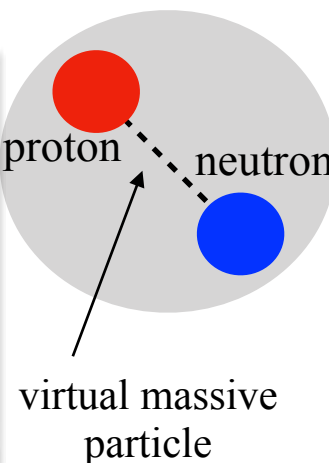
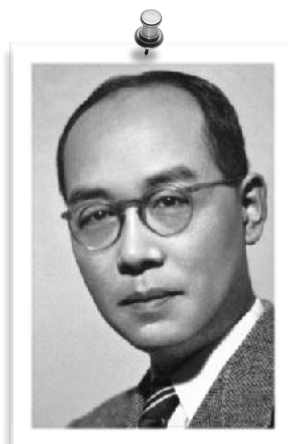
1931:

H. Urey discovers deuterium present in a residue of distilled liquid hydrogen



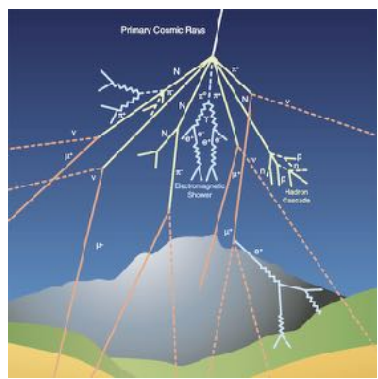
1935:

H. Yukawa proposes the NN interaction to be mediated by the exchange of a massive virtual particle



1947, 1948:

Charged pion discovered in cosmic rays (1947) and later artificially produced in Berkeley Lab (1948)



1930s:

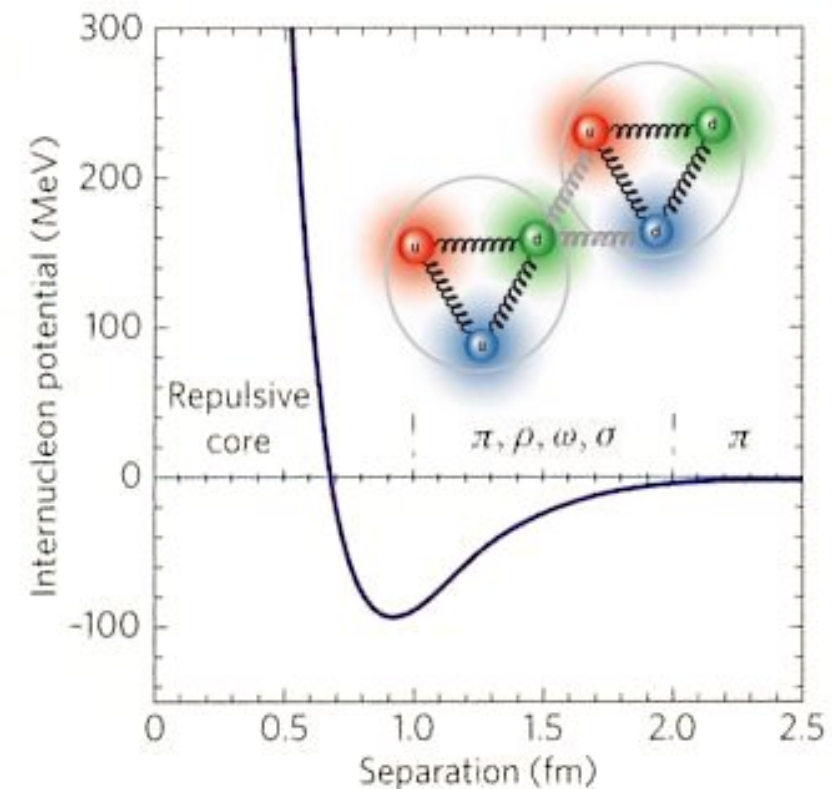
Efforts devoted to develop pion (meson) field theories motivated by pion discovery

- One-Pion Exchange Potential (OPEP) described NN scattering data successfully
- Meson Theory failed to describe multi-pion exchange (Meson Theory is NOT the fundamental theory of strong interactions)

1950s:

1951:

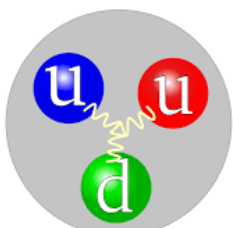
M. Taketani, S. Nakamura and M. Sasaki propose to divide the NN potential into 3 sub-ranges



A Brief History of the Nuclear Force: From Meson Theory to Phenomenology

Quark Model (1964)

- M. Gell-Mann and G. Zweig propose that baryons & mesons are bound states of sub-atomic particles termed “quarks” by Gell-Mann



1970s:

- Refined OBEP models
- relativistic OBE models developed
- sophisticated OBE models to include 2π exchange
- Paris potential (1972, 1979)

1970s:

1990s:

- High-precision NN potentials based on improved nn , pp , np scattering database
- e.g., Argonne V18 (AV18), Nijmegen I & II, Charge-dependent Bonn (CD-Bonn)

Fundamental problem of nuclear physics in present day:
derive the NN interaction from fundamental QCD principles

1960s:

- large amounts of NN scattering data accumulated since 1955
- Discovery of heavier mesons in experiments $\rho(770)$, $\omega(783)$,
- Development of the One-Boson Exchange Potential (OBEP)
e.g., Hamada-Johnston (HD), Yale-Group, Bryan-Scott (BS), Reid (1969) potentials

1980s:

- More sophisticated OBEP models constructed
- Argonne V14, V28 (AV14, AV28) potential
- 2π exchange contributions
- Full Bonn potential
- 2π exchange contributions, - relativistic effects

1990s:



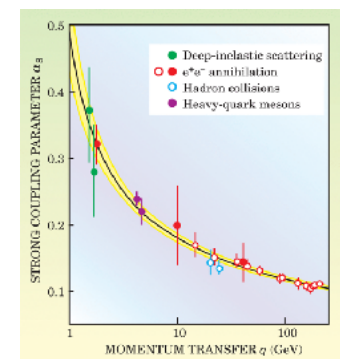
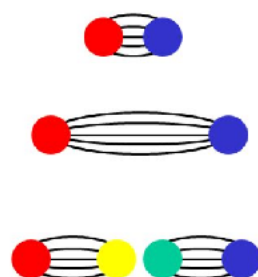
2000s:

- Chiral Effective Field Theories
- development of NN potentials based on χ EFT (experimental scattering data is used as input)
- QCD-based approaches are still a set of models and do NOT represent a true fundamental progress in understanding nuclear forces

Quantum Chromodynamics (QCD) (1973)

QCD established as the QFT of strong interactions
QCD exhibits 2 main properties:

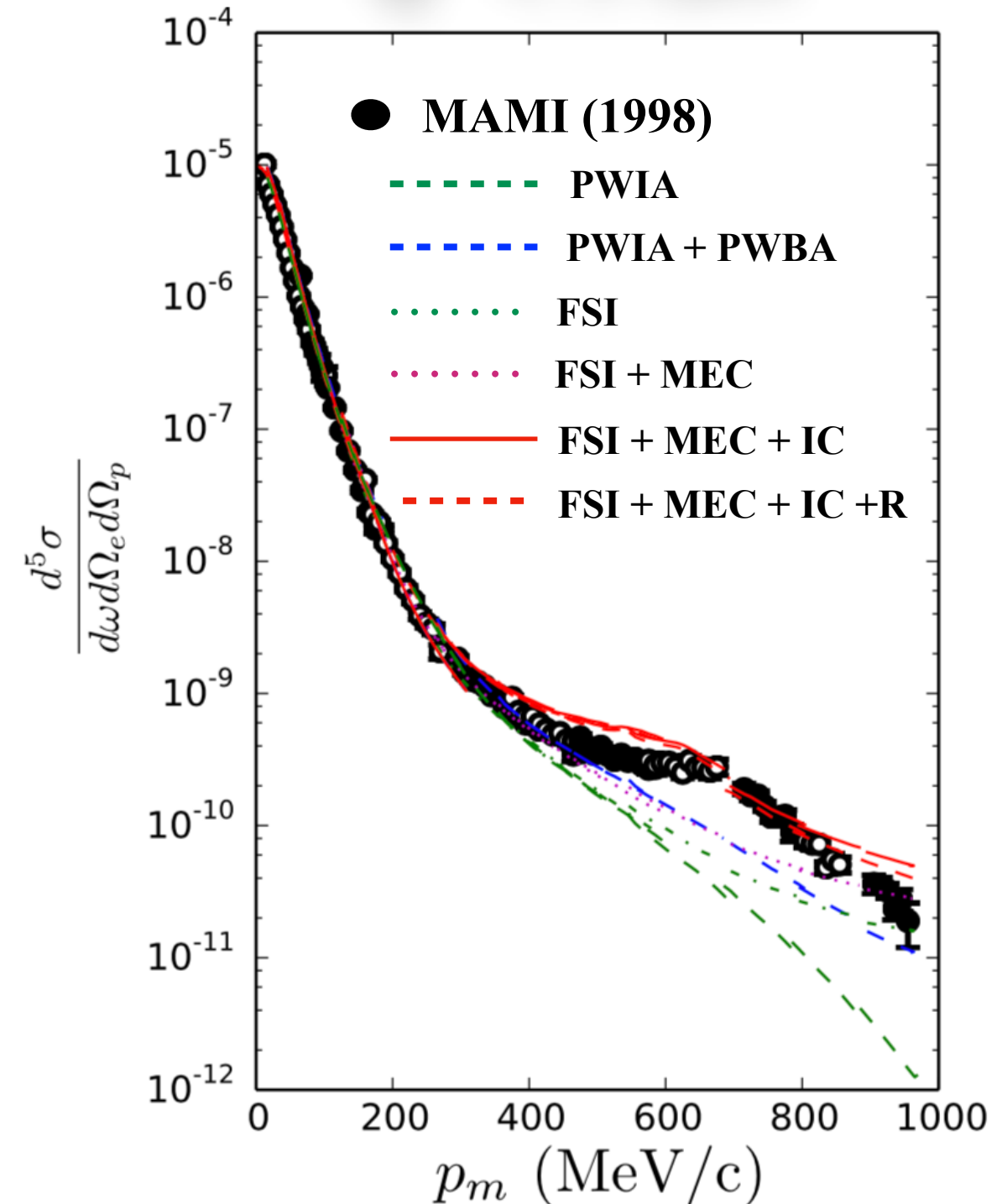
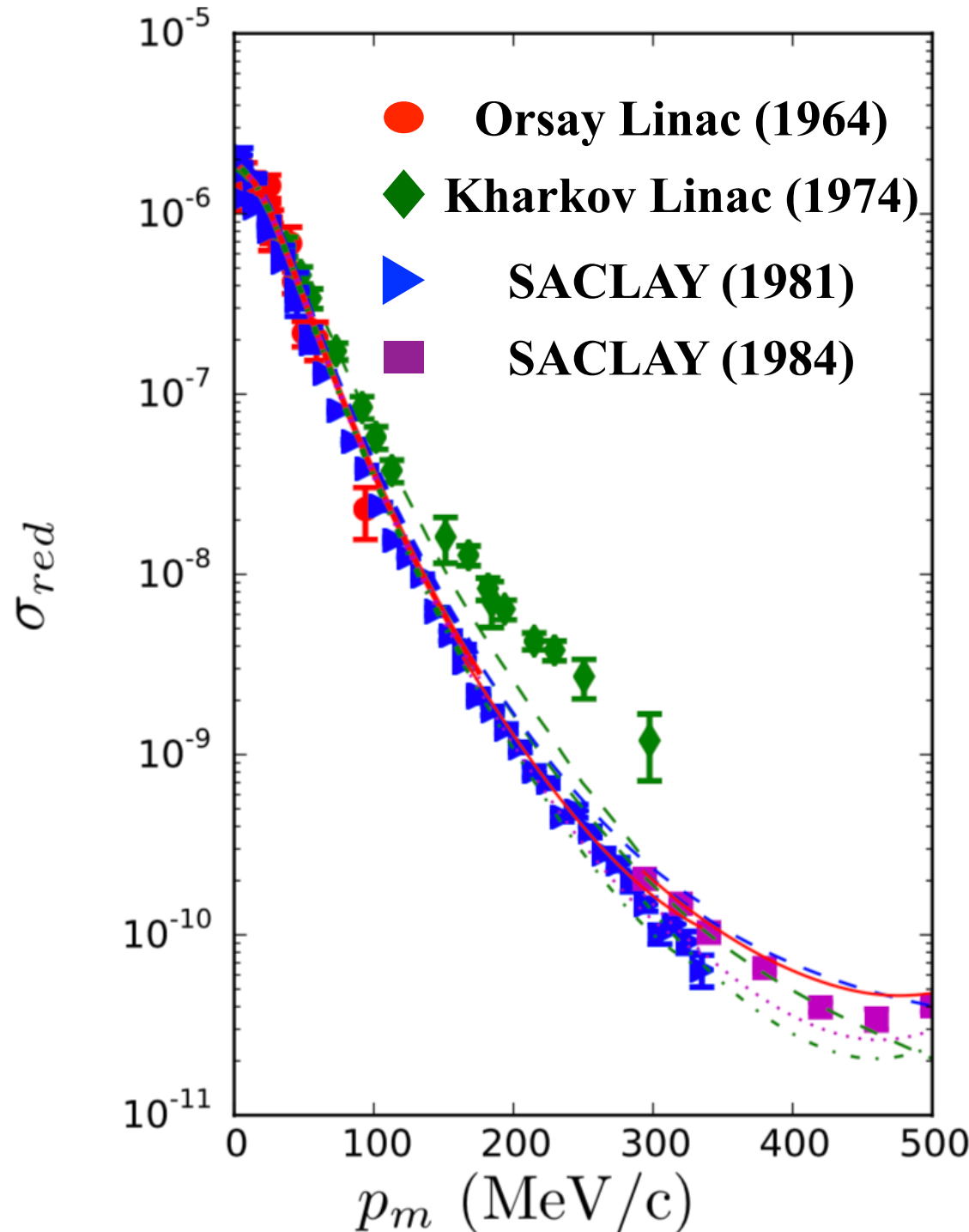
- Color confinement
- Asymptotic Freedom (Gross, Wilczek, Politzer)



D(e,e'p) Experiments

At $Q^2 < 1 \text{ GeV}^2$

Previous D(e,e'p)n Experiments at: $Q^2 < 1 \text{ GeV}^2$



Theoretical Calculations

W. Fabian and H. Arenhövel,
Nucl.Phys. A258, 461 (1976)

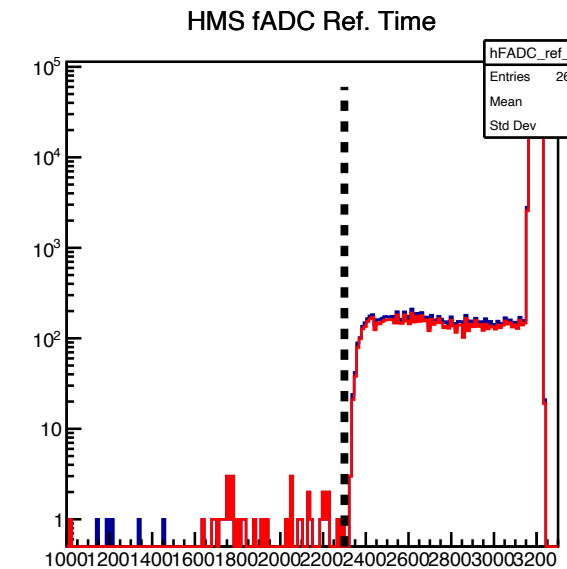
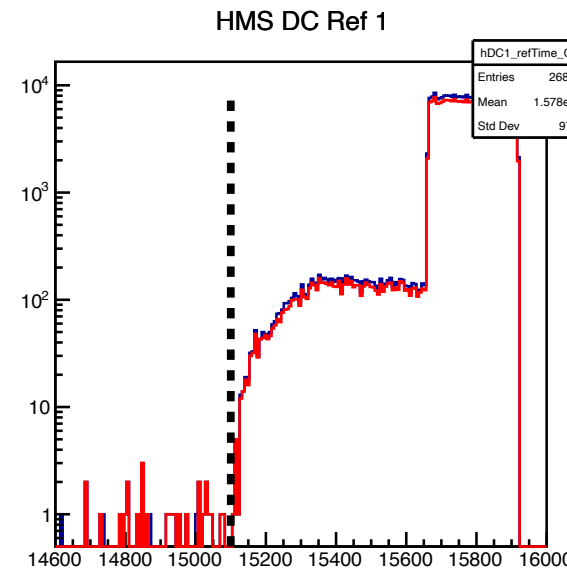
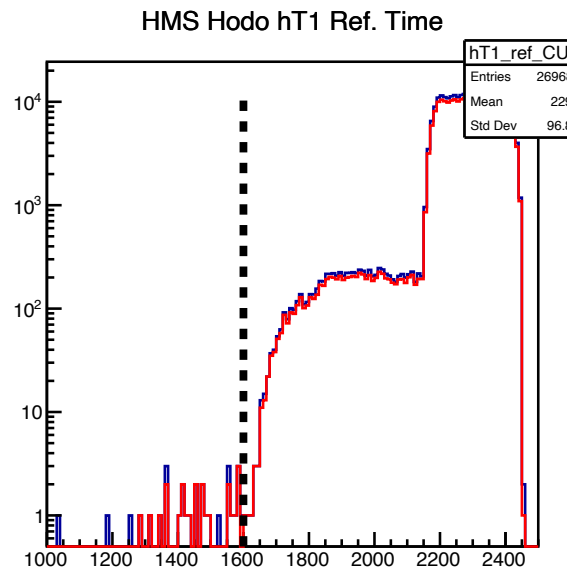
⦿ At $P_m > 300 \text{ MeV/c}$, FSI+MEC+IC all dominate the cross section

Plots Reference: [W.U.Boeglin and M. Sargsian Int.J.Mod.Phys. E24 \(2015\) no.03, 1530003](#)

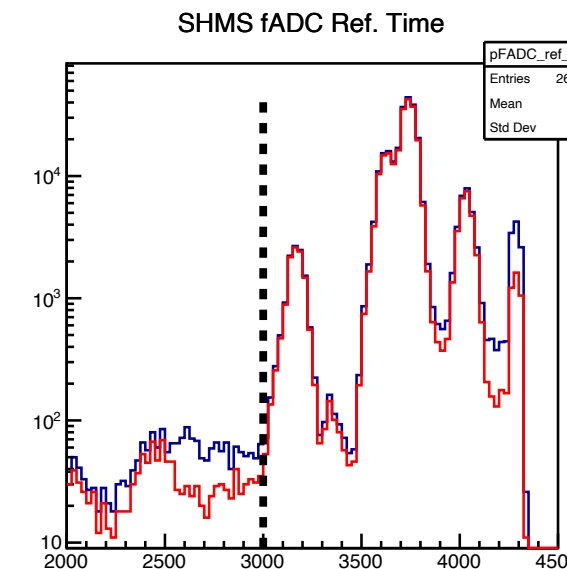
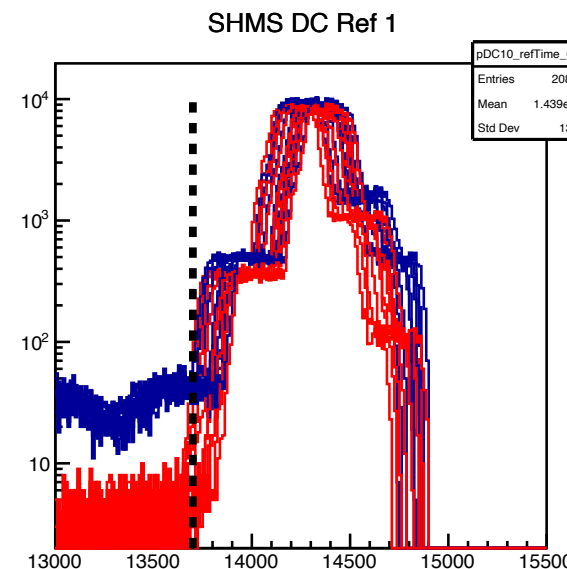
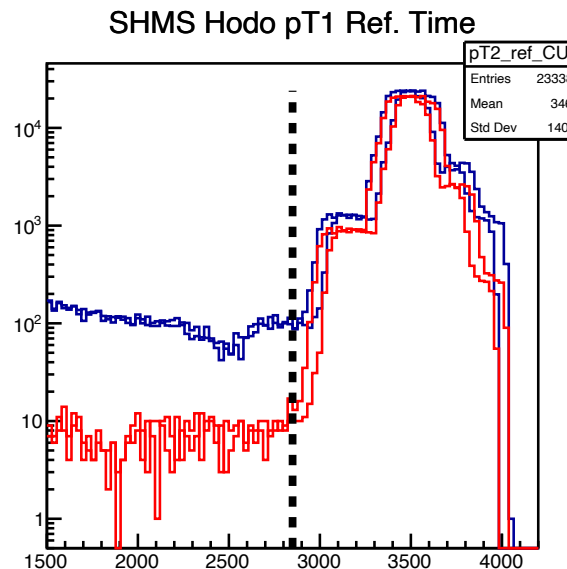
Data Analysis of the E12-10-003 Commissioning Experiment at Hall C

Reference Time Cuts

- Correct reference time (copy of the trigger) must be chosen so that the ADCs/TDCs subtract the correct reference time (to the right of the cut dashed line)



HMS
Reference Times

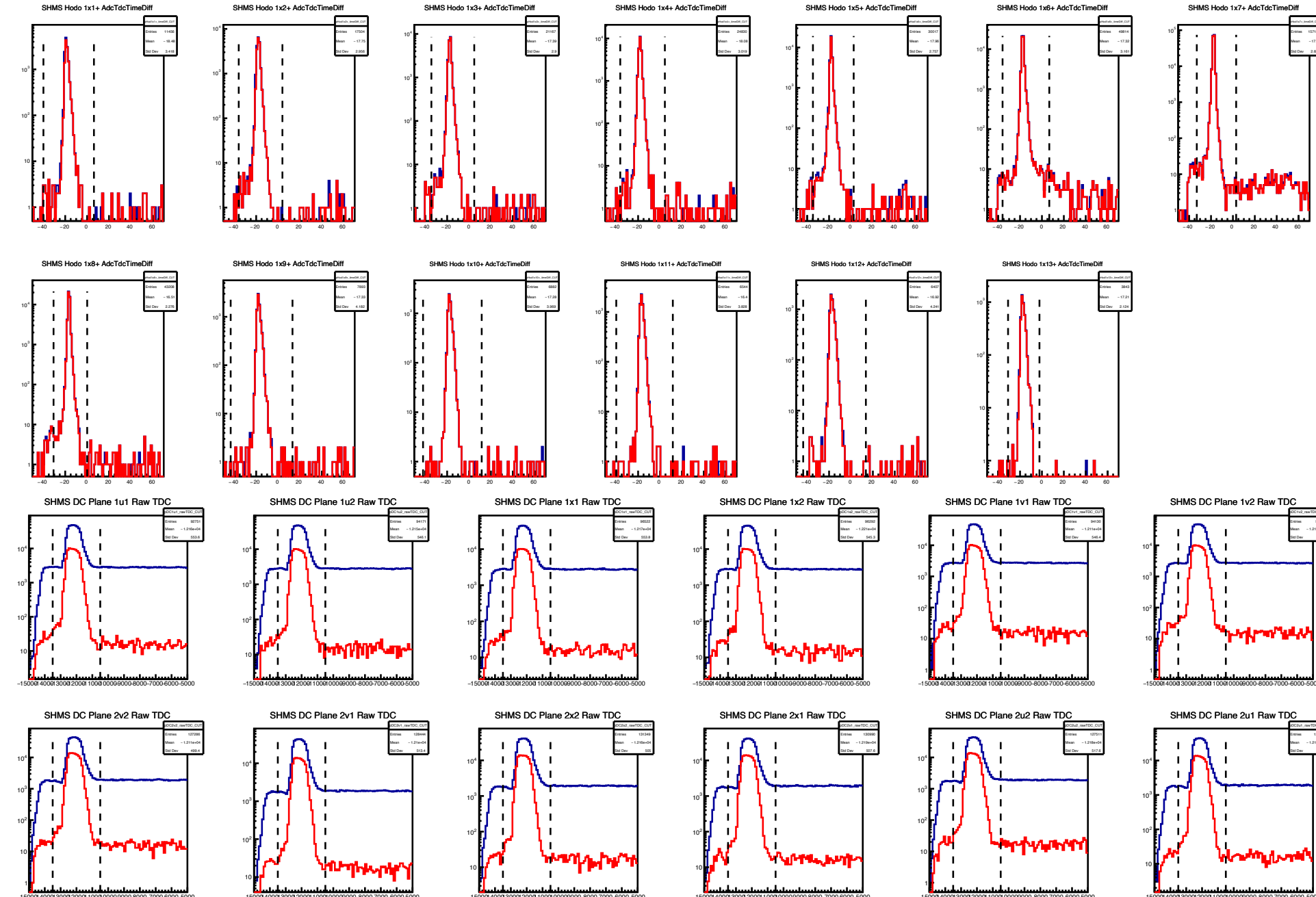


SHMS
Reference Times

TDC Time Window Cuts

A time window cut MUST be made around the main signal peak to reduce background from possible out-of-time events. (Specially on the DCs)

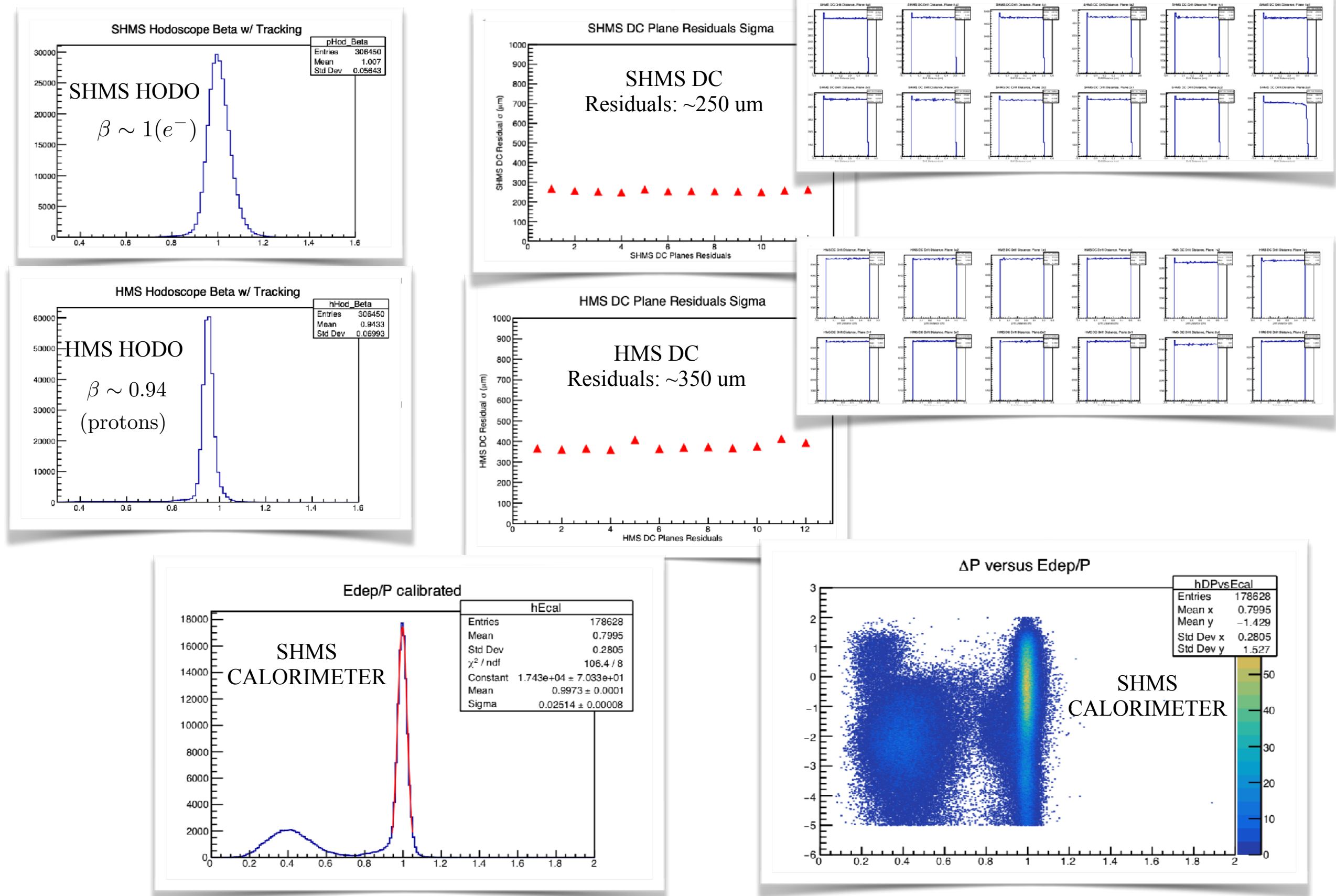
Legend: No Mult. Cut Multiplicity==1



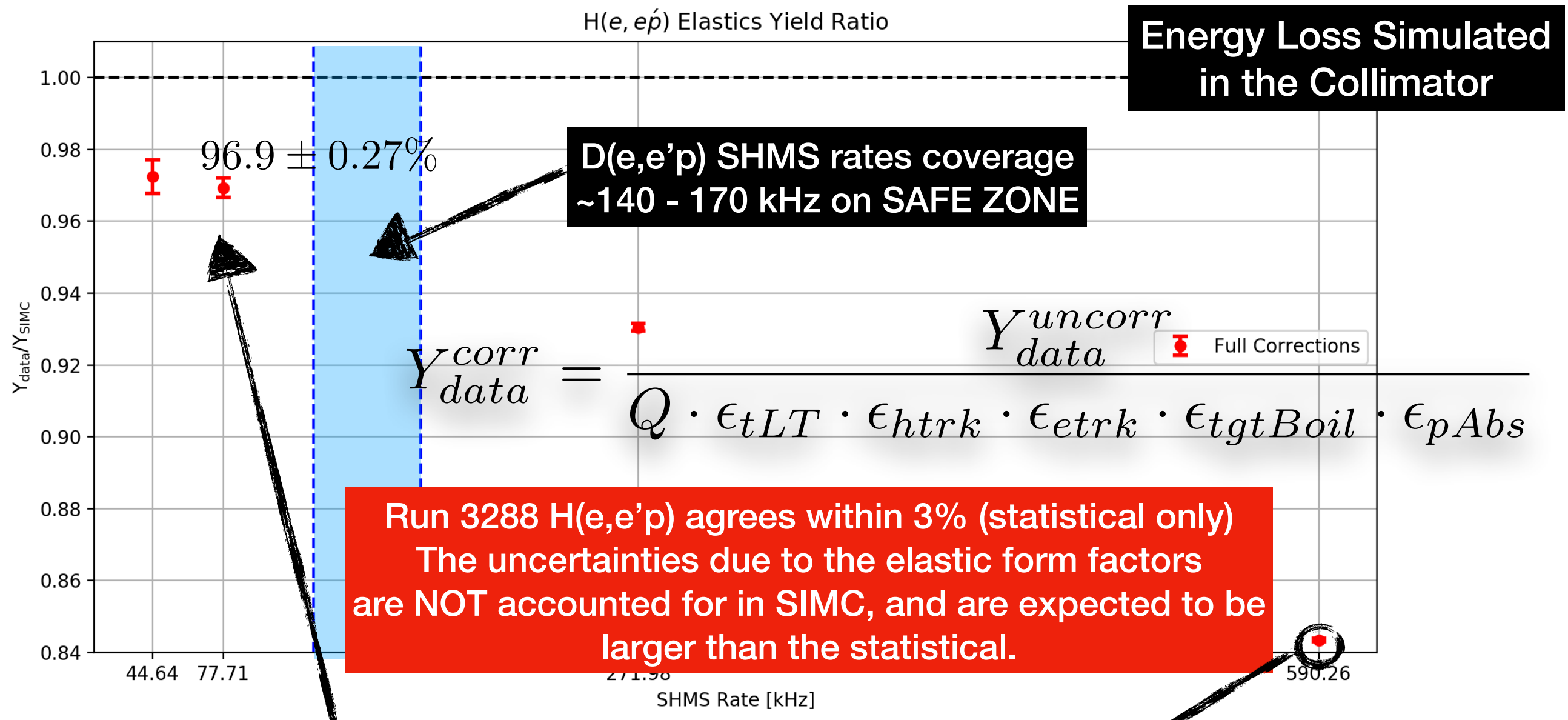
**SHMS
Hodoscope 1X+
(ADC-TDC) Time
Difference**

**SHMS
Drift Chambers
Raw TDC Time**

Detector Calibrations



H(e,e'p) Yield Ratio Check



Spectrometer acceptance is studied in detail for this run (3288), due to its proximity to the D(e,e'p)n 80 MeV kinematics

The general cuts applied were:

|HMS Delta| < 8 % SHMS Delta: (-10, 22) %

Inv. Mass W : (0.85, 1.05), HMS Coll. Cut

SHMS Optics Optimization for E12-10-003 Using H(e,e'p) Elastics

The SHMS optics optimization work done for the D(e,e'p)n experiment can be found at Hall C Document Database

Optics Optimization for the D(e,e'p)n Experiment (E12-10-003)

Carlos Yero

July 29, 2019

1 Introduction

The commissioning of the HMS/SHMS optics took place on the 2017-18 run period and underwent multiple revisions of the reconstruction matrix elements for both spectrometers during that period.^[3,4] This document presents the optics optimization checks and procedures done on the High Momentum Spectrometer (HMS) and superHMS (SHMS) for the Deuteron Electro-Disintegration Commissioning Experiment (E12-10-003) on April 2018. At the time, this experiment also served as part of the general optics commissioning as during data-taking, it was found that the SHMS Q3 magnet had an un-necessary correction in the matrix elements. As a result, the data for this experiment is divided into two sections. Only the section after the fix in the SHMS optics was used in the optimization procedure.

The problem of optics optimization can be approached in different ways, depending on the circumstances of the experiment. In this particular experiment, a series of H(e,e'p) elastic runs were taken at different configurations such as to cover the entire HMS momentum range in the D(e,e'p)n reaction kinematics. The original and corrected H(e,e'p) kinematics are summarized below.

Run	HMS Angle [deg]	HMS Momentum [GeV]	SHMS Angle [deg]	SHMS Momentum [GeV]
3288	37.338	2.938	12.194	8.7
3371	33.545	3.48	13.93	8.7
3374	42.9	2.31	9.928	8.7
3377	47.605	1.8899	8.495	8.7

Table 1: Original H(e,e'p) Elastic Kinematics in E12-10-003.

Run	HMS Angle [deg]	HMS Momentum [GeV]	SHMS Angle [deg]	SHMS Momentum [GeV]
3288	37.338	2.9355	12.194	8.5342
3371	33.545	3.4758	13.93	8.5342
3374	42.9	2.3103	9.928	8.5342
3377	47.605	1.8912	8.495	8.5342

Table 2: Corrected H(e,e'p) Elastic Kinematics in E12-10-003.

Spec	$\delta\theta$ [rad]	$\delta\phi$ [rad]	X'_{tar} -offset[rad]	Y'_{tar} -offset[rad]
HMS	0.0	1.521×10^{-3}	2.852×10^{-3}	9.5×10^{-4}
SHMS	0.0	0.0	0.0	0.0

Table 3: Spectrometer Offsets determined from H(e,e'p) Elastic Run 3288 in E12-10-003. See Section 4 of this document for more information.

Since this is a coincidence experiment, the spectrometers are highly correlated which makes the optics optimization more complicated, as changes in one spectrometer can affect the other. Based on the kinematics, it was determined to focus on the HMS first, as the momentum is well below the Dipole saturation (~ 5 GeV), and the optics are much better understood from the 6 GeV era.



Optimize SHMS delta matrix



Used sieve data to optimize Y_{tar}



Determined spectrometer kinematics offsets

Details can be found in documentation

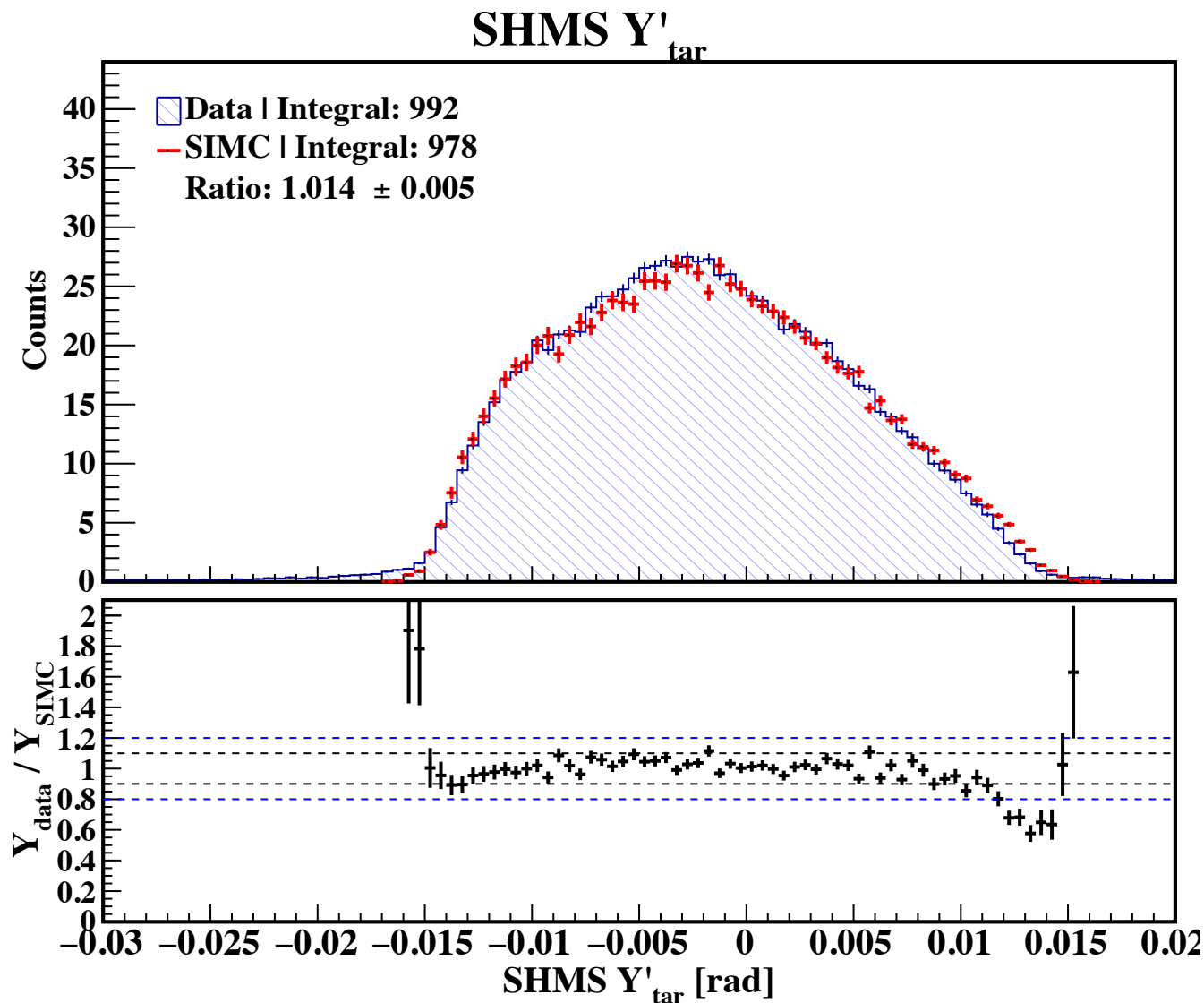
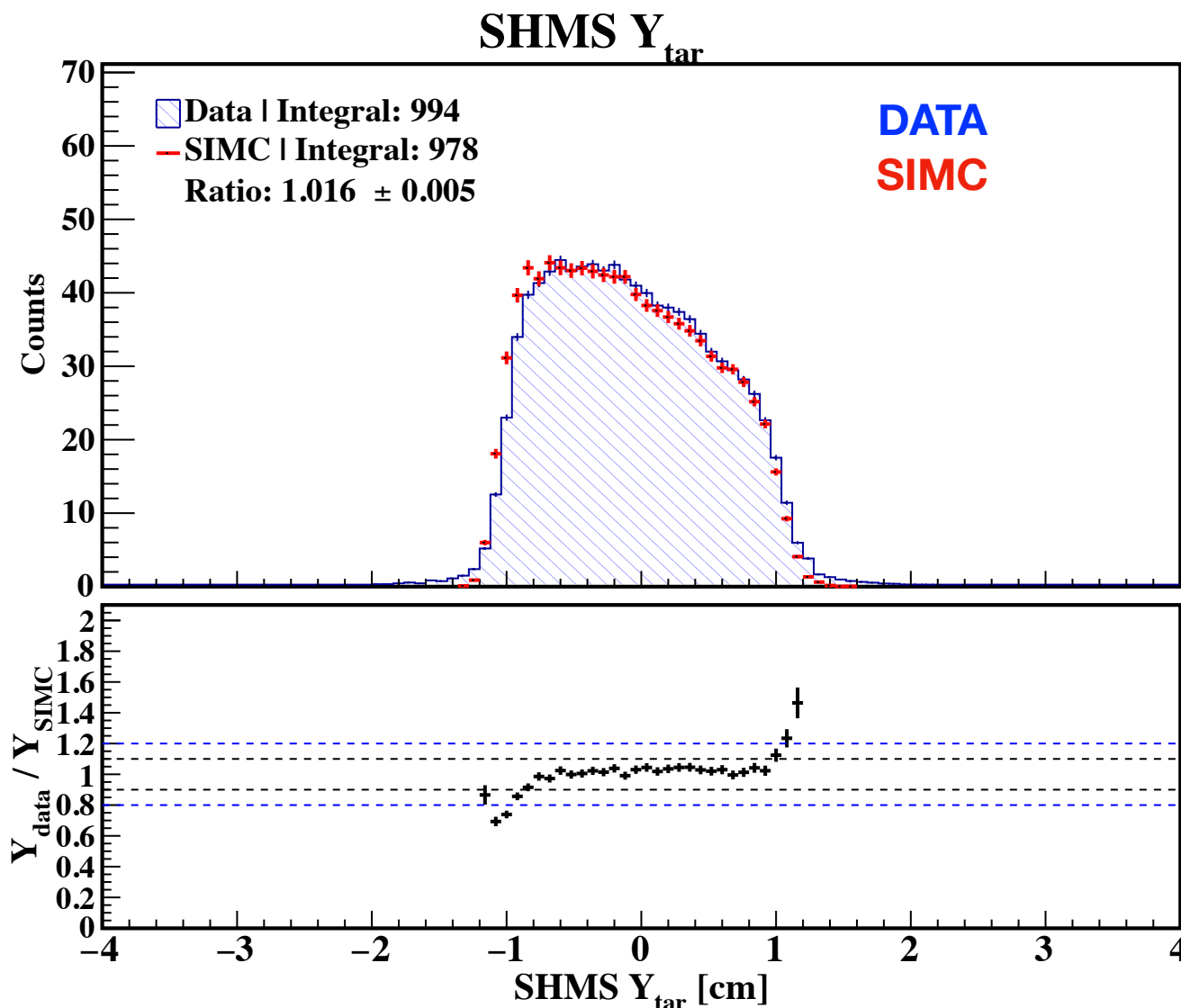
HALLC DOC-DB LINK

Spectrometer Acceptance DATA/SIMULATION

(used H(e,e'p) Elastics data taken on D(e,e'p)n Experiment)

SHMS Reconstructed Variables

**** Data is fully corrected for inefficiencies**

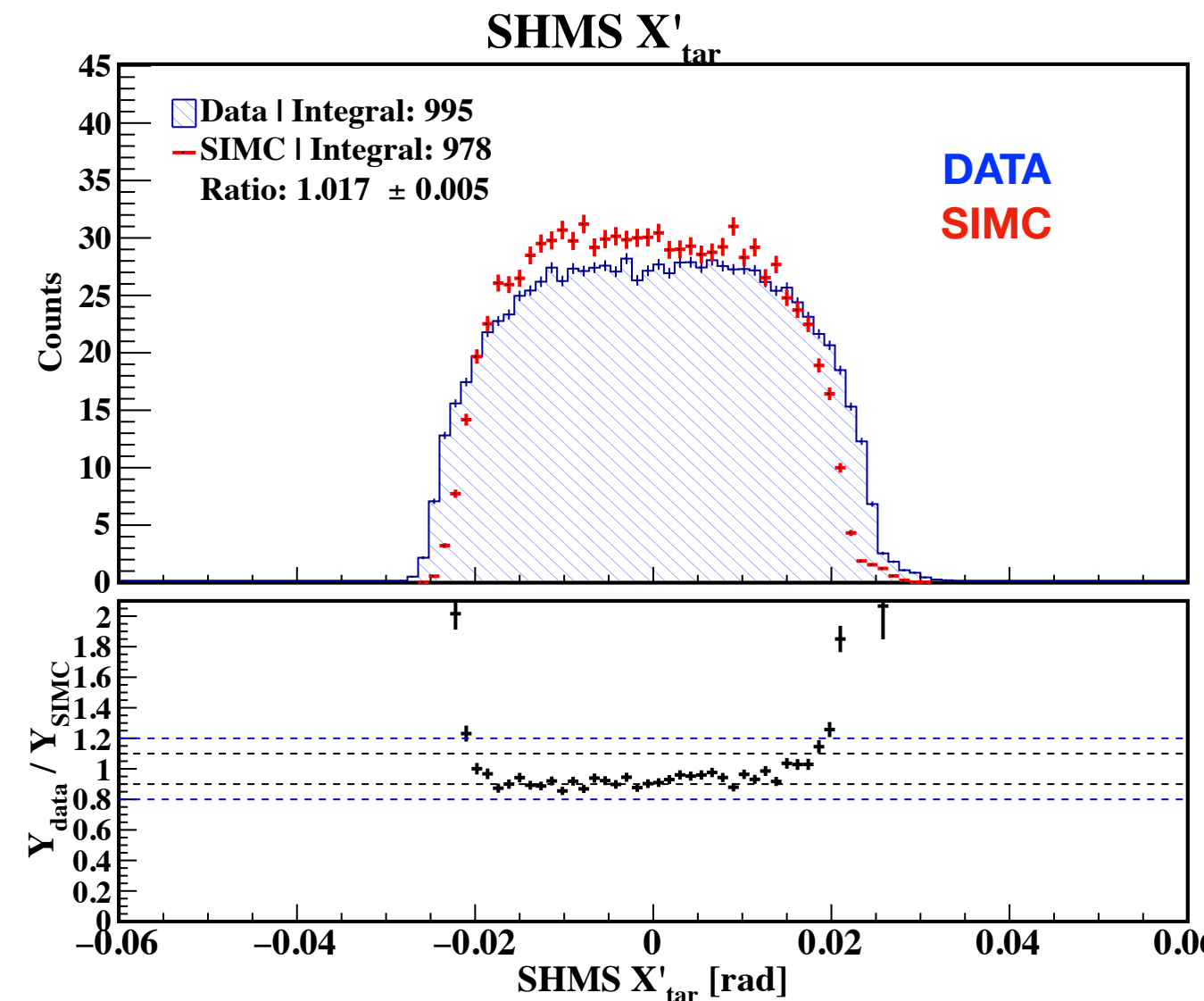


Spectrometer Acceptance DATA/SIMULATION

(used H(e,e'p) Elastics data taken on D(e,e'p)n Experiment)

SHMS Reconstructed Variables

**** Data is fully corrected for inefficiencies**

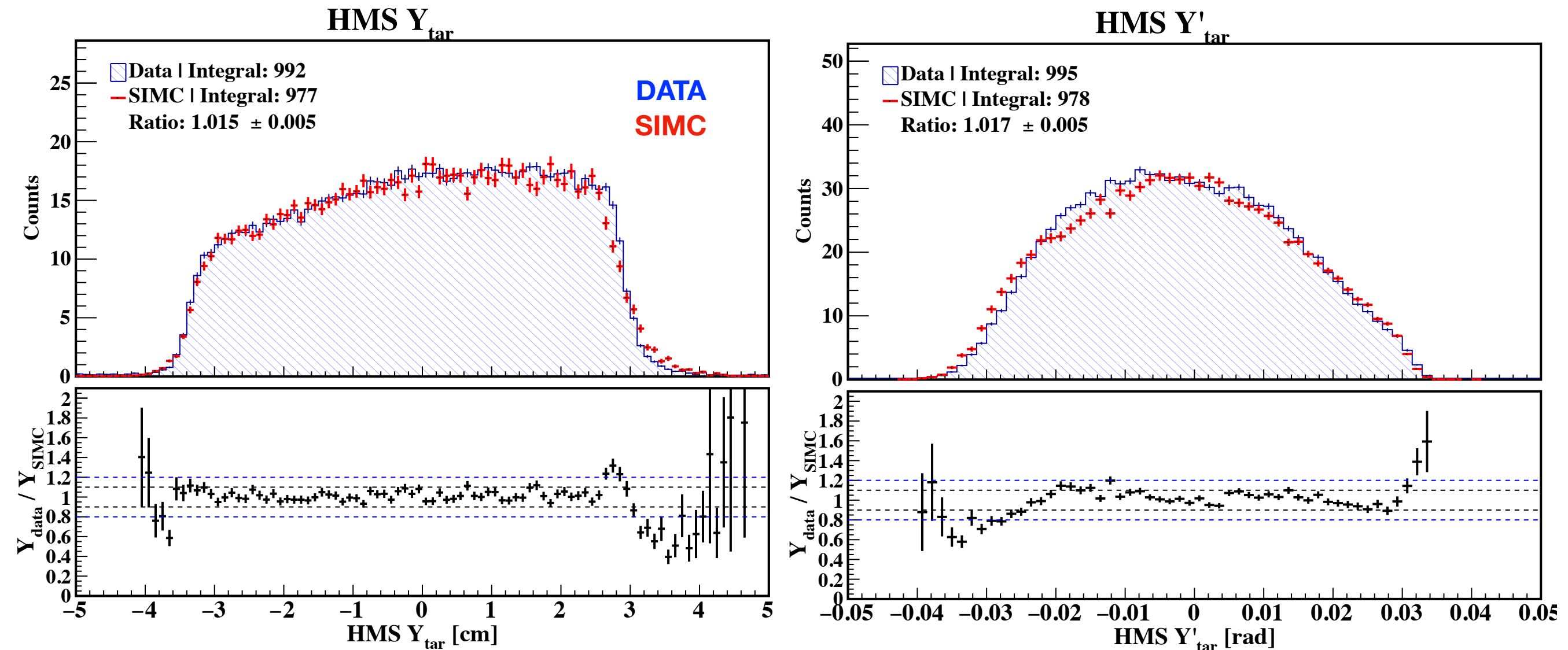


Spectrometer Acceptance DATA/SIMULATION

(used H(e,e'p) Elastics data taken on D(e,e'p)n Experiment

HMS Reconstructed Variables

**** Data is fully corrected for inefficiencies**

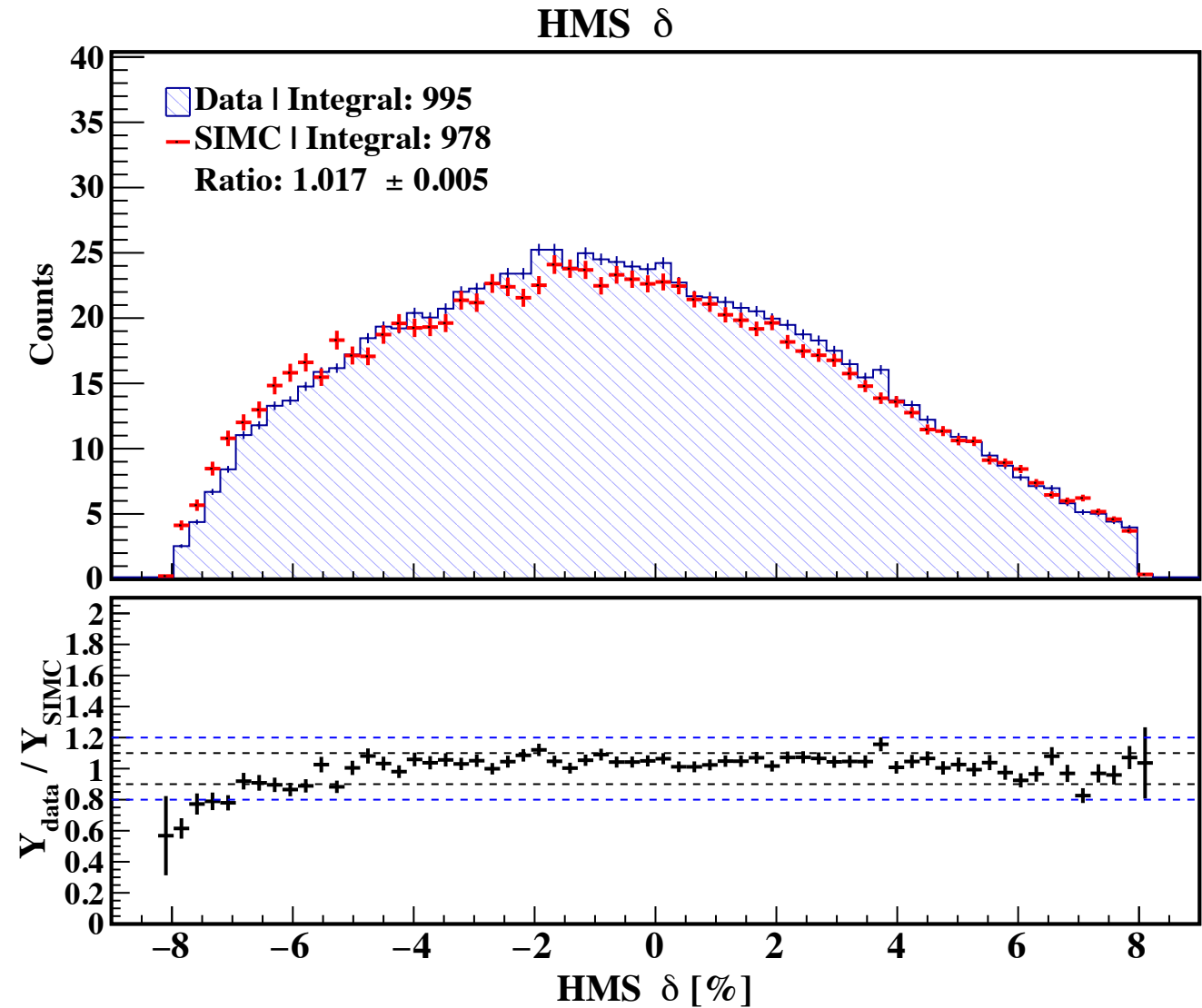
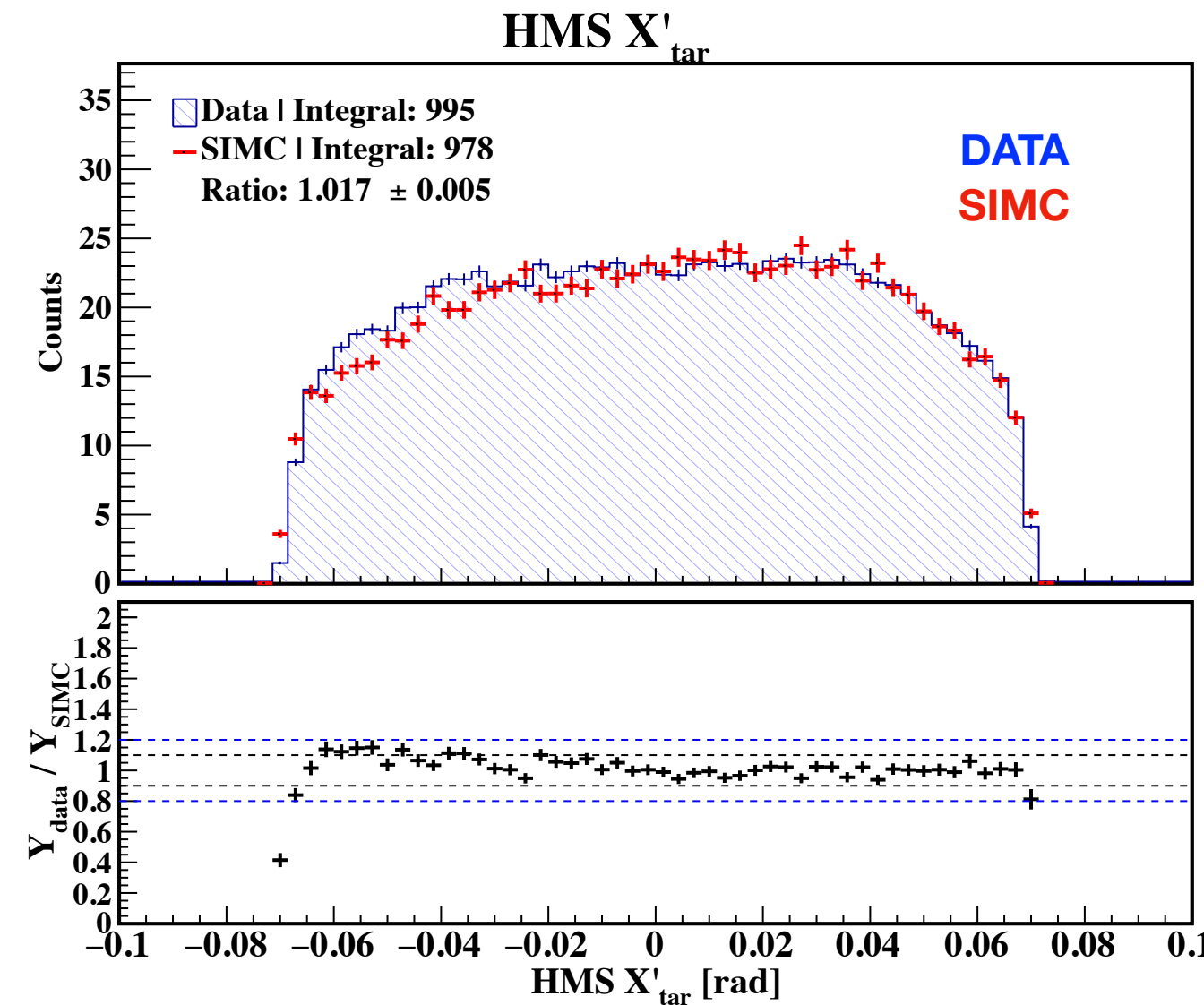


Spectrometer Acceptance DATA/SIMULATION

(used H(e,e'p) Elastics data taken on D(e,e'p)n Experiment

HMS Reconstructed Variables

**** Data is fully corrected for inefficiencies**

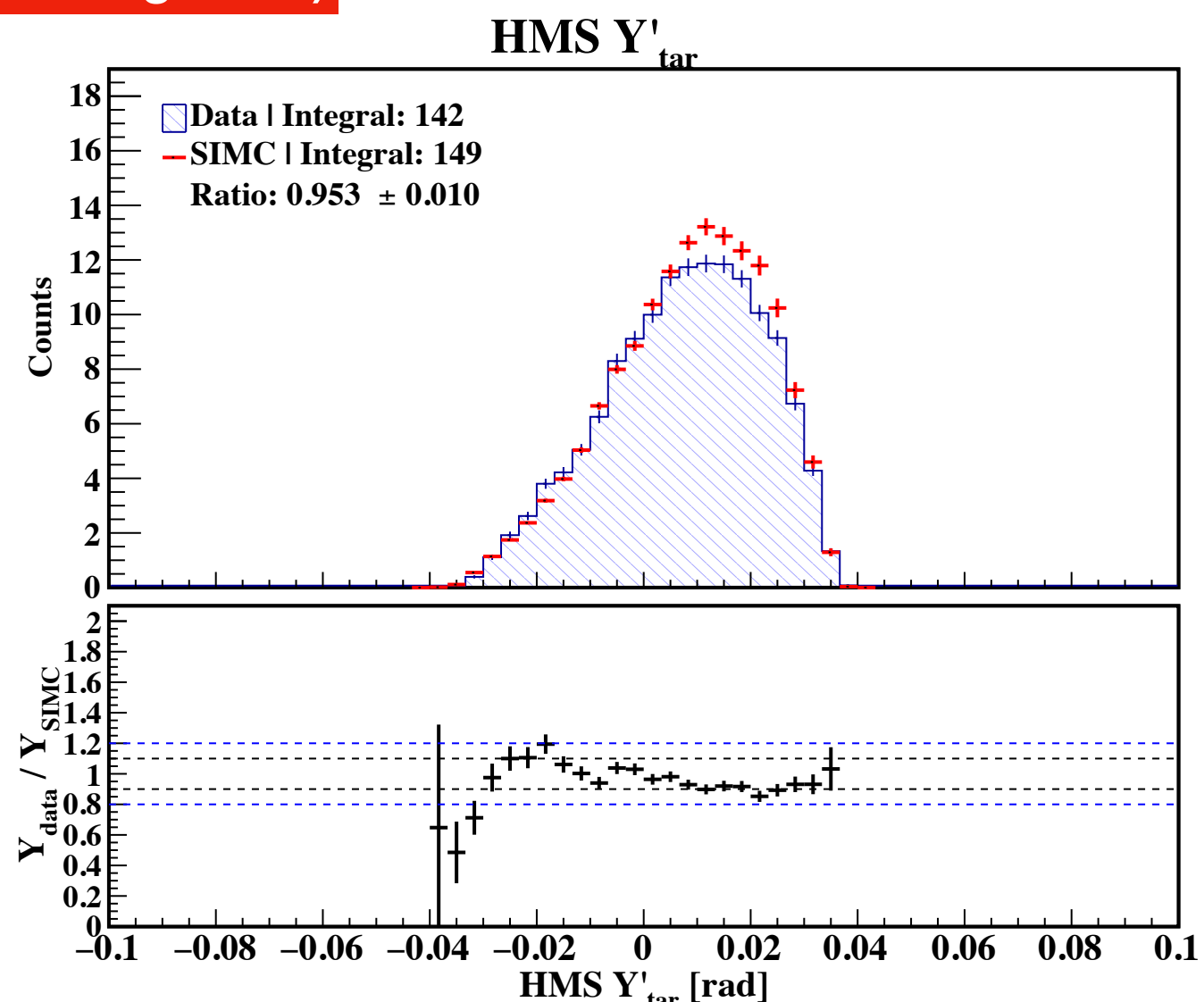
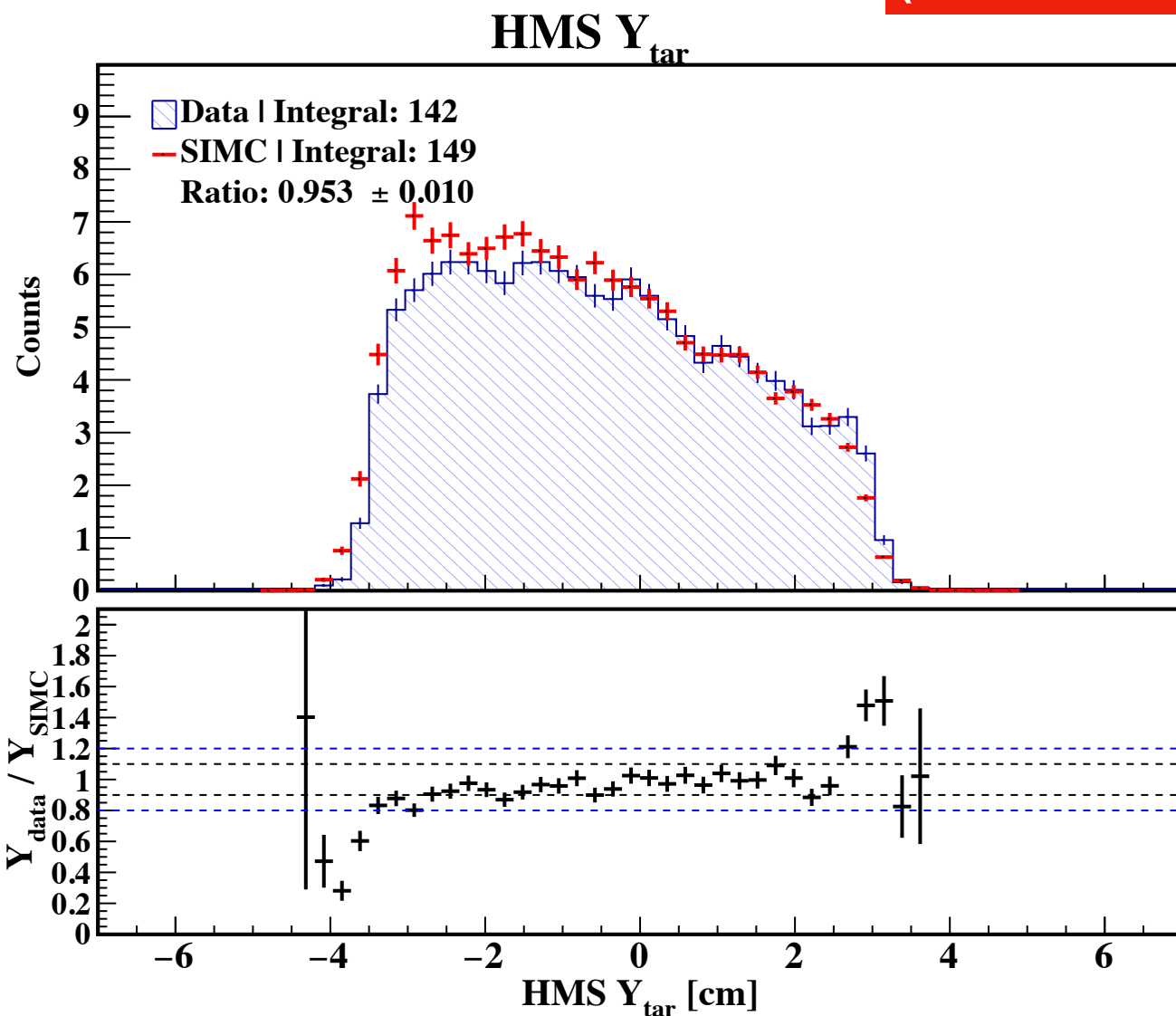


Spectrometer Acceptance Checks on $D(e,e'p)n$ using 80 MeV setting

HMS Reconstructed Variables

**** Data is fully corrected for inefficiencies**

(SIMC MODEL: Laget FSI)

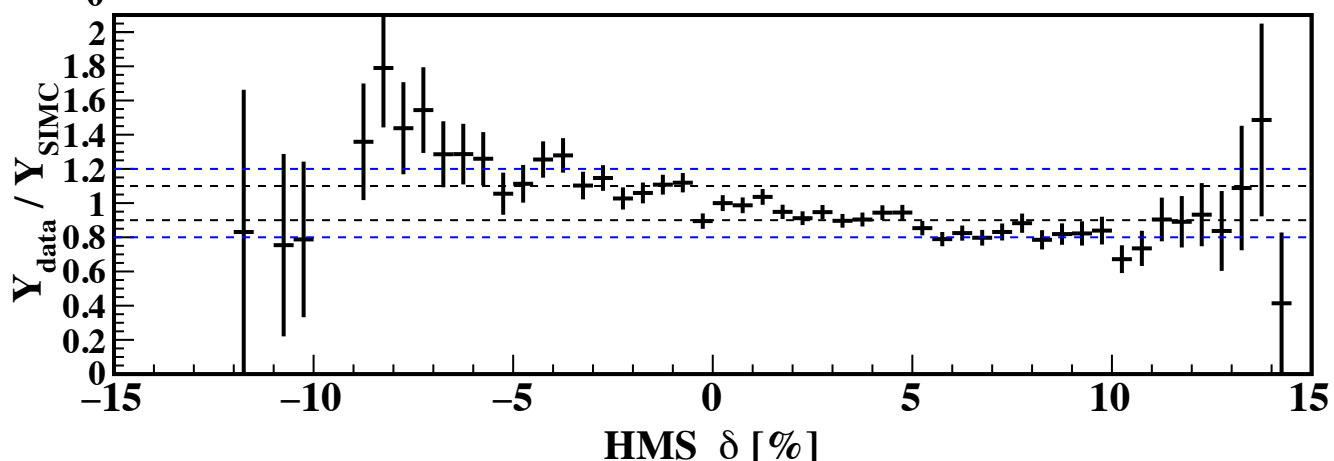
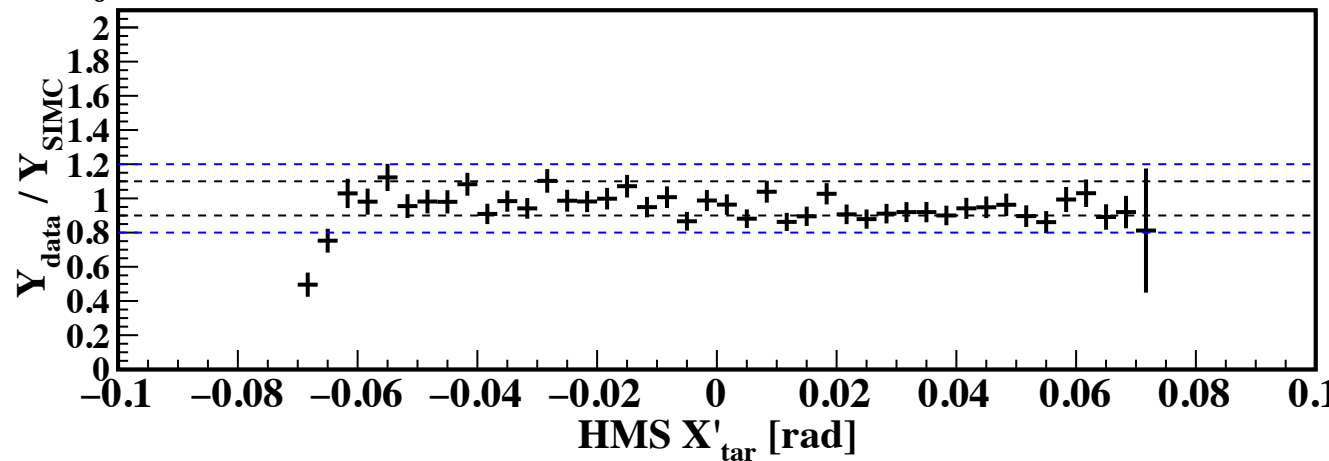
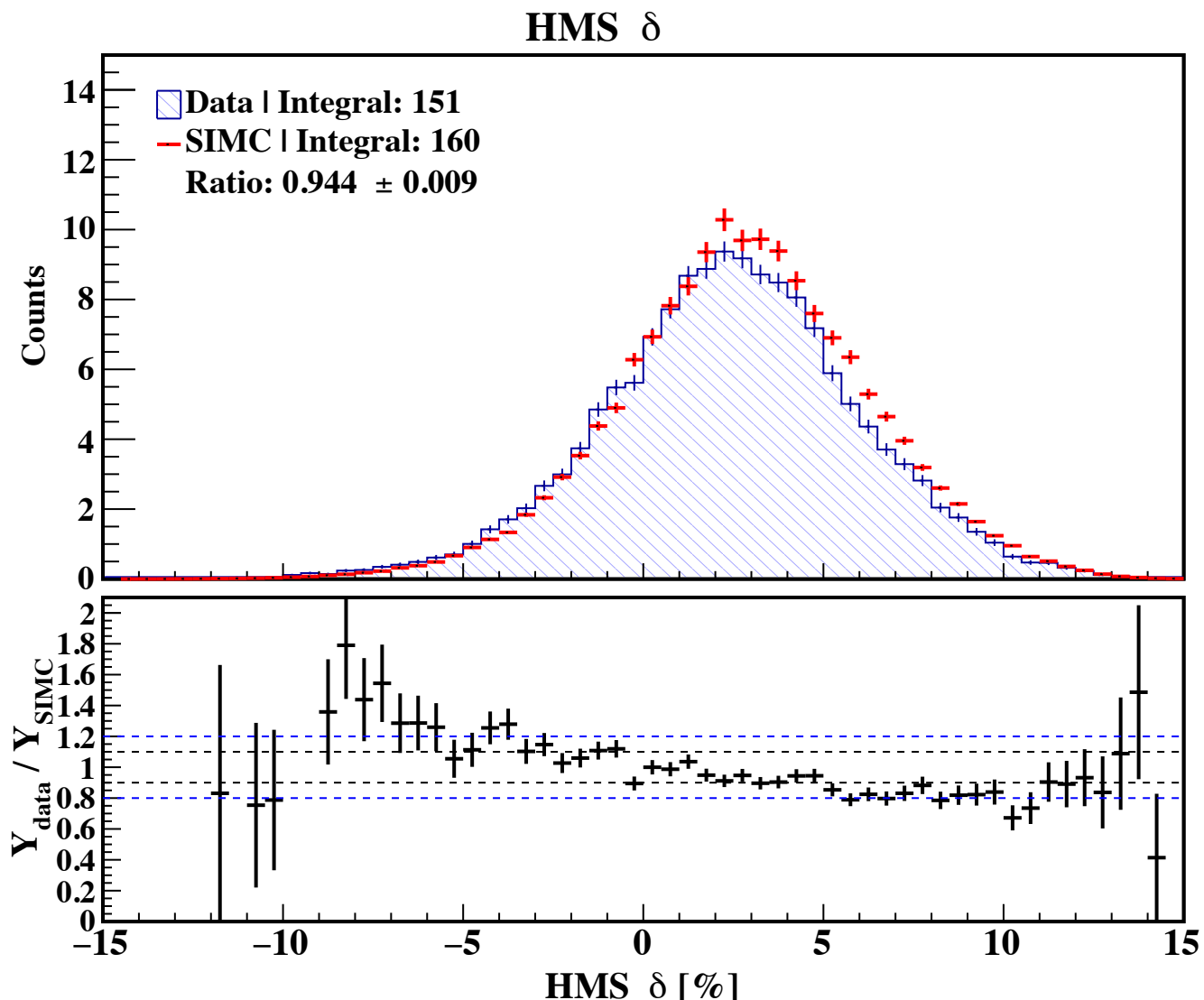
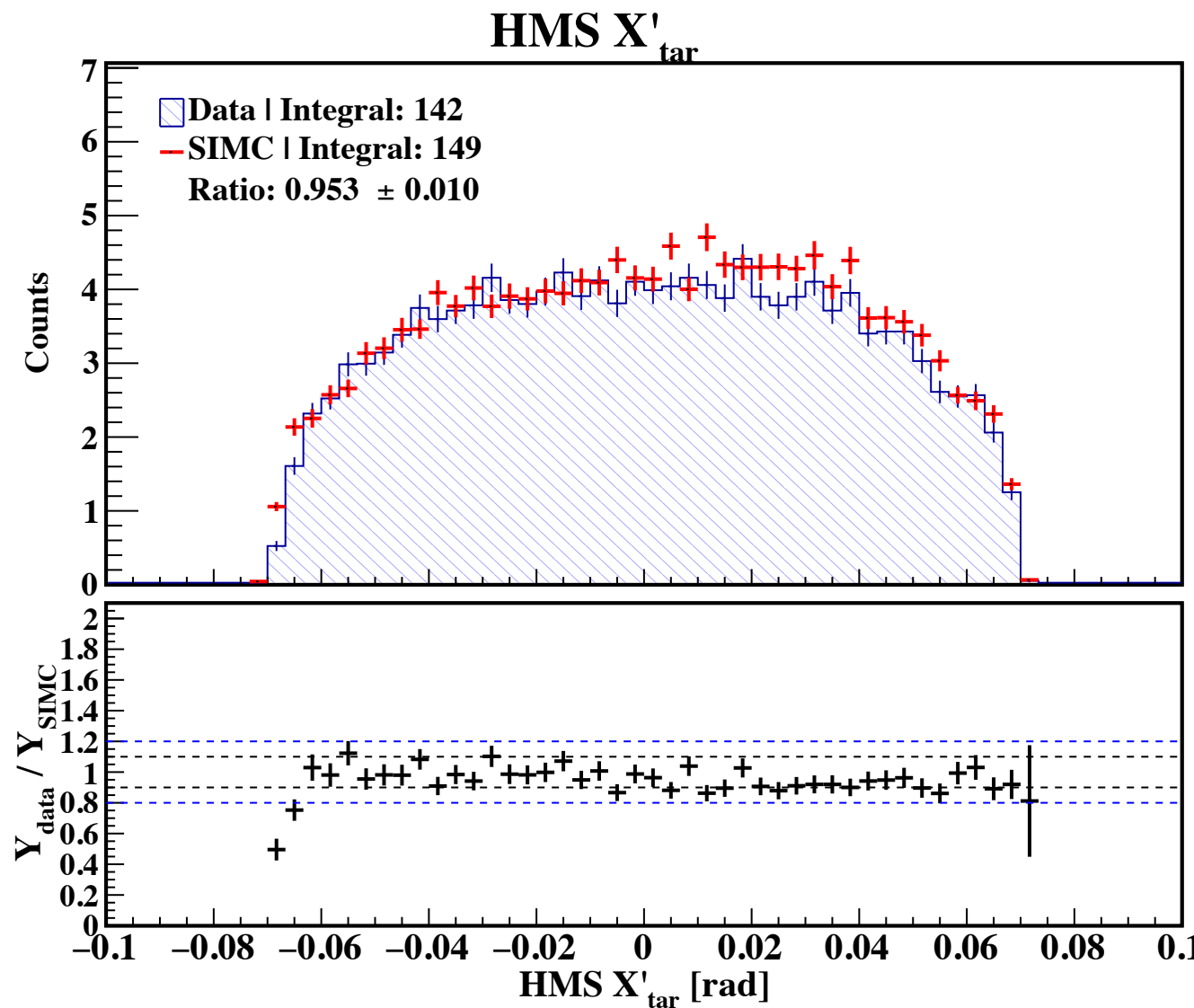


Spectrometer Acceptance Checks on $D(e,e'p)n$ using 80 MeV setting

HMS Reconstructed Variables

**** Data is fully corrected for inefficiencies**

(SIMC MODEL: Laget FSI)

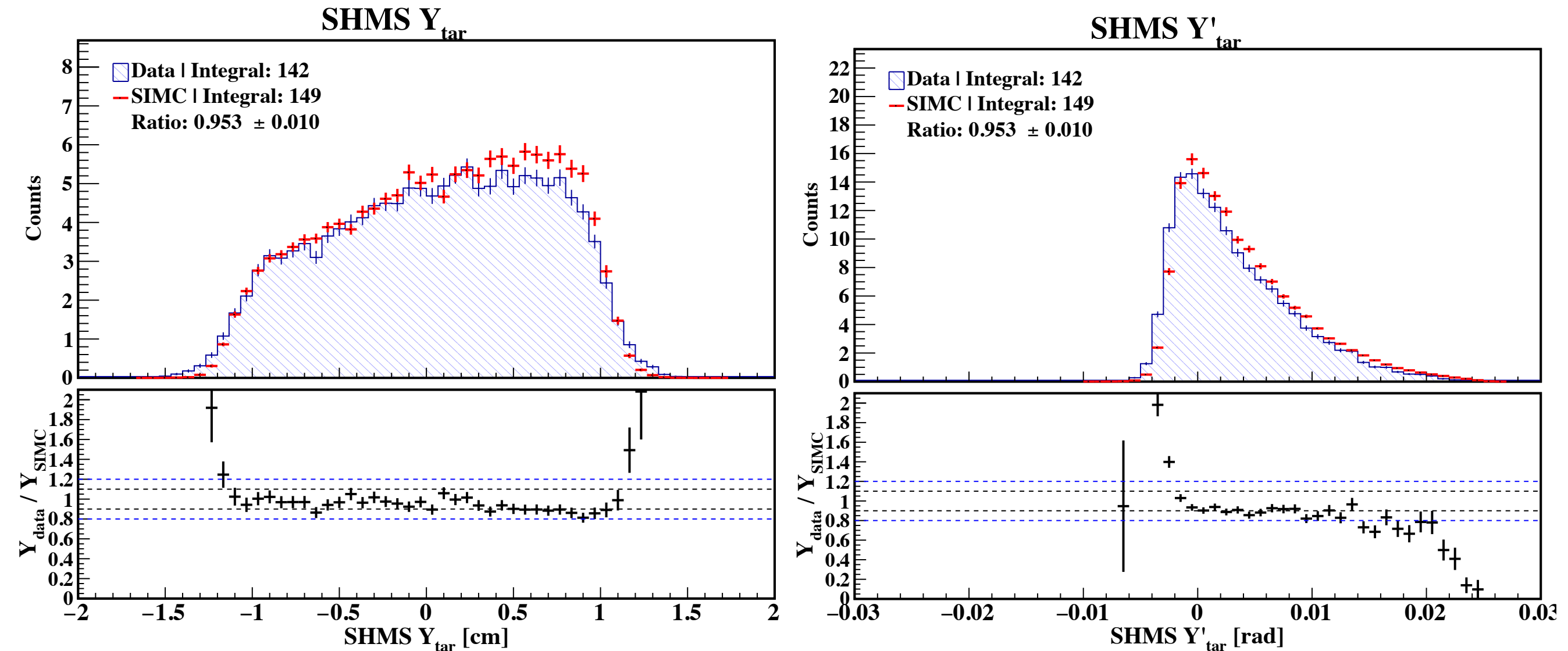


Spectrometer Acceptance Checks on $D(e,e'p)n$ using 80 MeV setting

SHMS Reconstructed Variables

**** Data is fully corrected for inefficiencies**

(SIMC MODEL: Laget FSI)

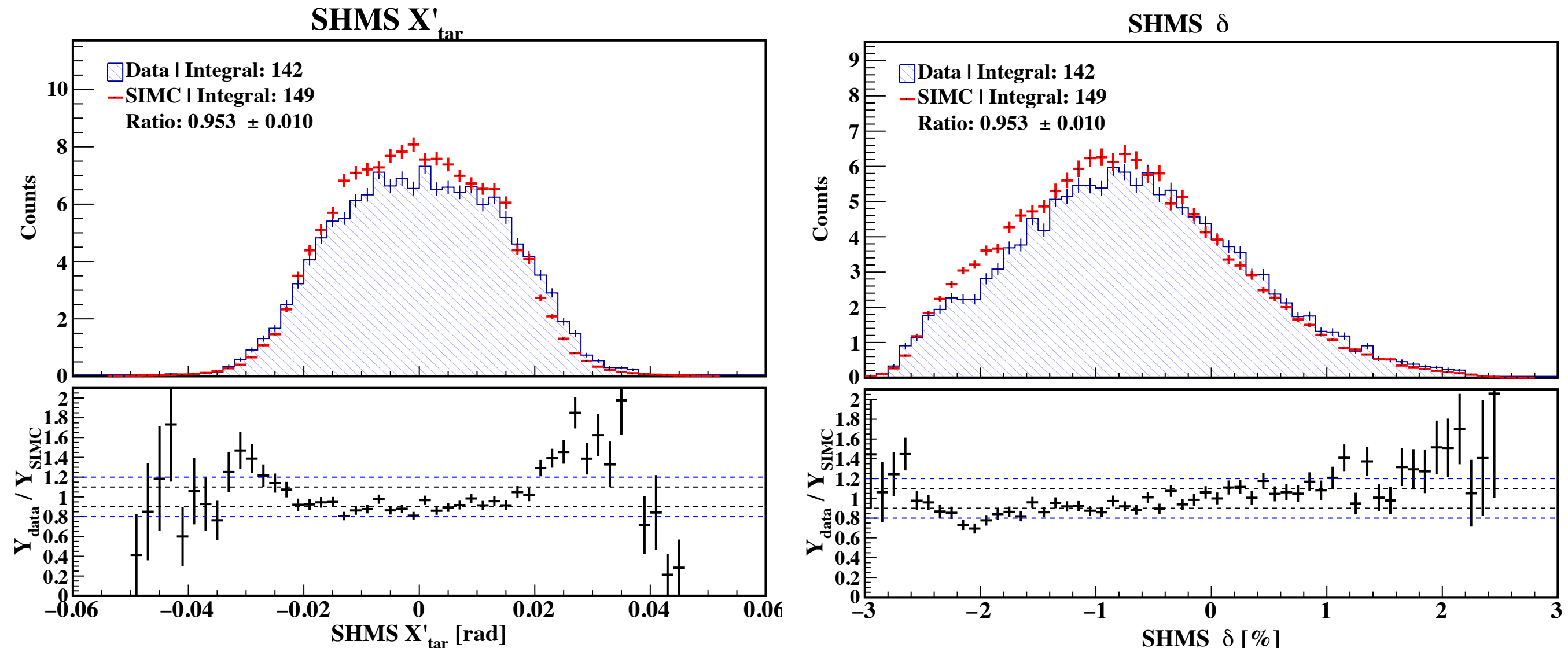


Spectrometer Acceptance Checks on $D(e,e'p)n$ using 80 MeV setting

SHMS Reconstructed Variables

**** Data is fully corrected for inefficiencies**

(SIMC MODEL: Laget FSI)

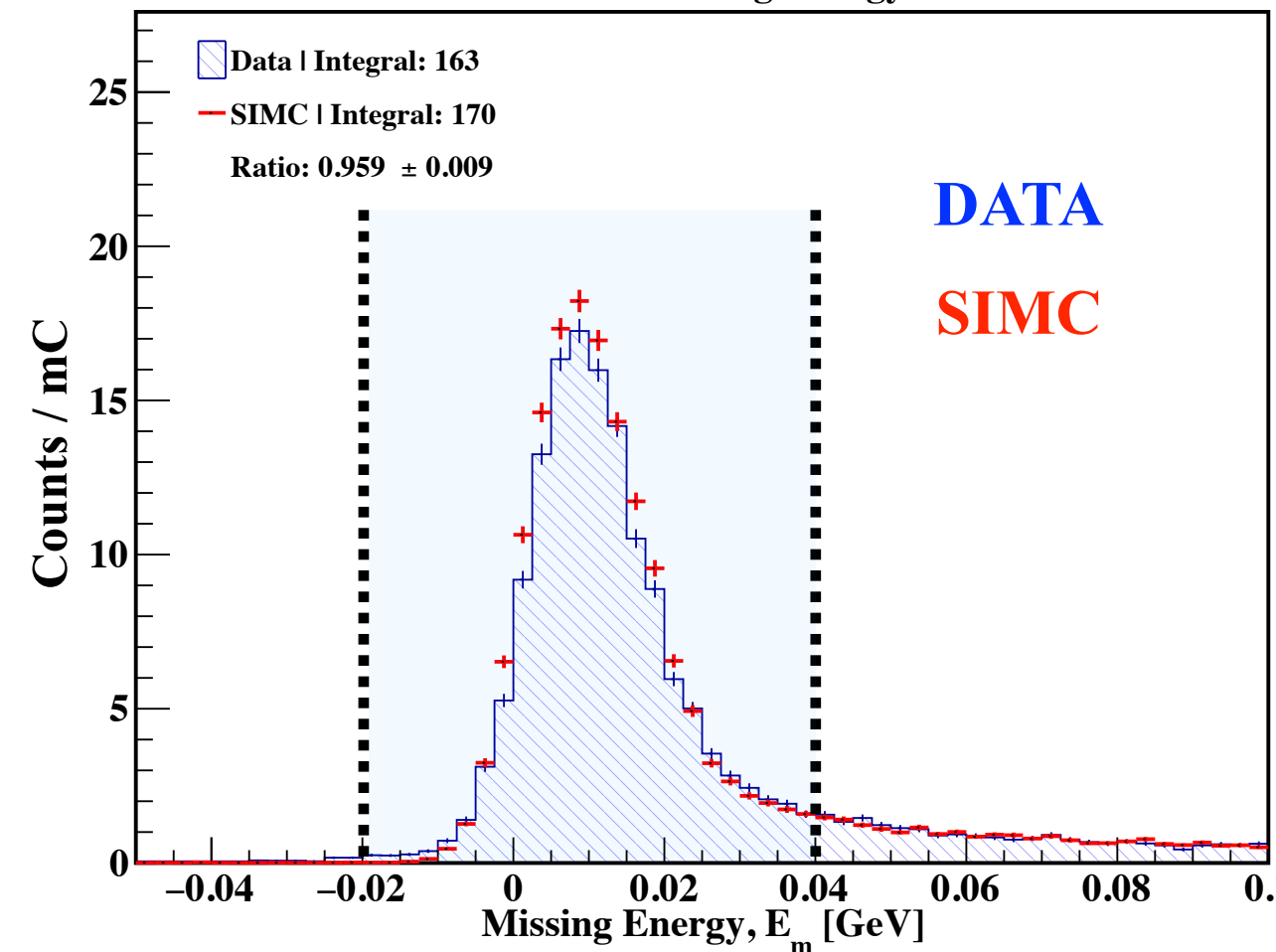


$D(e,e'p)n$

Data Analysis Cuts

(shown only for 80 MeV setting but are
also applied to high missing momentum data)

Nuclear Missing Energy



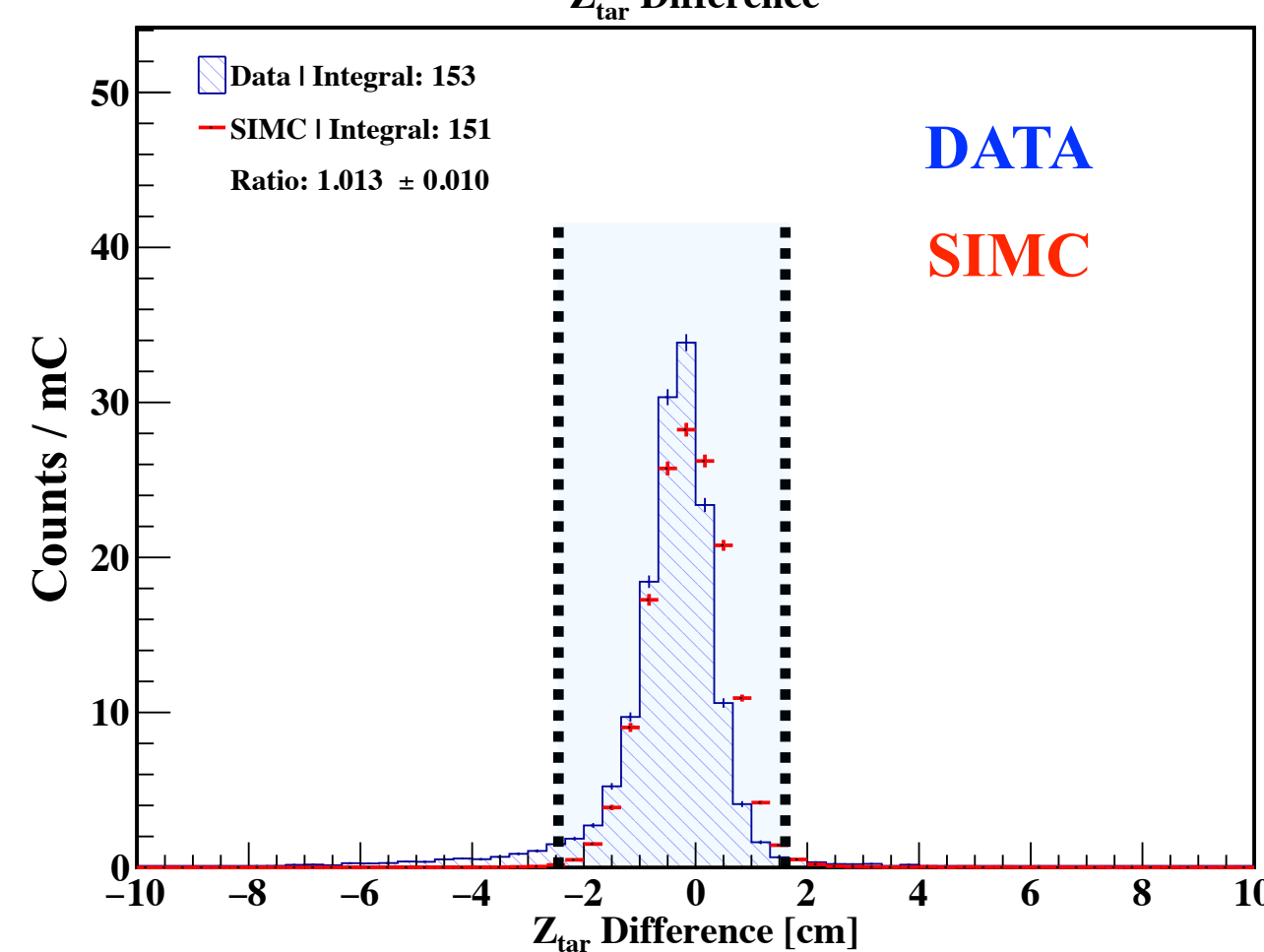
Missing Energy Cut: (-20, 40) MeV

Select true D(e,e'p)n events

$$E_m = \omega - T_p - T_r$$

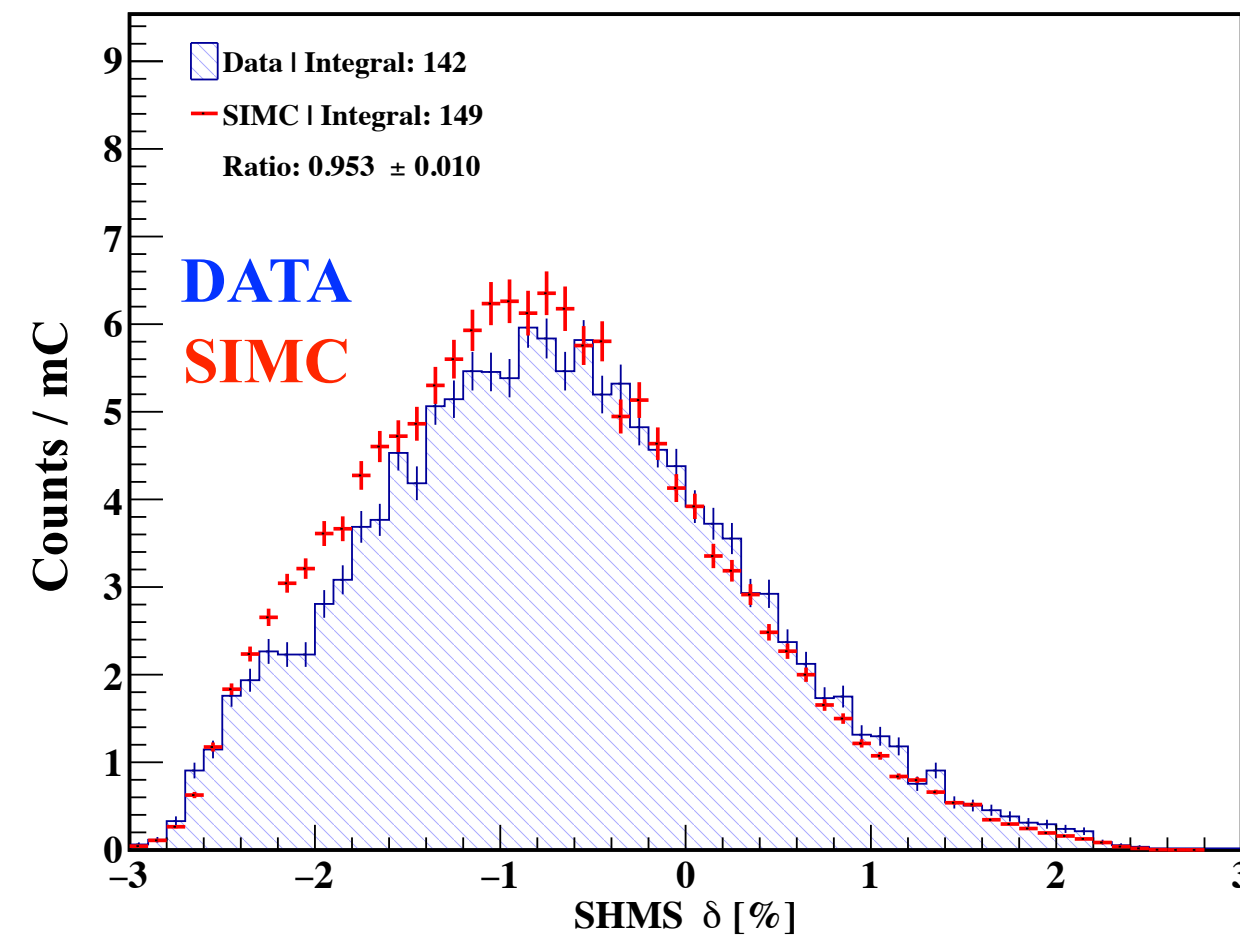
↑
Missing energy
is the B.E. of deuteron
(~2.22 MeV)

↑
Assume the mass
of the neutron



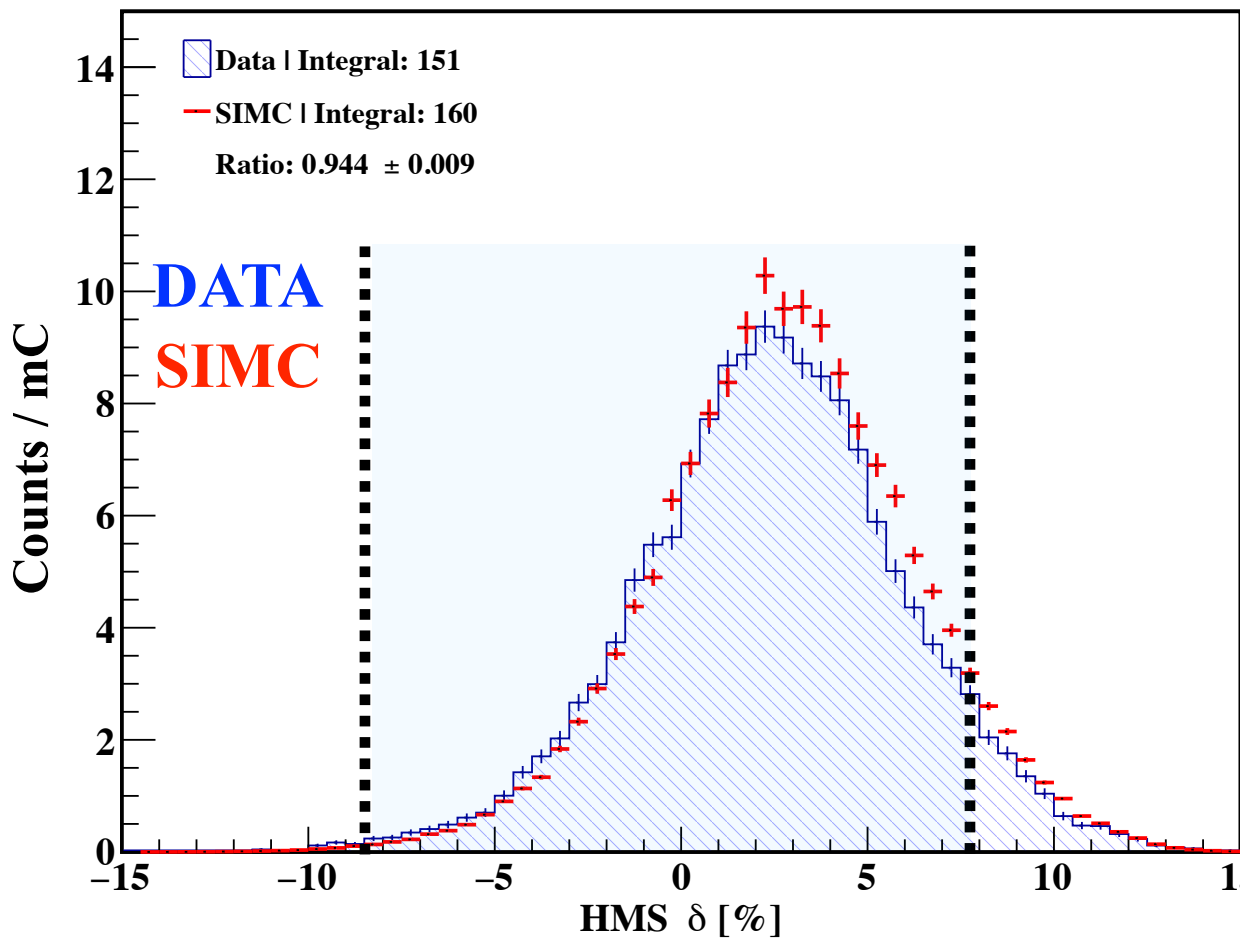
Reconstructed Z vertex difference Cut:
 ± 2 cm relative the peak value

require event Z-vertex position
to be the same for both HMS and SHMS to
select true coincidences and not
accidental events

SHMS δ 

SHMS Delta Acceptance (-3, 3) %

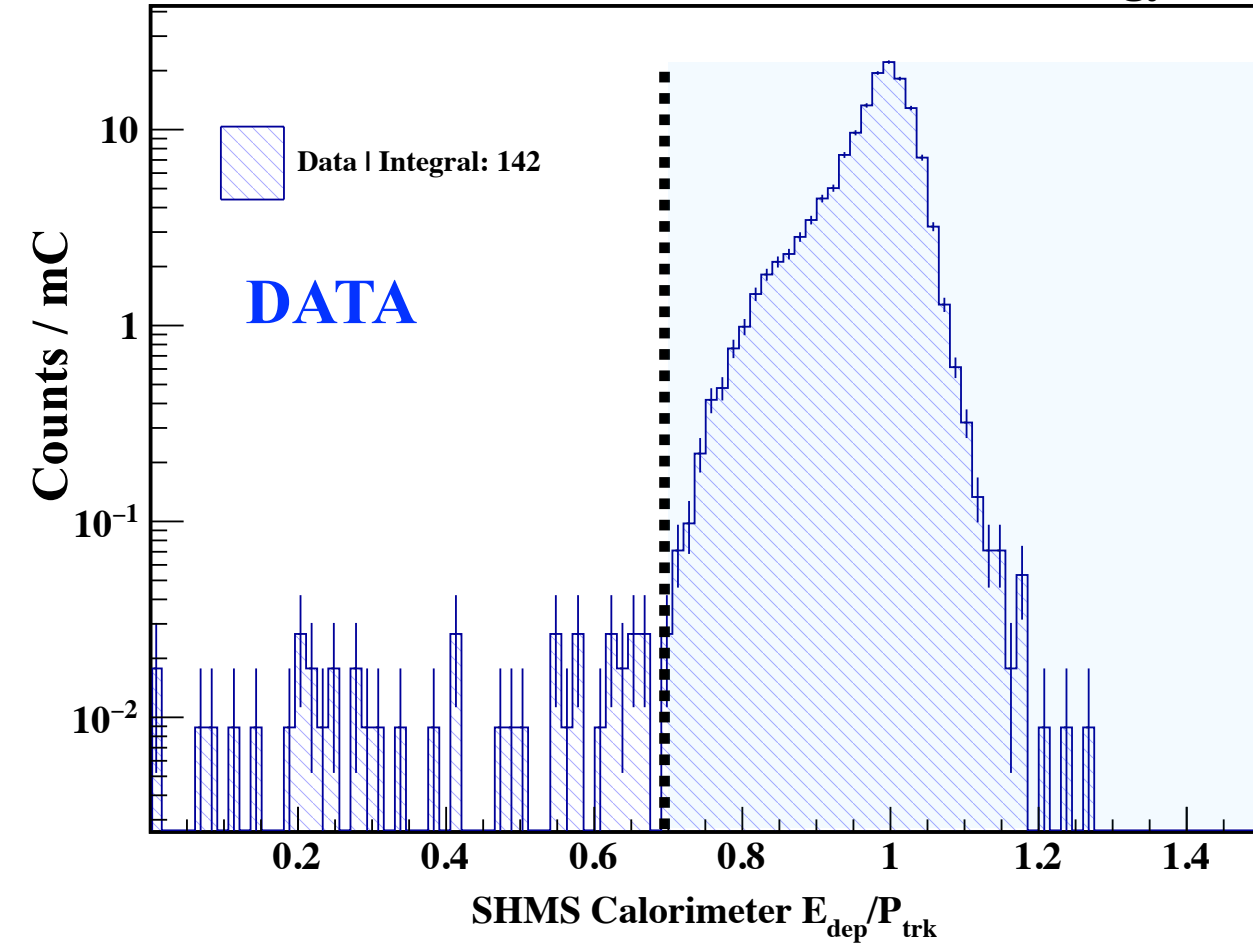
SHMS Delta Acceptance is constrained by the HMS Acceptance to be in the range (-3, 3)%

HMS δ 

HMS Delta Acceptance Cut: (-8, 8) %

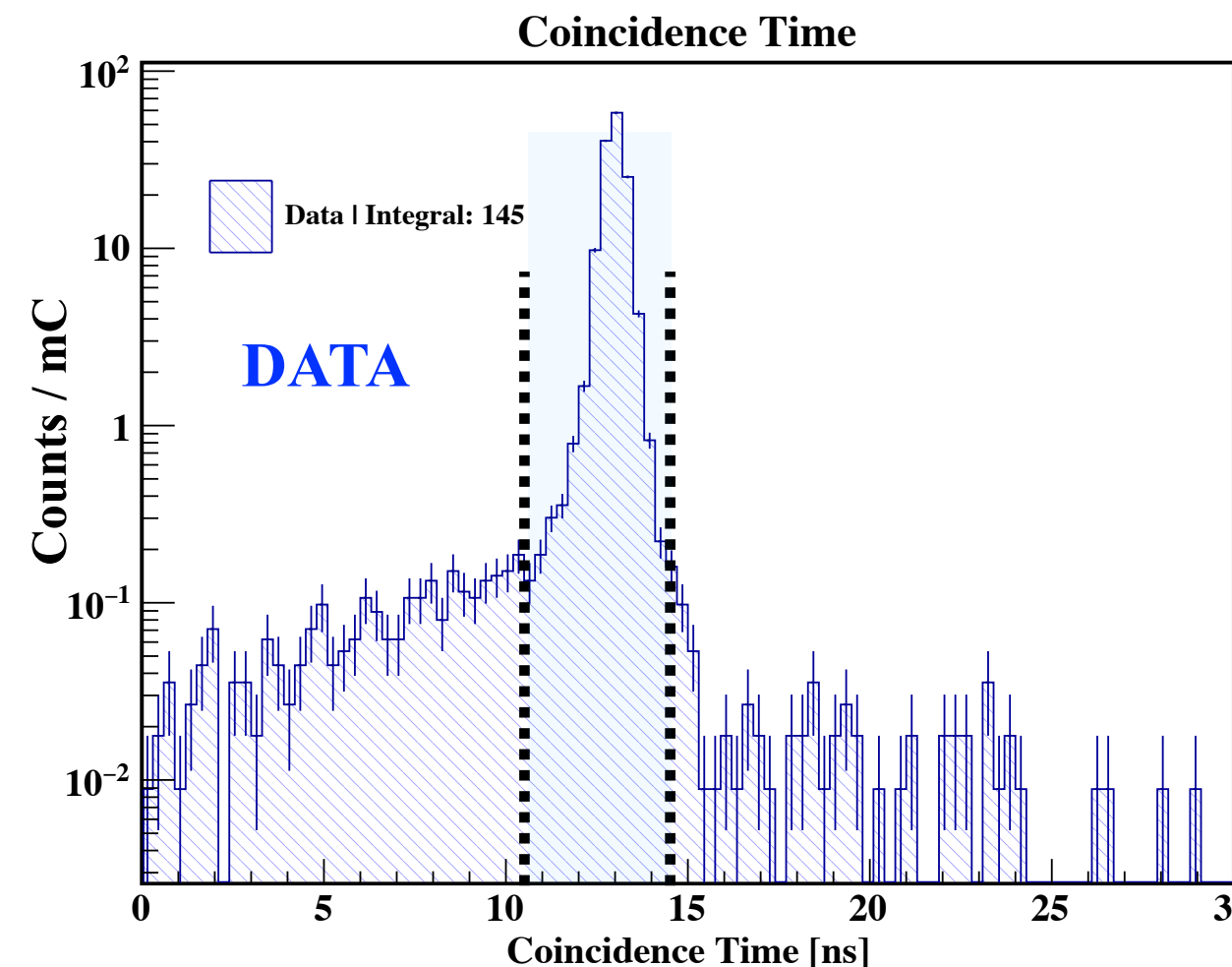
Select HMS acceptance region where Optics Reconstruction is reliable

SHMS Calorimeter Total Normalized Energy



**SHMS: Total energy deposited in
Calorimeter normalized by the best track
CUT: > 0.7**

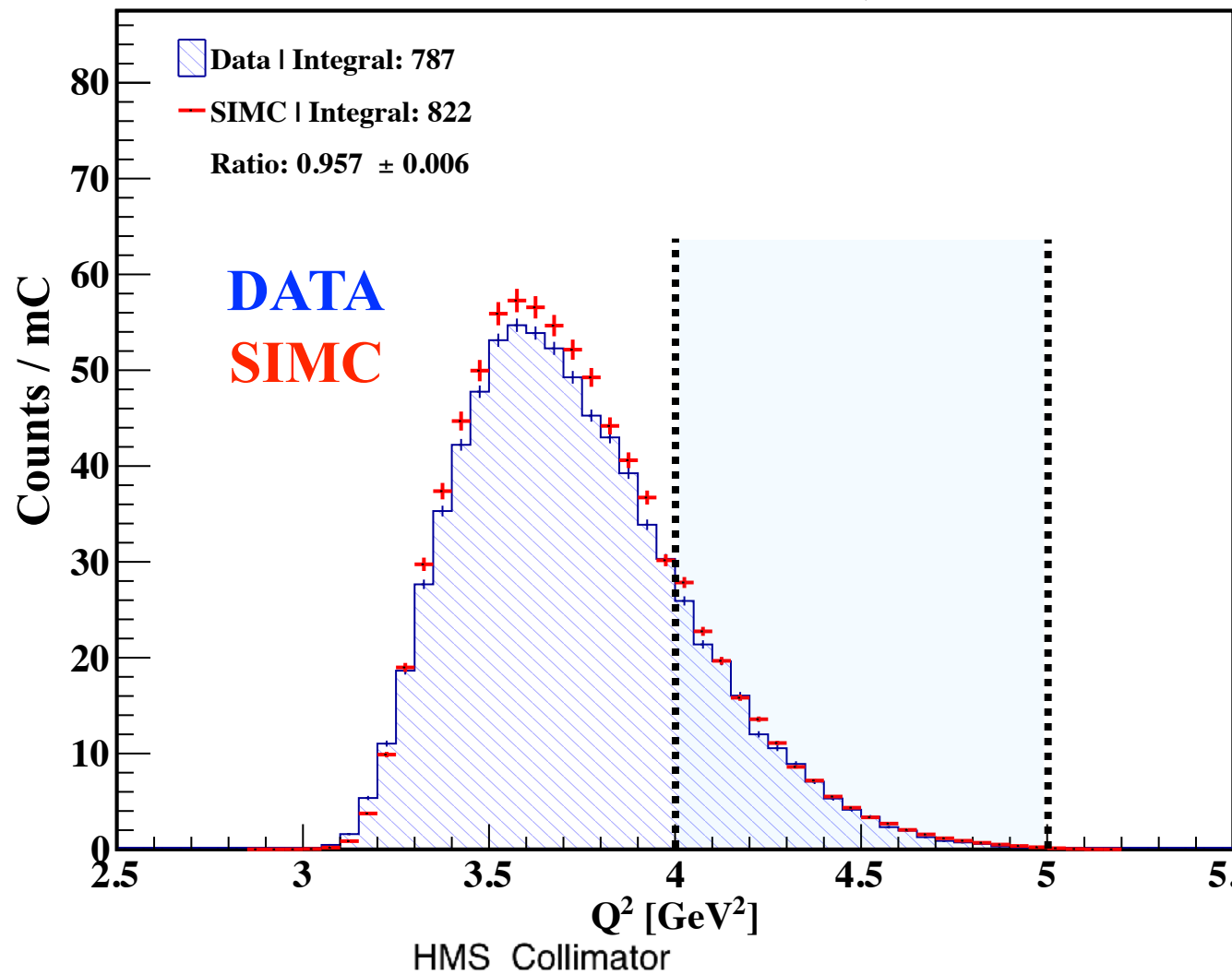
select true electrons in SHMS
and not pions (looks very clean!)



**Coincidence Time Cut
CUT: (10.5, 14.5) ns**

select true electron-proton coincidences

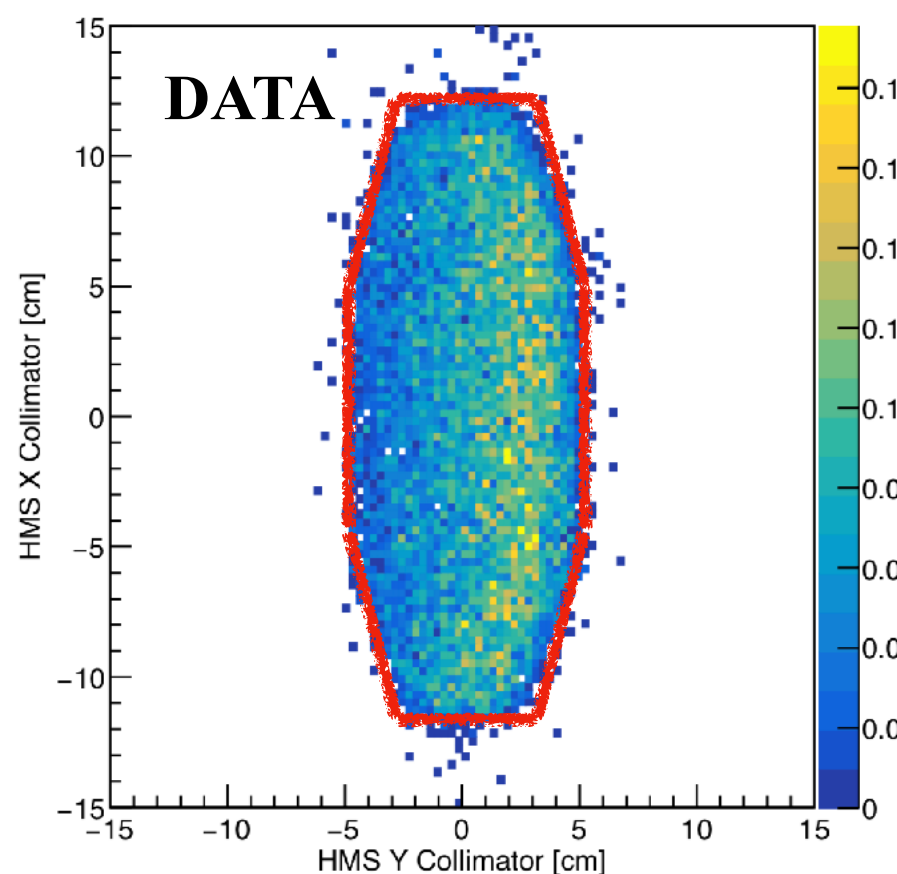
4-Momentum Transfer, Q^2



4-Momentum Transfer Cut

CUT: $Q^2 = 4.5 \pm 0.5$ GeV 2

Kinematics cut to select only events with high momentum transfer (as stated on the proposal)



HMS Collimator Cut
(Geometrical cut on collimator dimensions)

Select events that passed through collimator and NOT scattered at the edges of the collimator

Extraction of the D(e,e'p)n Cross Section

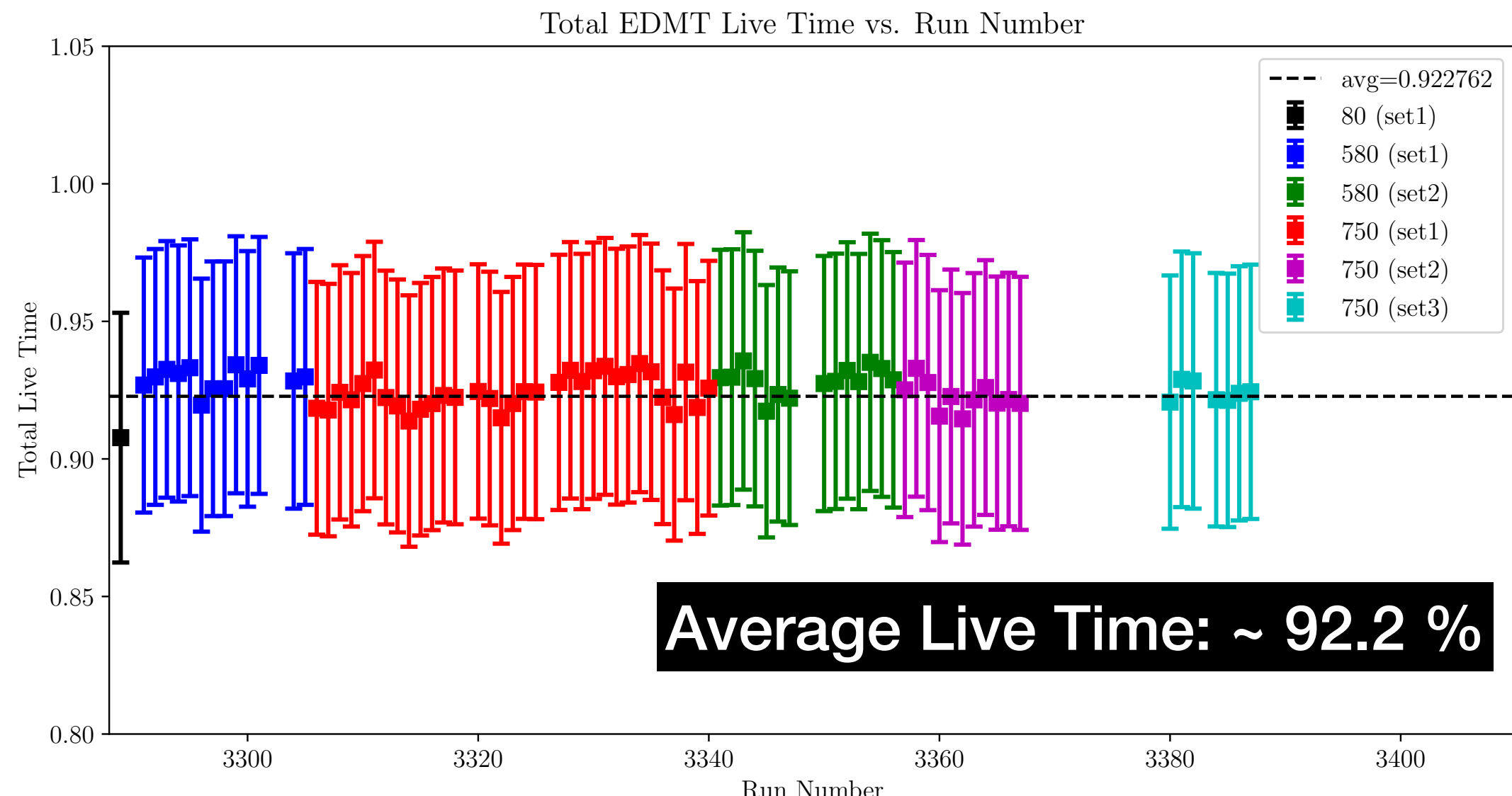
Efficiencies and Correction Factors Determination

$$Y_{data}^{corr} = \frac{Y_{data}^{uncorr} \cdot f_{rad} \cdot f_{bc}}{Q \cdot \epsilon_{tLT} \cdot \epsilon_{htrk} \cdot \epsilon_{etrk} \cdot \epsilon_{tgtBoil} \cdot \epsilon_{pAbs}}$$

$$Y_{data}^{corr} = \frac{Y_{data}^{uncorr} \cdot f_{rad}}{Q \cdot \epsilon_{tLT} \cdot \epsilon_{htrk} \cdot \epsilon_{etrk} \cdot \epsilon_{tgtBoil} \cdot \epsilon_{pAbs}}$$

Correct for total Data Acquisition (DAQ) dead time

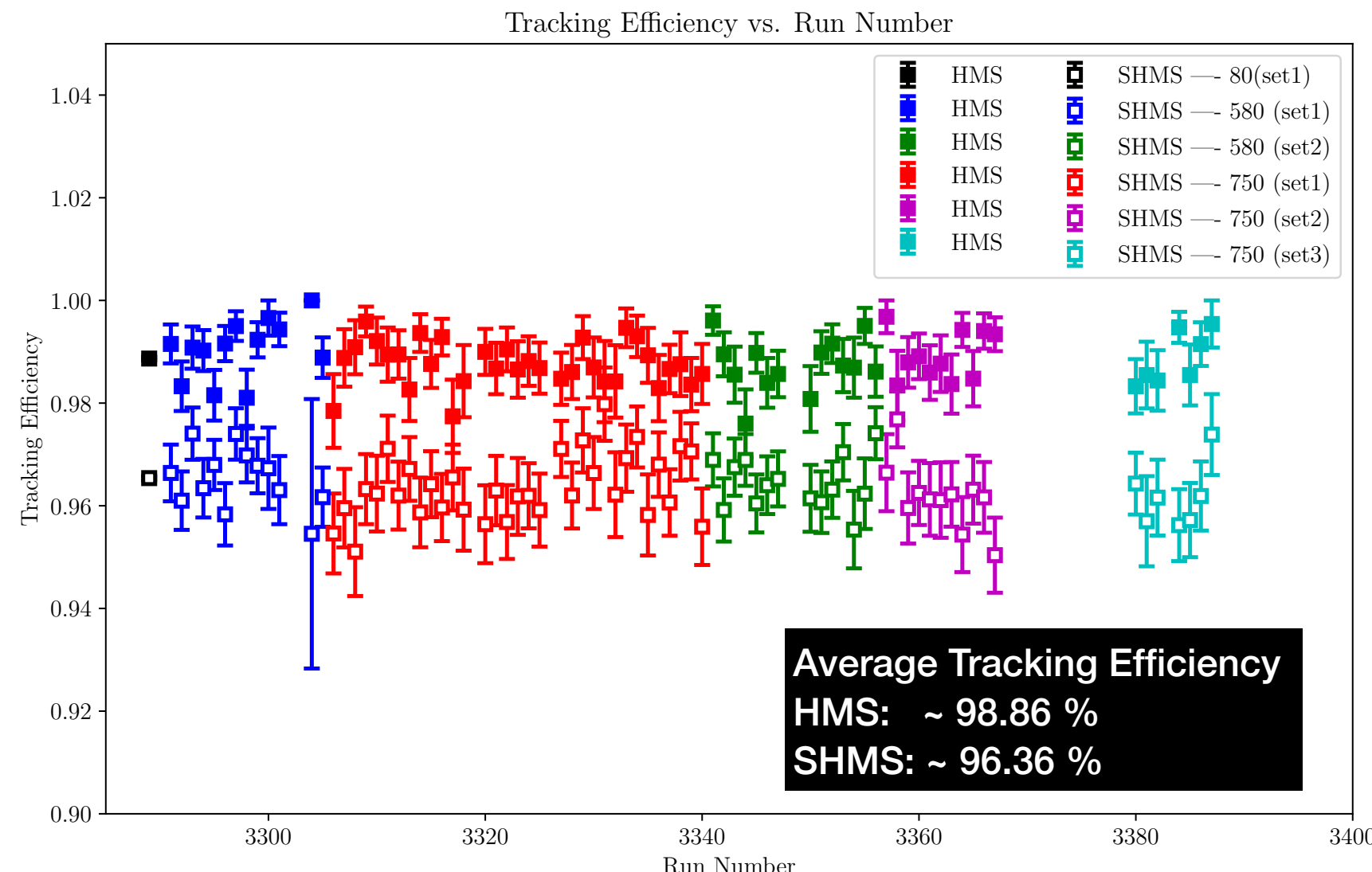
- Time that the DAQ is unable to register/process triggers results in event loss which must be accounted for



$$Y_{data}^{corr} = \frac{Y_{data}^{uncorr} \cdot f_{rad}}{Q \cdot \epsilon_{tLT} \cdot \epsilon_{htrk} \cdot \epsilon_{etrk} \cdot \epsilon_{tgtBoil} \cdot \epsilon_{pAbs}}$$

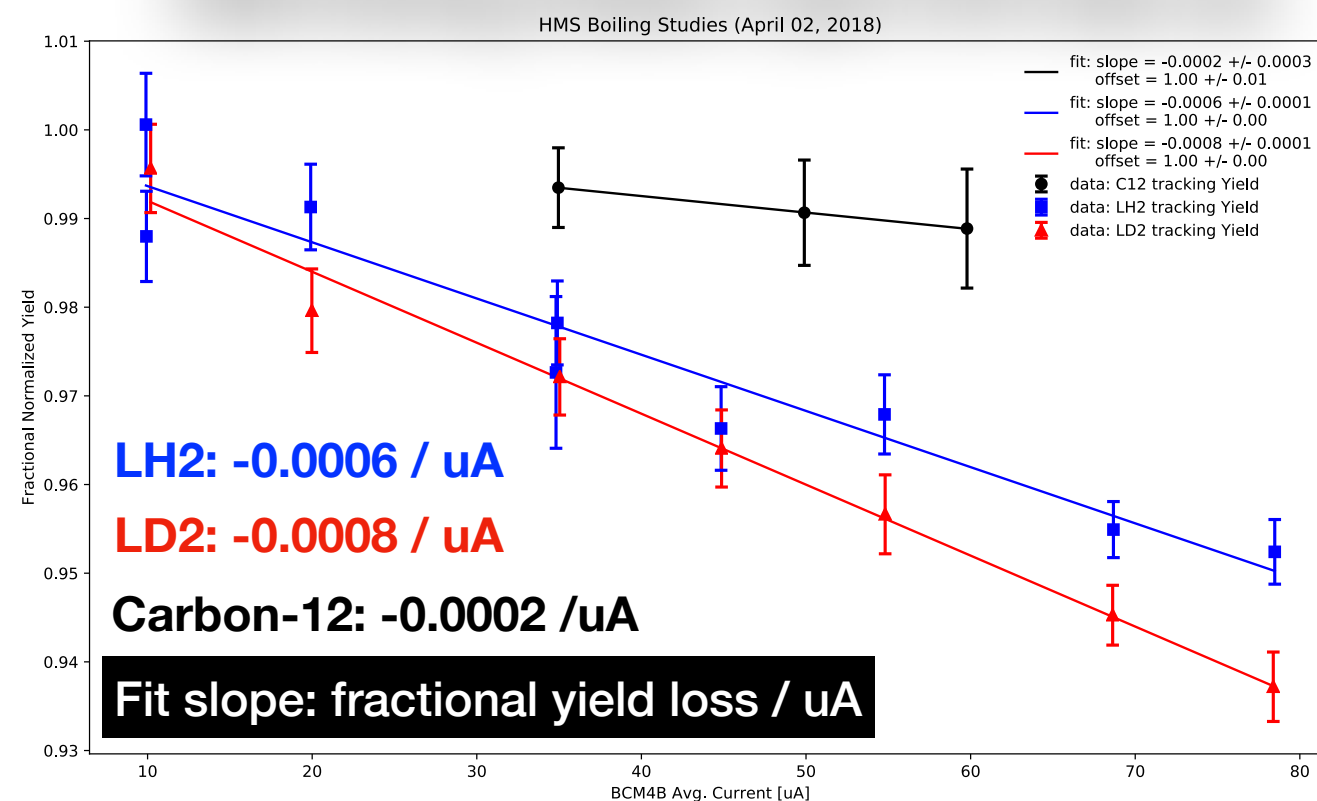
Correct for inefficiency due to tracking reconstruction

- Account for potential lost tracks due to bad track reconstruction by the tracking algorithm

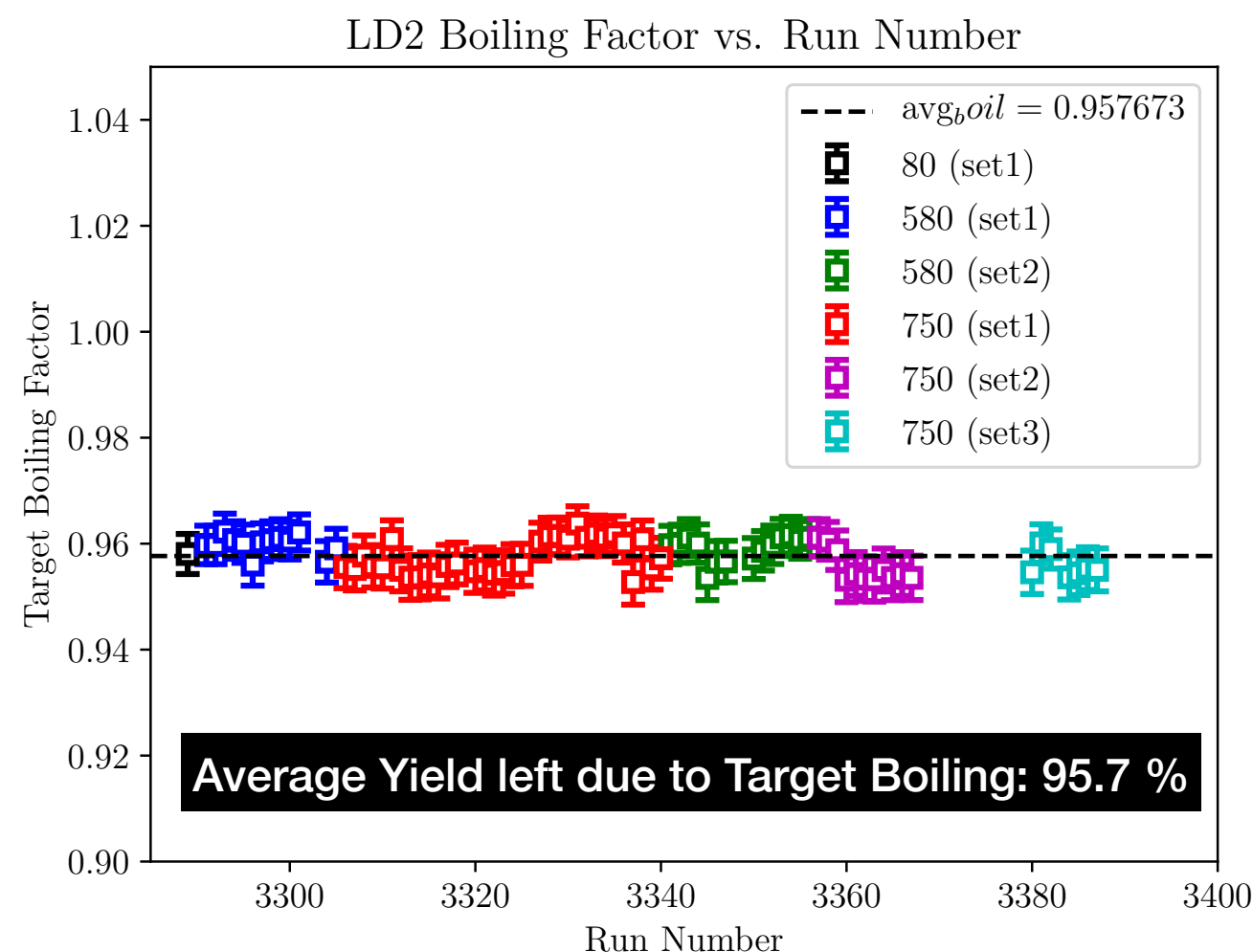


$$Y_{data}^{corr} = \frac{Y_{data}^{uncorr} \cdot f_{rad}}{Q \cdot \epsilon_{tLT} \cdot \epsilon_{htrk} \cdot \epsilon_{etrk} \cdot \epsilon_{tgtBoil} \cdot \epsilon_{pAbs}}$$

HMS Boiling Studies (April 2018 data set)



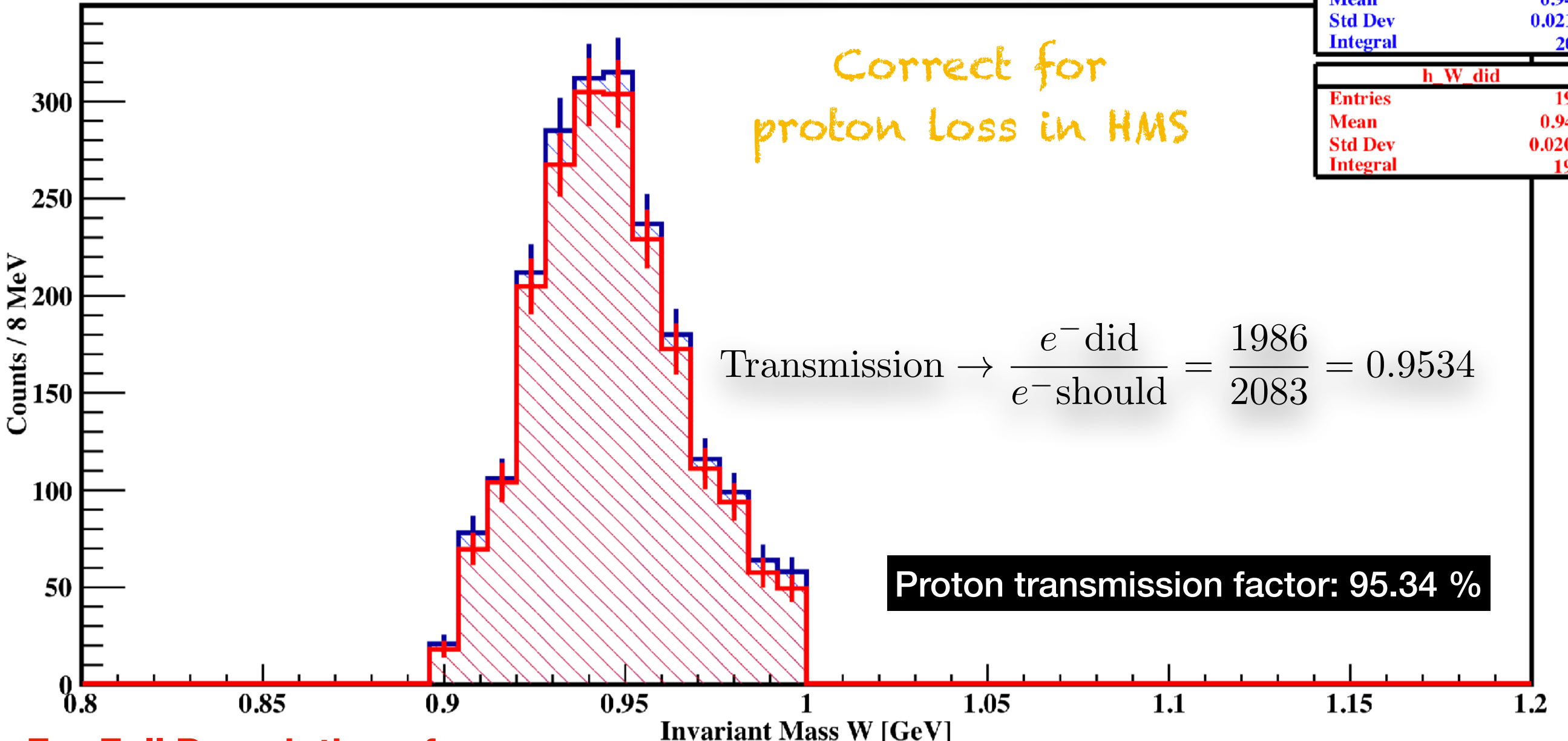
Correct for yield loss due
to target boiling



Target Boiling Corrections
See DOC DB Link HERE !

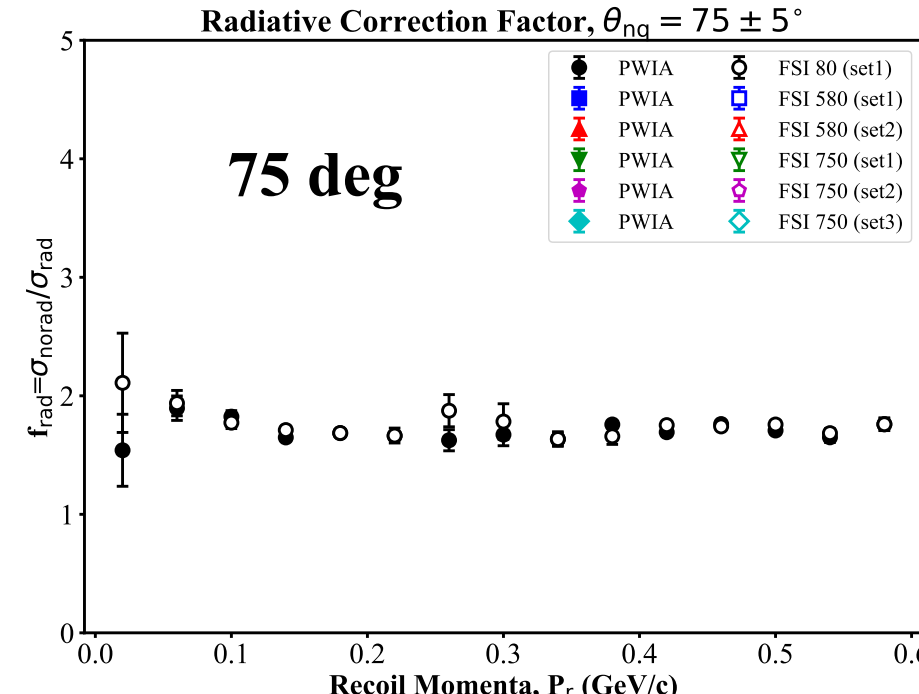
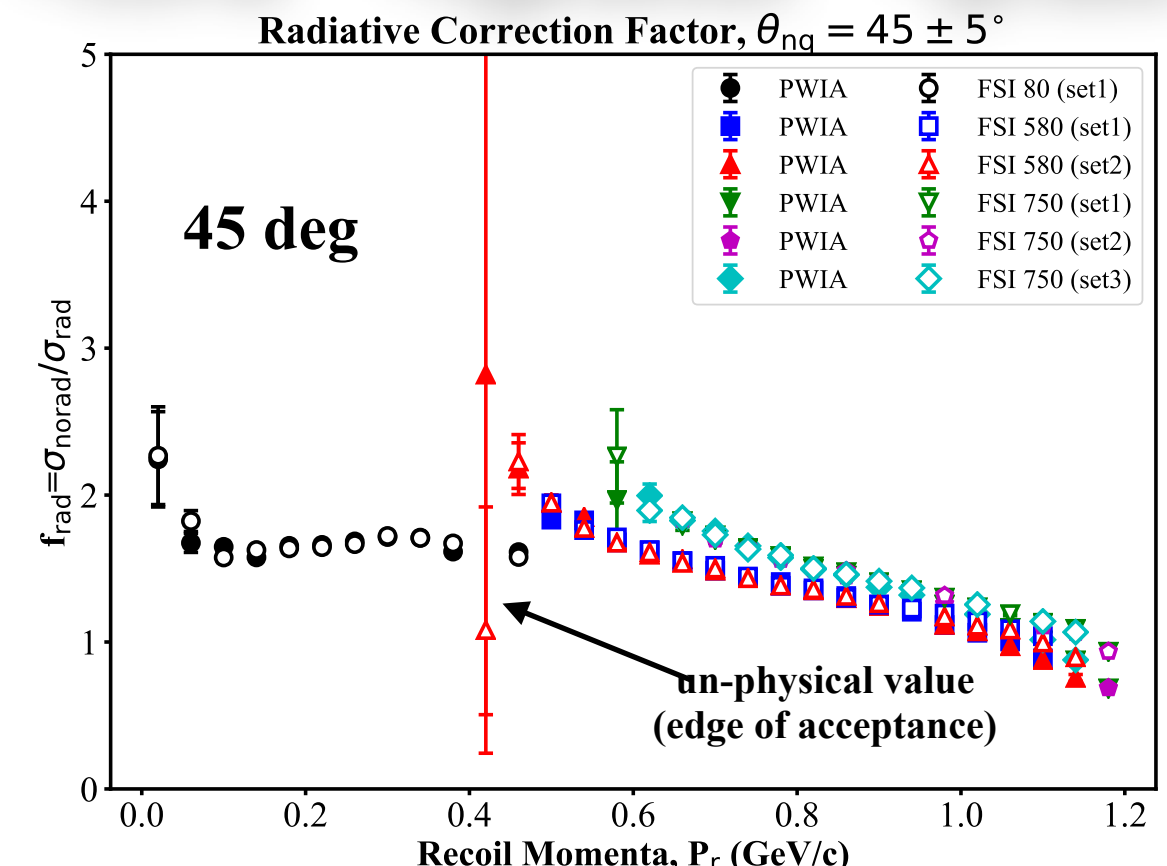
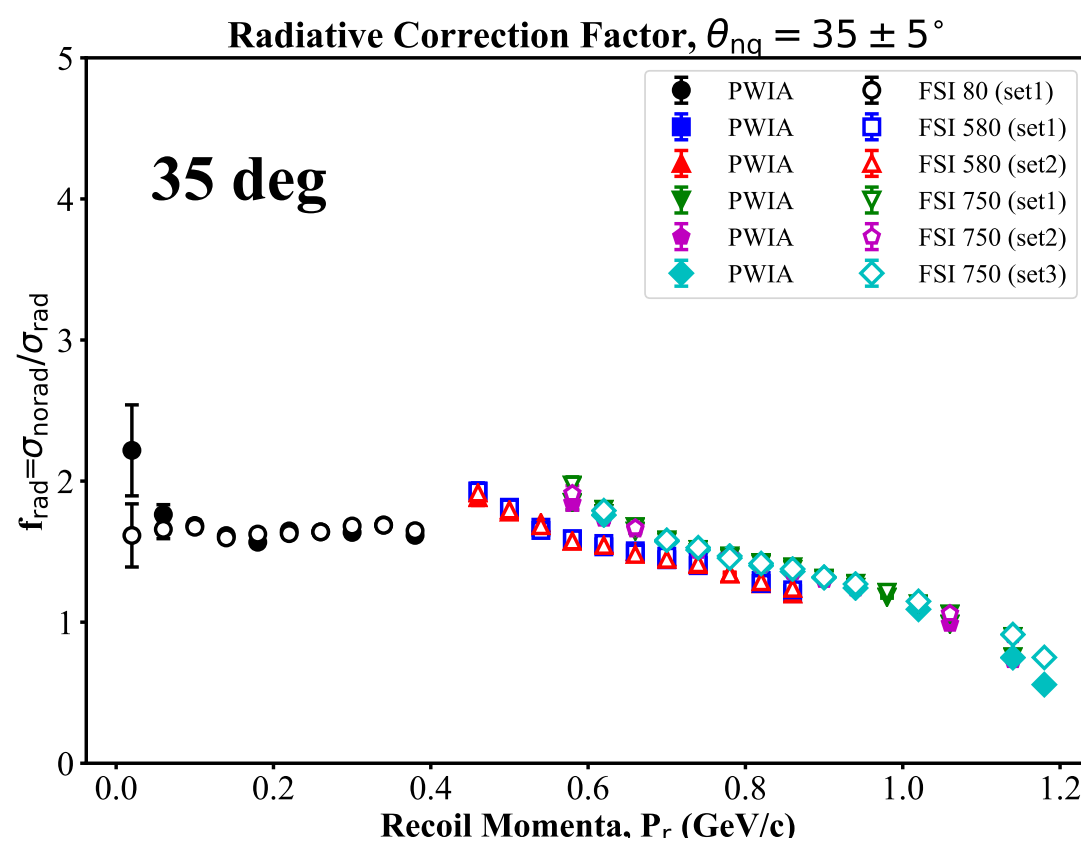
$$Y_{data}^{corr} = \frac{Y_{data}^{uncorr} \cdot f_{rad}}{Q \cdot \epsilon_{tLT} \cdot \epsilon_{htrk} \cdot \epsilon_{etrk} \cdot \epsilon_{tgtBoil} \cdot \epsilon_{pAbs}}$$

Proton Absorption = $4.66 \pm 0.472\%$



For Full Description of
Proton Absorption Analysis,
See DOC DB Link [HERE](#) !

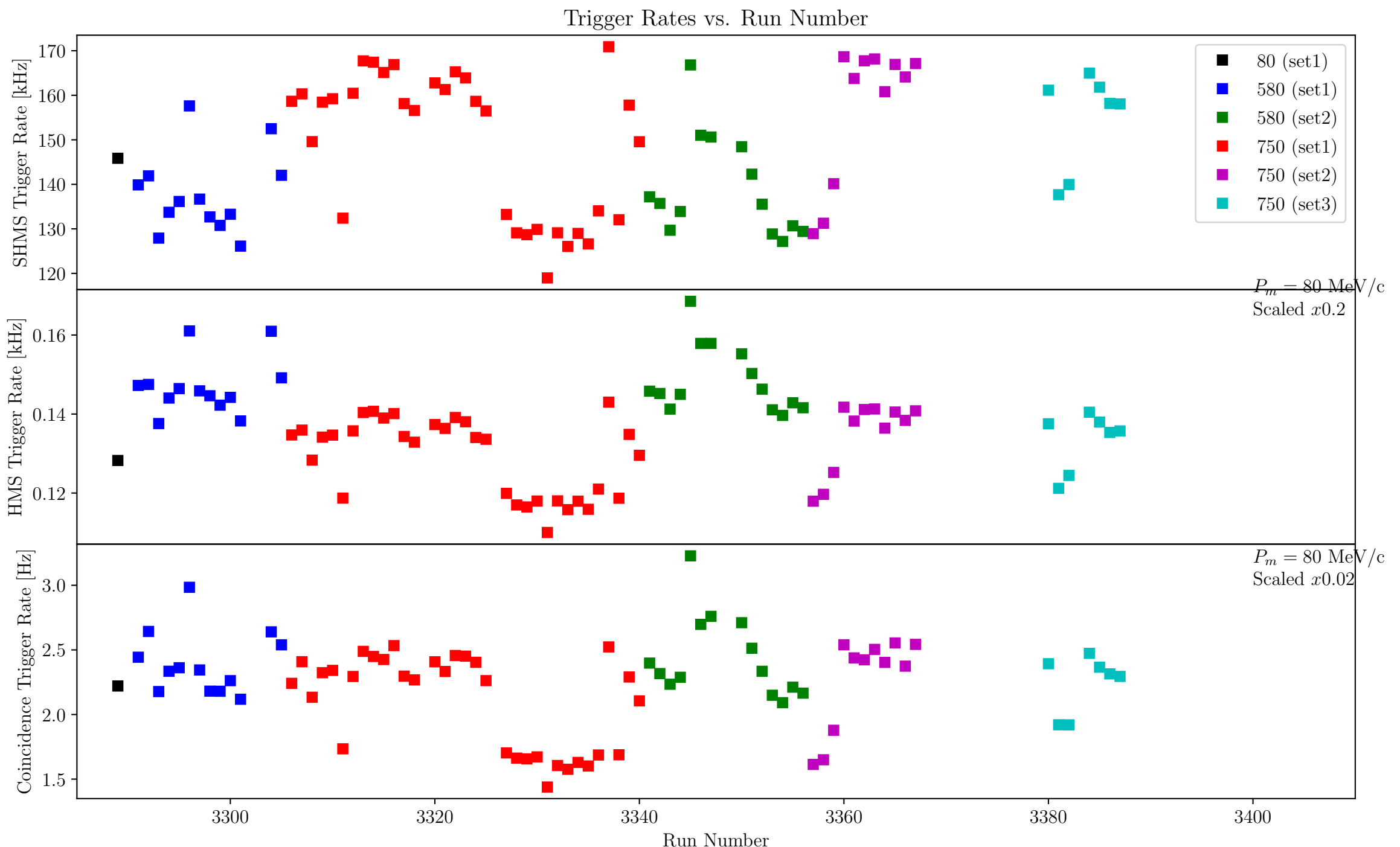
$$Y_{data}^{corr} = \frac{Y_{data}^{uncorr} \cdot f_{rad}}{Q \cdot \epsilon_{tLT} \cdot \epsilon_{htrk} \cdot \epsilon_{etrk} \cdot \epsilon_{tgtBoil} \cdot \epsilon_{pAbs}}$$



Radiative Correction factor

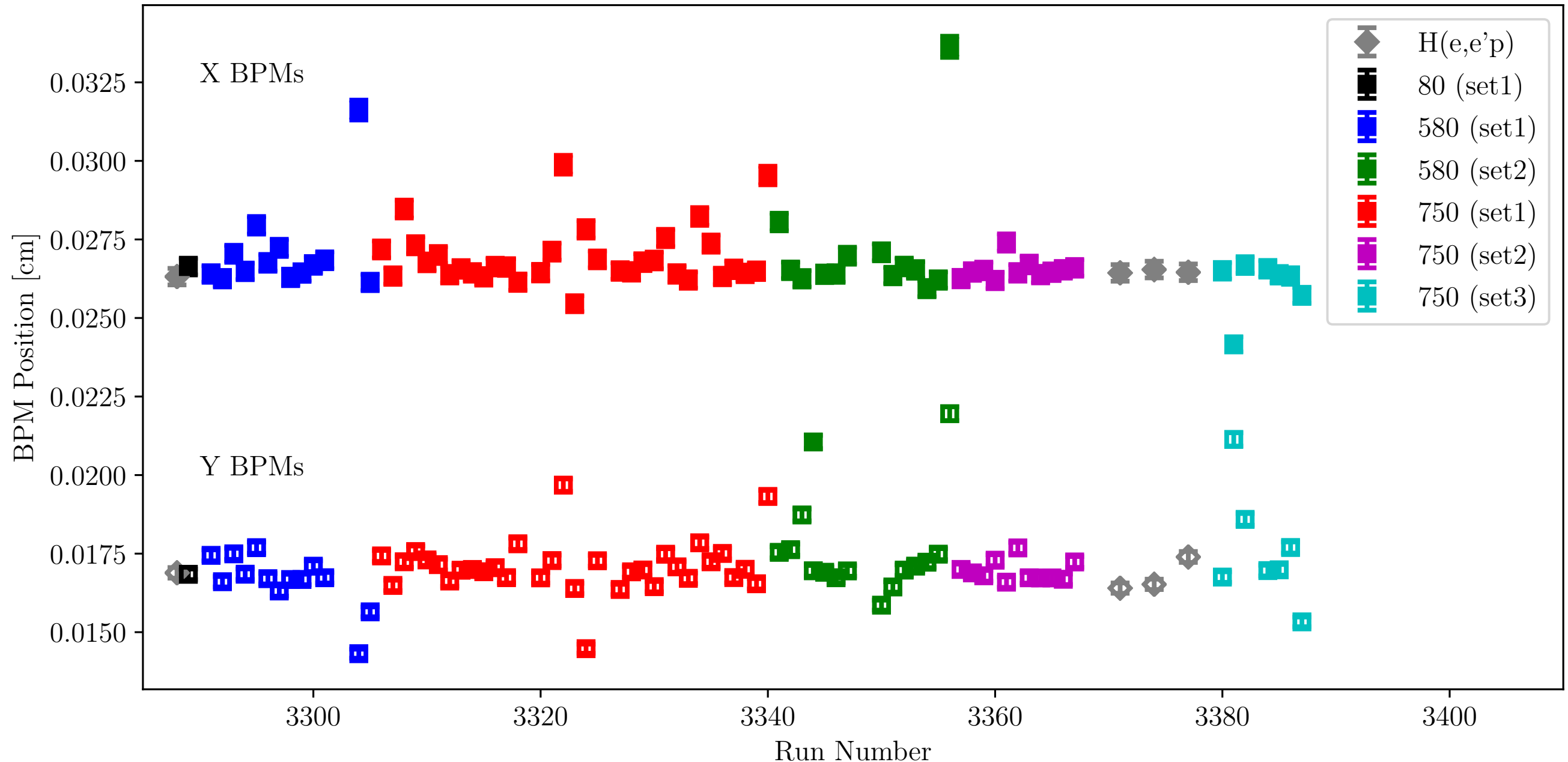
$$f_{rad} = \frac{Y_{norad}^{\text{SIMC}}}{Y_{rad}^{\text{SIMC}}}$$

TRIGGER RATES

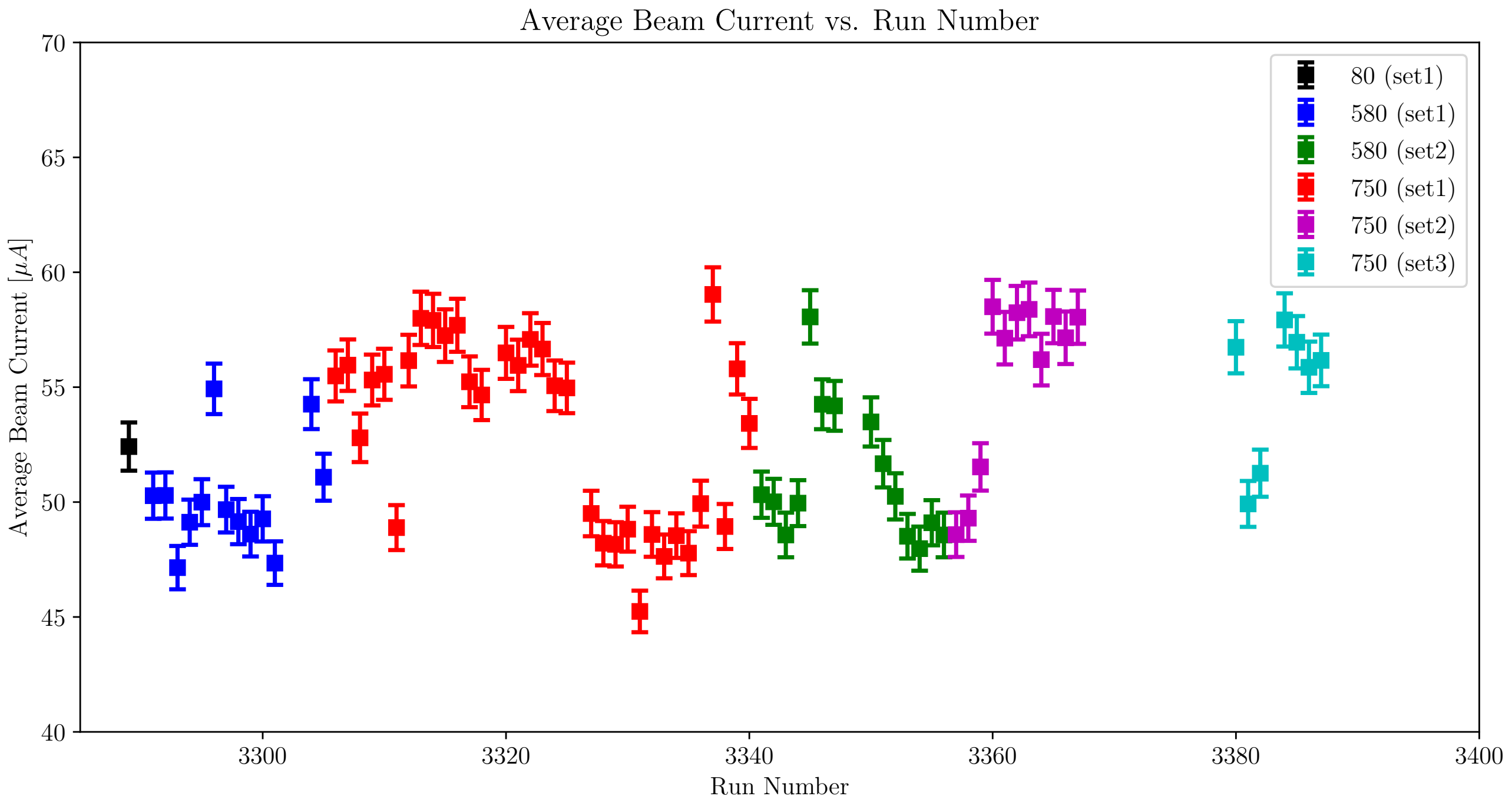


BEAM POSITION MONITORING (BPMs)

Beam Position Monitor vs. Run Number

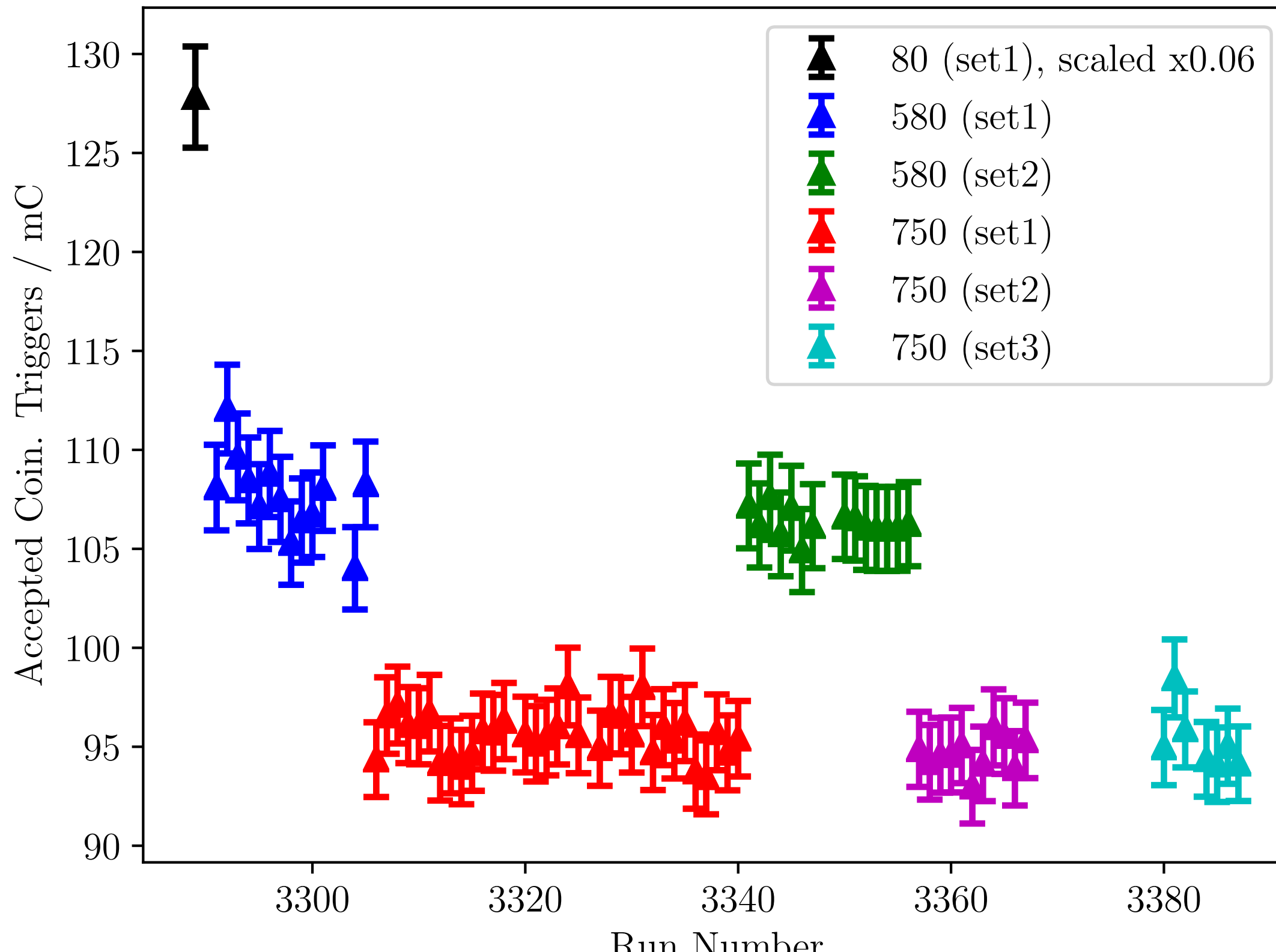


AVERAGE BEAM CURRENT



ACCEPTED COUNTS / CHARGE

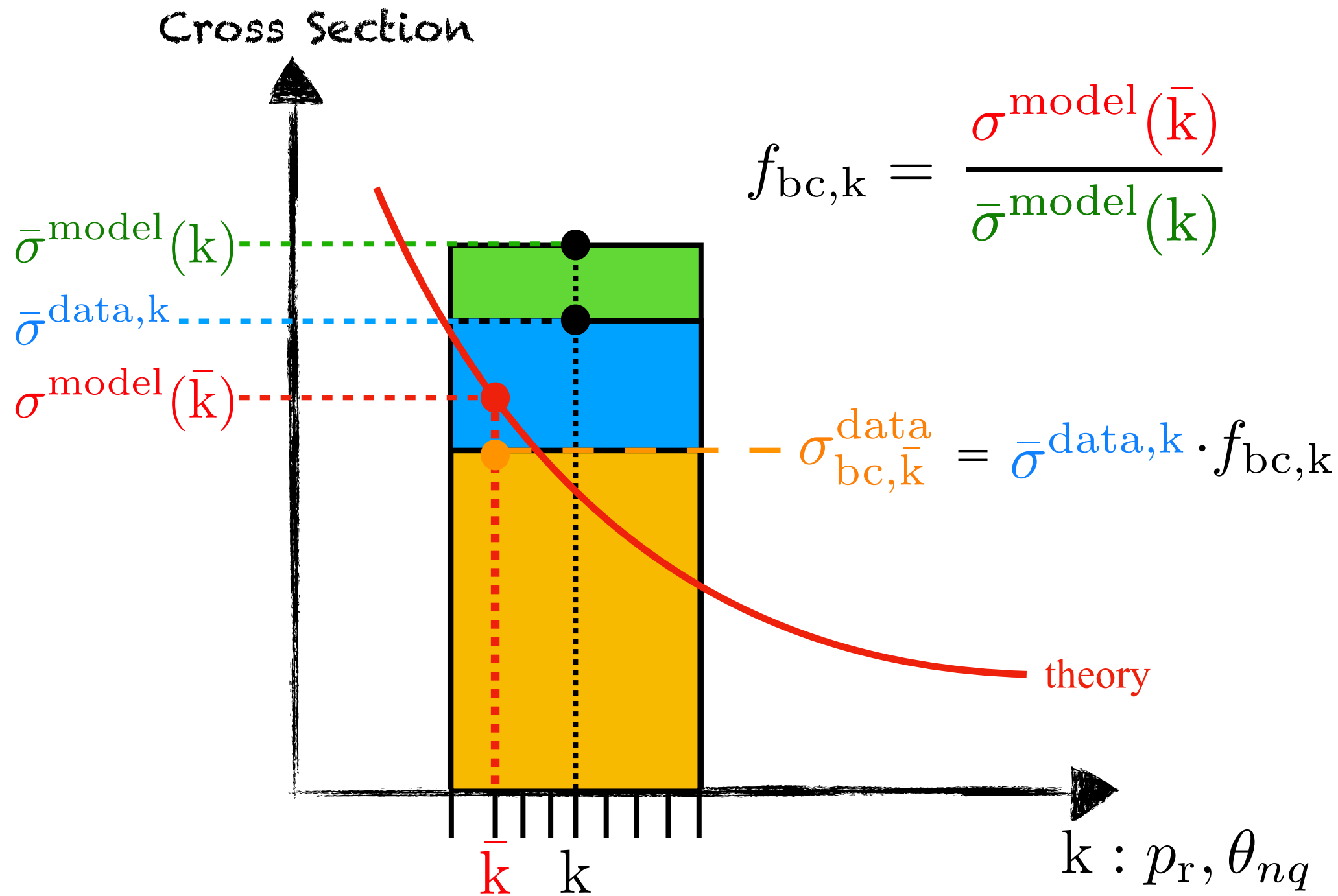
Accepted Coincidence Triggers / Charge vs. Run Number



BIN-CENTERING

CORRECTIONS

Bin Centering Corrections



$\sigma^{\text{model}}(\bar{k})$ Model cross section evaluated at the averaged kinematic bin

$\bar{\sigma}^{\text{model}}(k)$ Average (SIMC) model cross section evaluated over a kinematic bin, k

$\sigma_{\text{bc},\bar{k}}^{\text{data}}$ Bin-center corrected data cross section at kinematic bin, k

Bin Centering Corrections

- ❖ Currently, Hall C software does **NOT** do energy loss corrections, therefore, the average kinematics were calculated from vertex quantities in simulation.

$$\bar{x}_k = \left(\frac{\sum_i w_i x_i}{\sum_i w_i} \right)_k$$

Kinematic bin (e.g. Pm bin where cross section is stored)

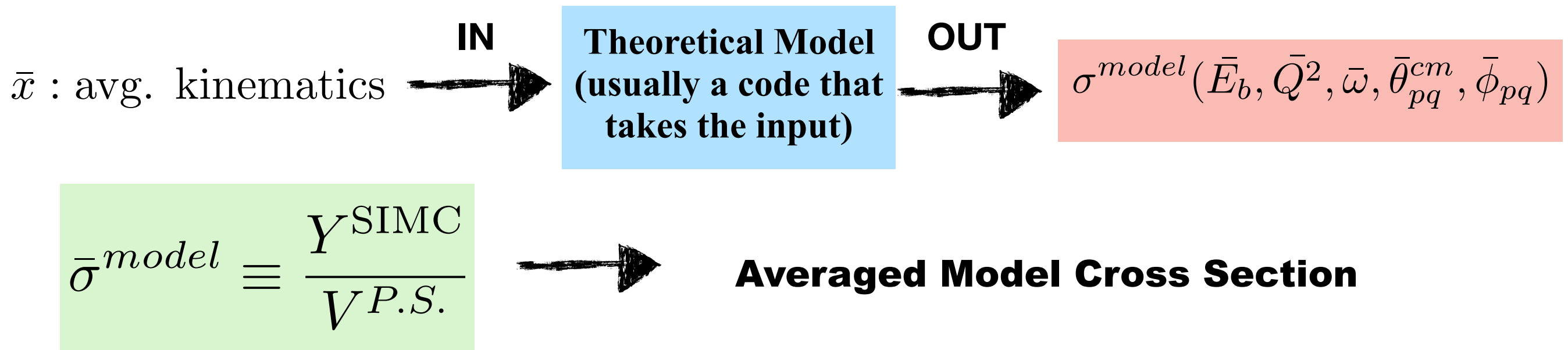
Averaged kinematic variable x over kinematic bin k

Weight times kinematic variable summed over all events

Sum of the weights over all events

Bin Centering Corrections

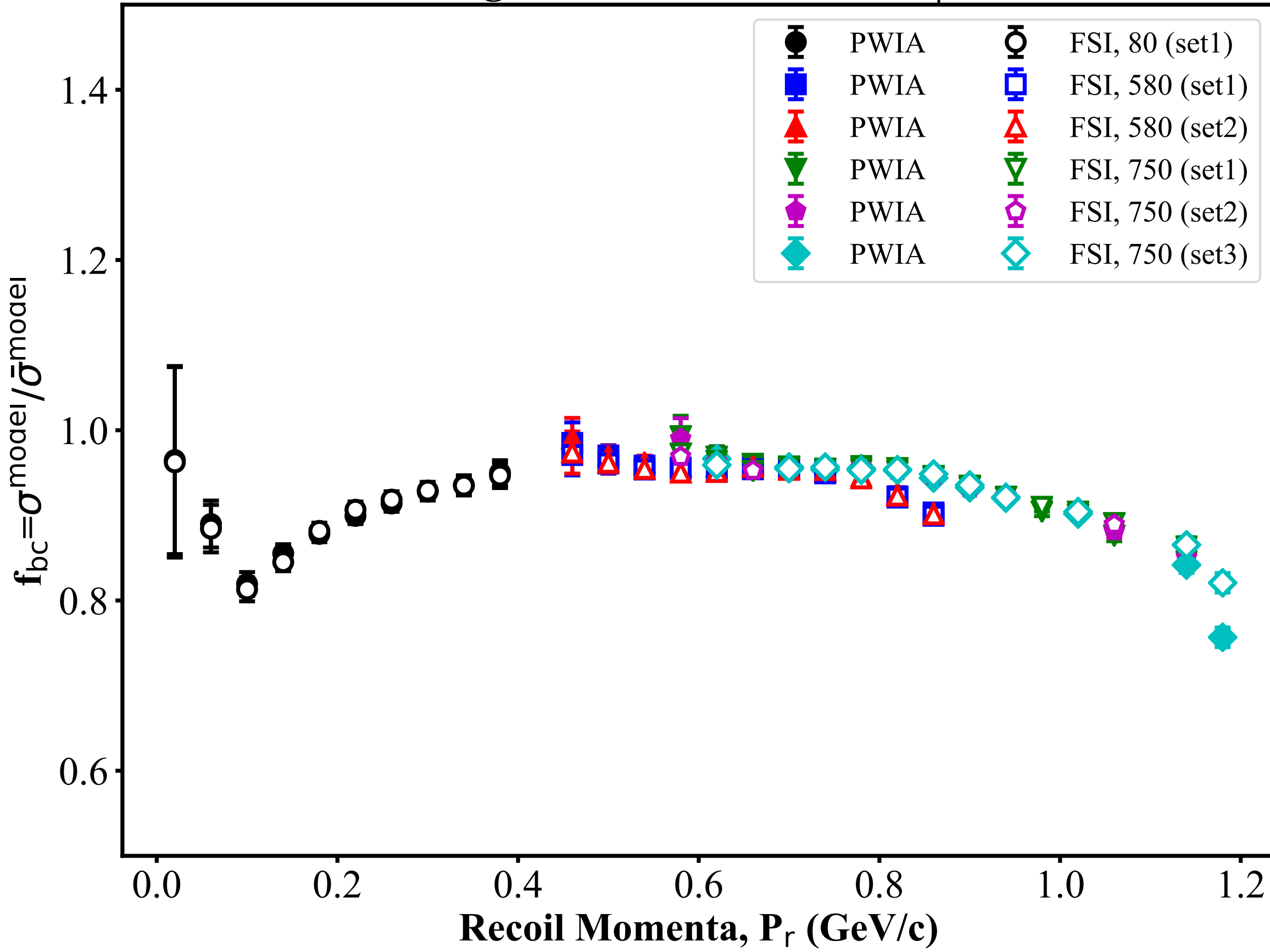
- ❖ Once the averaged kinematics have been calculated, . . .



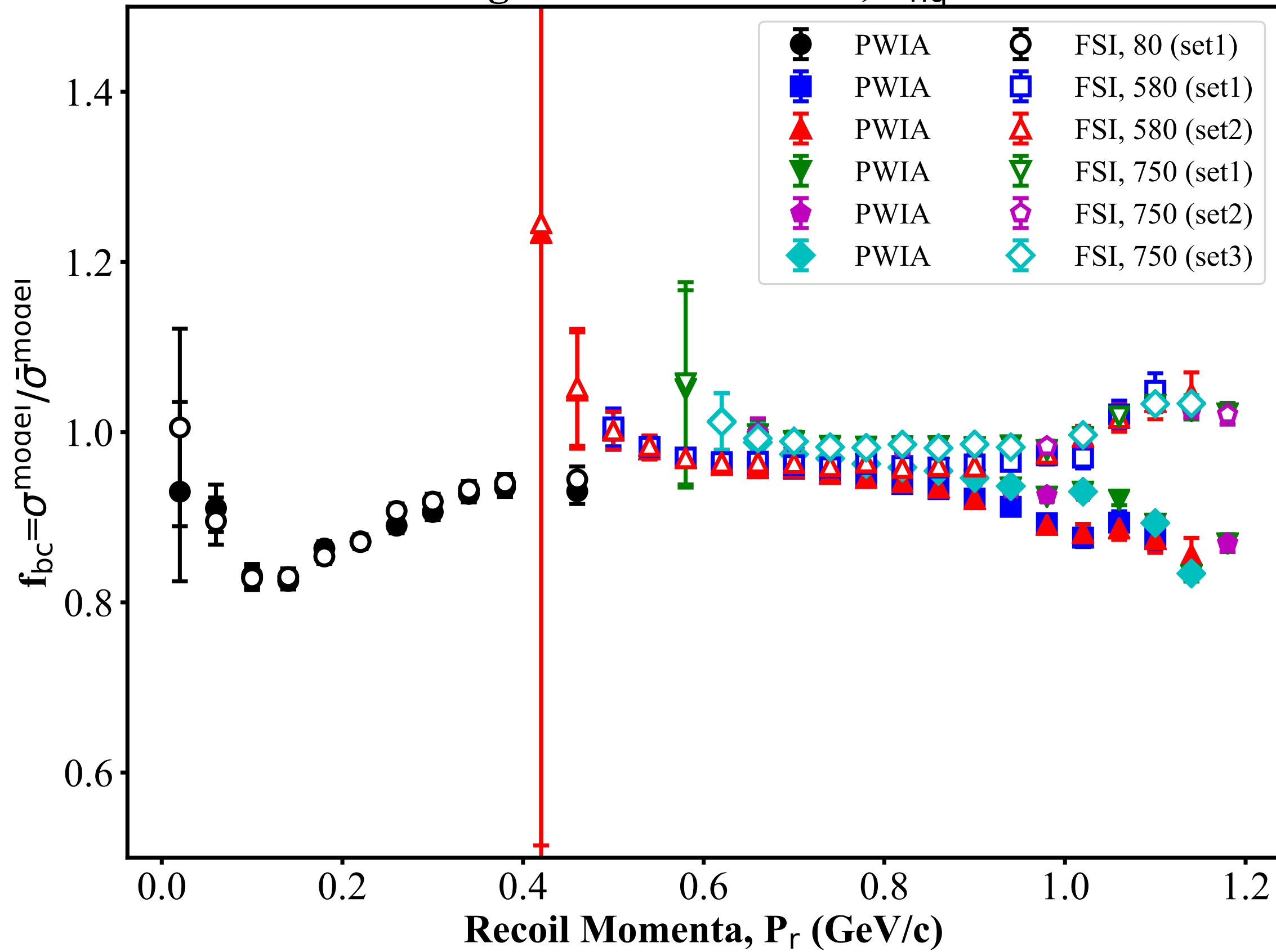
- ❖ Correct the data bin-by-bin using the model cross sections ratio . . .

$$\sigma_{bc}^{exp} = \bar{\sigma}^{exp} \cdot \frac{\sigma^{model}(\bar{E}_b, \bar{Q}^2, \bar{\omega}, \bar{\theta}_{pq}^{cm}, \bar{\phi}_{pq})}{\bar{\sigma}^{model}}$$

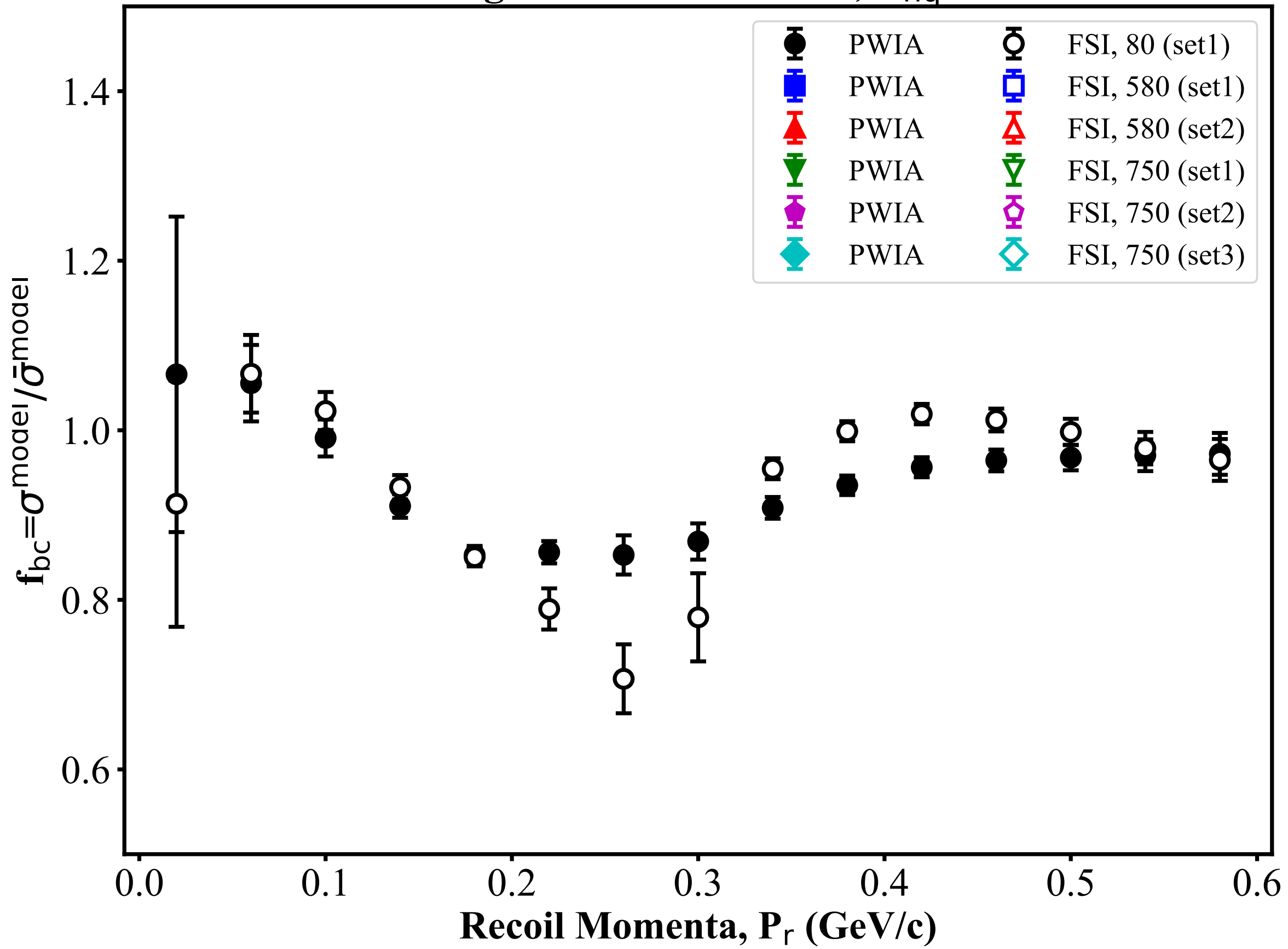
Bin Centering Correction Factor, $\theta_{\text{hq}} = 35 \pm 5^\circ$



Bin Centering Correction Factor, $\theta_{nq} = 45 \pm 5^\circ$



Bin Centering Correction Factor, $\theta_{nq} = 75 \pm 5^\circ$



Error Analysis of D(e,e'p)n Cross Section

NORMALIZATION CORRECTION FACTORS for D(e,e'p)n

Pm	HMS Tracking Efficiency	sHMS Tracking Efficiency	Target Boiling Correction	Proton Absorption Correction	Total Live Time	Total Charge (mC)
80	0.989	0.965	0.958	0.953	0.908	142.140
580 (set 1)	0.990	0.965	0.960	0.953	0.929	1686.830
580 (set 2)	0.987	0.964	0.959	0.953	0.929	1931.770
750 (set 1)	0.988	0.964	0.957	0.953	0.924	5329.490
750 (set 2)	0.989	0.962	0.956	0.953	0.923	1894.010
750 (set 3)	0.989	0.962	0.956	0.953	0.924	1083.700

◆ Correction factors were averaged over all runs of individual data sets

UNCERTAINTY (%) IN NORMALIZATION CORRECTION FACTORS for D(e,e'p)n

Pm	HMS Tracking Efficiency Err.	sHMS Tracking Efficiency Err.	Target Boiling Correction Err.	Proton Absorption Correction Err.	Total Live Time Err.	Total Charge (mC) Err.
80	0.034%	0.040%	0.378%	0.472%	—	—
580 (set 1)	0.396%	0.732%	0.362%	0.472%	—	—
580 (set 2)	0.473%	0.583%	0.369%	0.472%	—	—
750 (set 1)	0.526%	0.689%	0.384%	0.472%	—	—
750 (set 2)	0.467%	0.682%	0.401%	0.472%	—	—
750 (set 3)	0.507%	0.729%	0.397%	0.472%	—	—

** Uncertainty on EDTM and BCM is not finalized. Conservative estimates on the cross section error were made (See next slide)



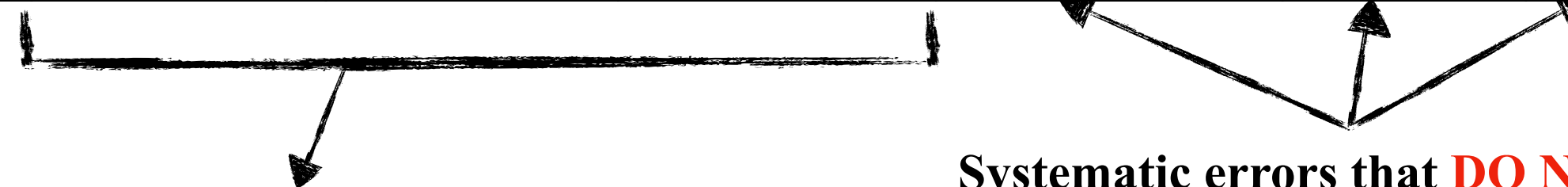
SYSTEMATIC UNCERTAINTY ON NORMALIZATION

$$\bar{\sigma}_{corr}^{exp} = \bar{\sigma}_{uncorr}^{exp} \cdot f_1 \cdot f_2 \dots f_i \longrightarrow \frac{d\bar{\sigma}_{corr}^{exp}}{\bar{\sigma}_{corr}^{exp}} \Big|_i = \frac{df_i}{f_i}$$

f_i : normalization correction factors

df_i : error in normalization correction factors

Relative Systematic Error (%) on the Cross Section due to:						
Pm	HMS Tracking Efficiency	sHMS Tracking Efficiency	Target Boiling Correction	Proton Absorption Correction	Total Live Time	Total Charge (mC)
80	0.0344%	0.0413%	0.3948%	0.4951%	3.0%	2.0%
580 (set 1)	0.3999%	0.7586%	0.3766%	0.4951%	3.0%	2.0%
580 (set 2)	0.4786%	0.6041%	0.3842%	0.4951%	3.0%	2.0%
750 (set 1)	0.5329%	0.7155%	0.4013%	0.4951%	3.0%	2.0%
750 (set 2)	0.4719%	0.7089%	0.4196%	0.4951%	3.0%	2.0%
750 (set 3)	0.5127%	0.7584%	0.4150%	0.4951%	3.0%	2.0%



added in quadrature for overlapping Pm bins

Systematic errors that **DO NOT** vary are added in quadrature to the final result

SPECTROMETER KINEMATIC SYSTEMATIC UNCERTAINTIES on D(e,e'p)n

$\delta\theta_e [mr]$	+/- 0.17
$\delta\theta_p [mr]$	+/- 0.24
$\delta E_f / E_f$	+/- 9.1E-04
$\delta E_b / E_b$	+/- 7.5E-04
$d\sigma_{exp}$	6.5%

Uncertainty in SHMS angle

Uncertainty in HMS angle

Uncertainty in SHMS momentum

Uncertainty in Beam Energy

Determined from
fit to H(e,e'p) coincidence
elastic data.
(See DOC DB link HERE!)

← Max. Kin. Systematic
Error on Cross
Section

$$d\sigma_{exp}^2 = \left(\frac{d\sigma}{d\theta_e} \delta\theta_e \right)^2 + \left(\frac{d\sigma}{d\theta_p} \delta\theta_p \right)^2 + \left(\frac{d\sigma}{dE_f} \frac{\delta E_f}{E_f} E_f \right)^2 + \left(\frac{d\sigma}{dE_b} \frac{\delta E_b}{E_b} E_b \right)^2 +$$

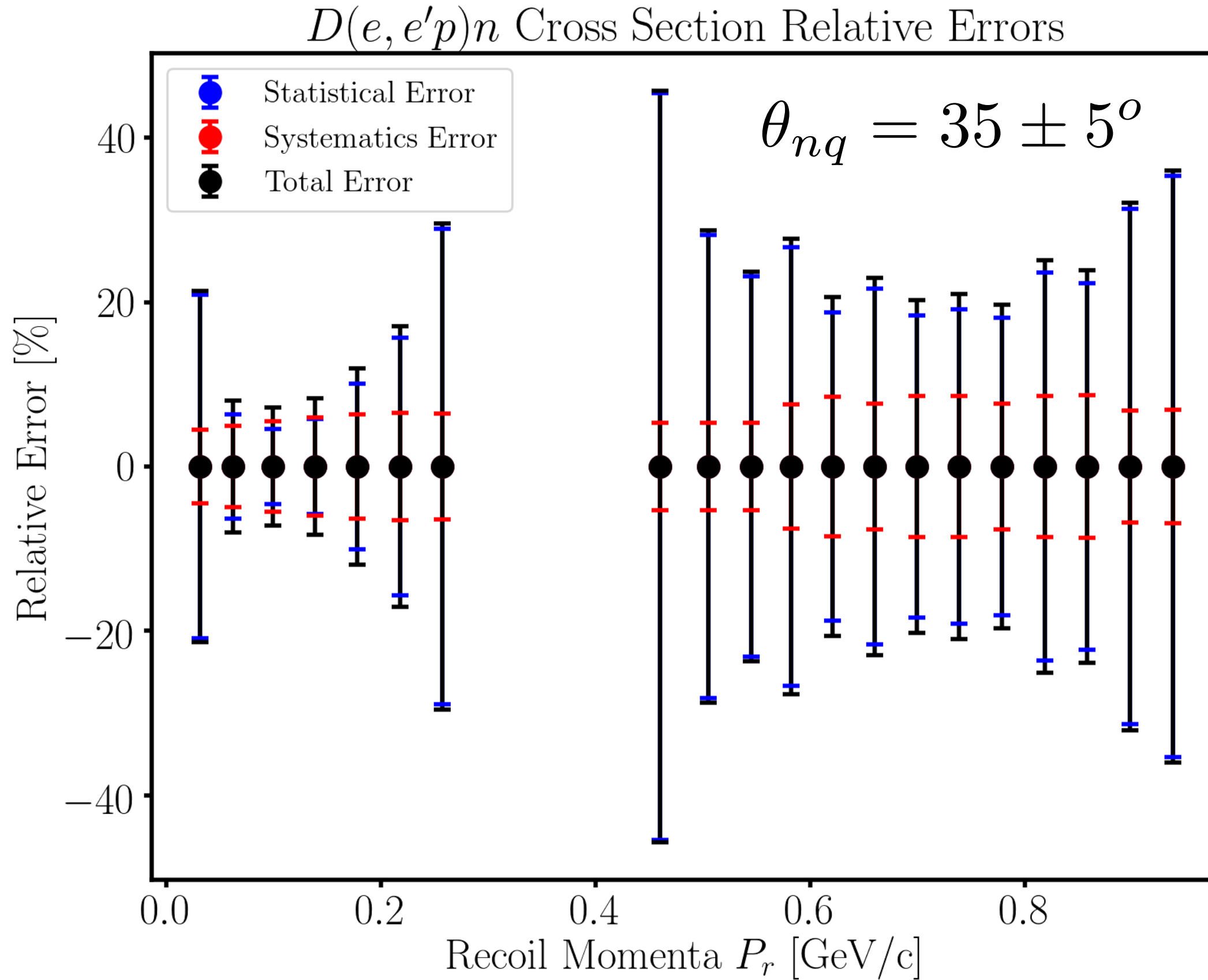
Covariance Errors

Kinematic uncertainties are due to our limited knowledge of the beam, spectrometer momenta and angles. Each of these uncertainties affects our knowledge of the cross section, since the cross section depends on these kinematics

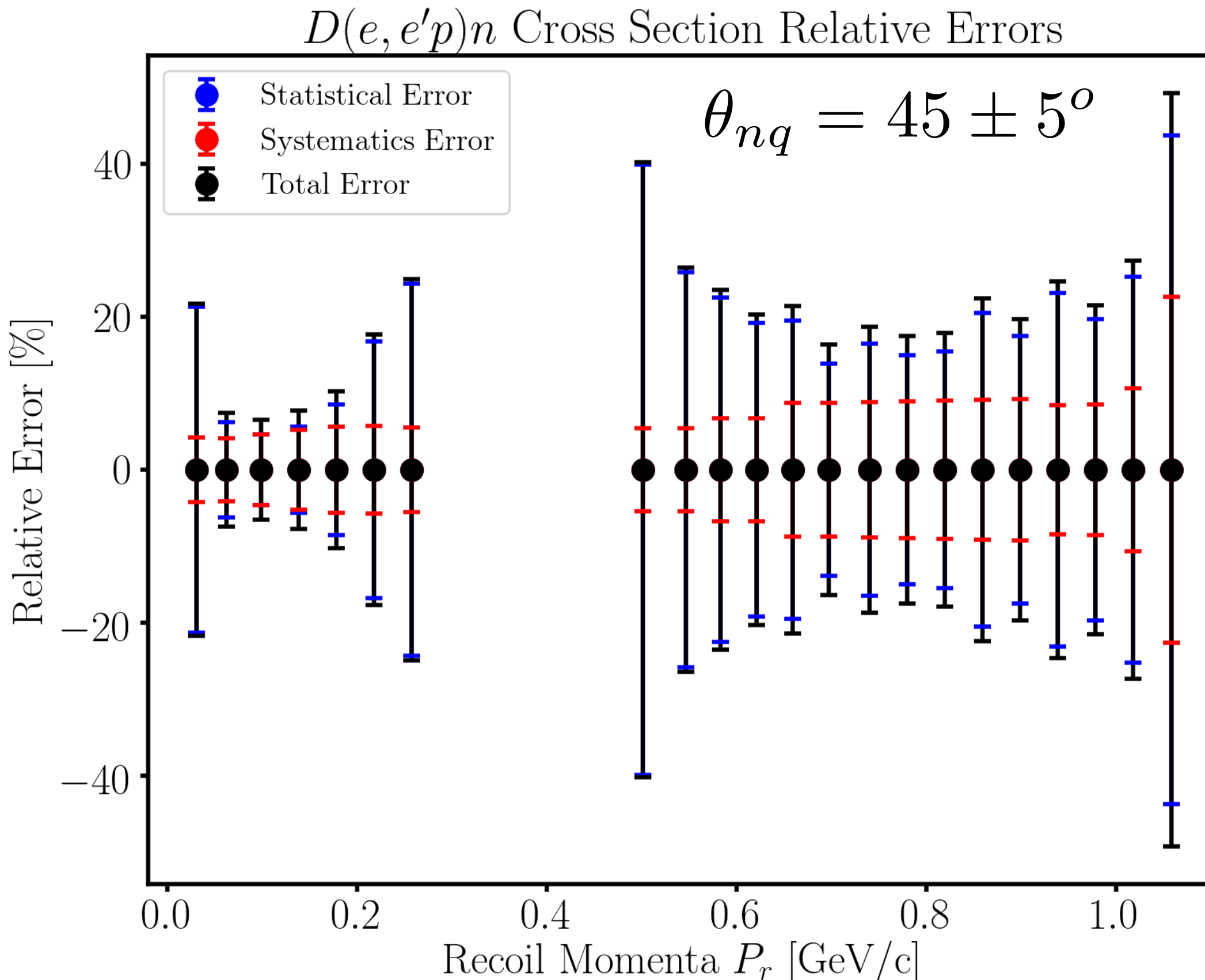
The kinematic uncertainties are point-to-point which means they vary depending for each data point, as each corresponds to a different missing momentum kinematic bin.

The tables of the PWIA Laget Cross section derivatives with respect to the kinematic variables were used

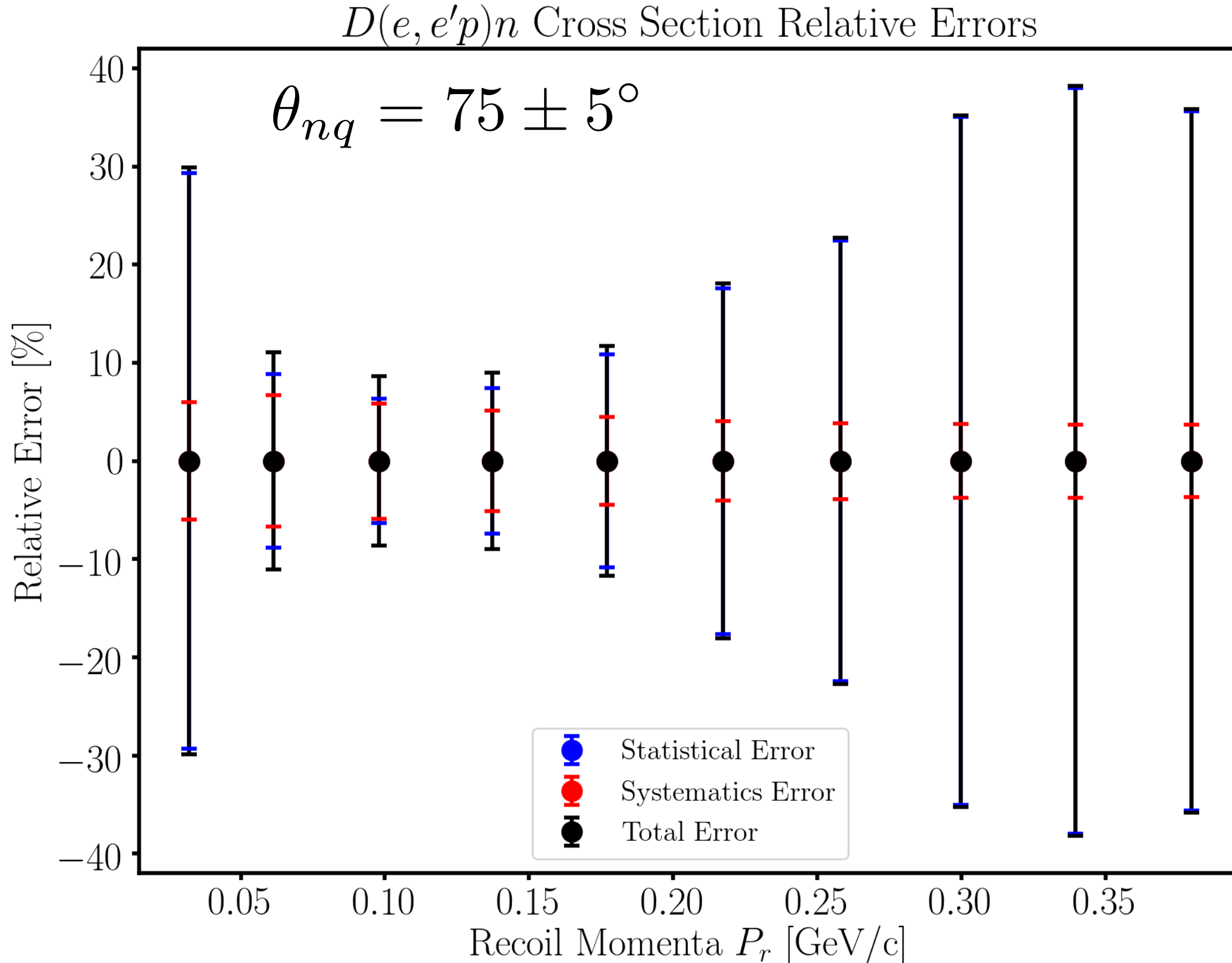
D(e,e'p)n Cross Section Relative Errors Summary Plots



D(e,e'p)n Cross Section Relative Errors Summary Plots

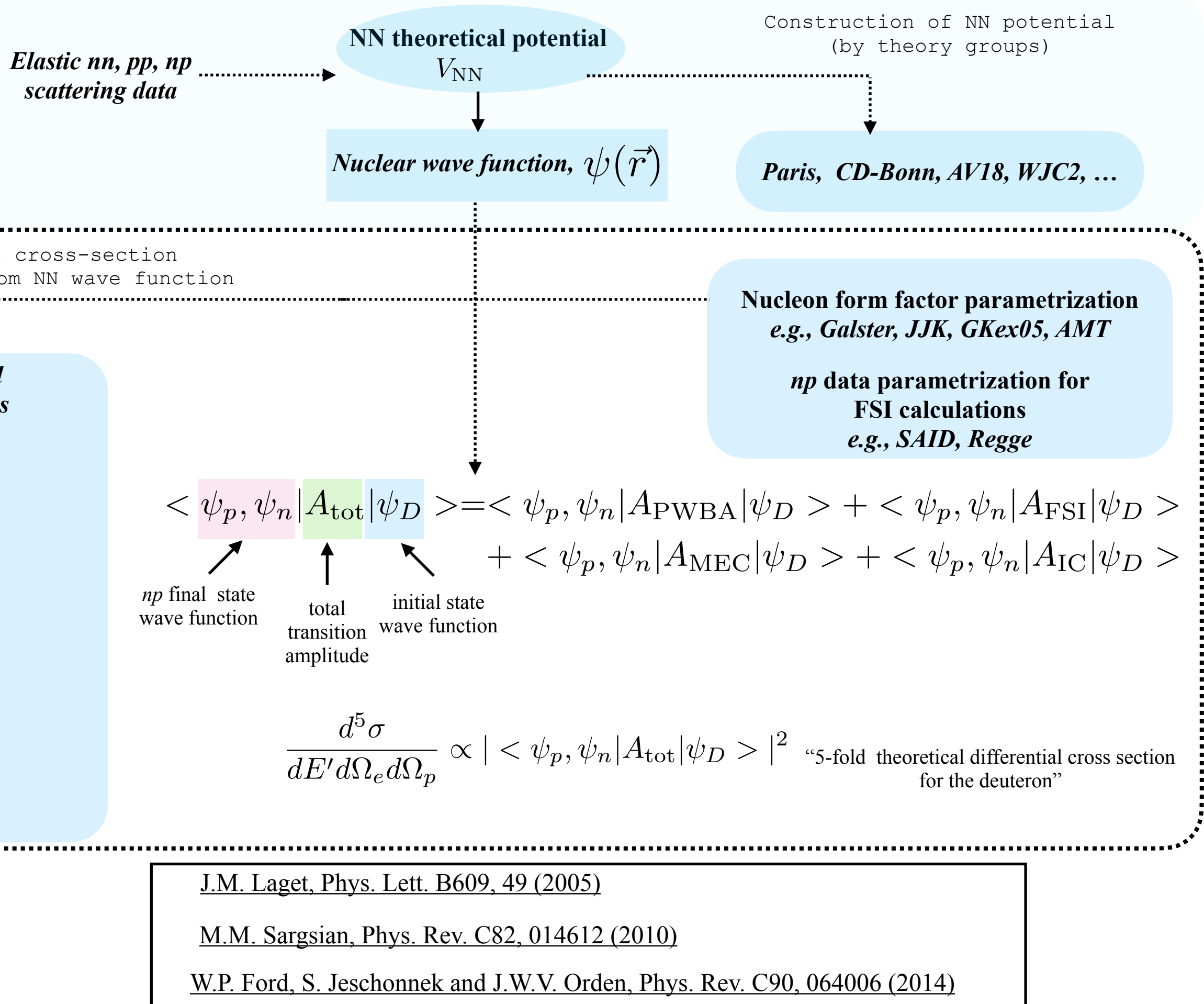


D(e,e'p)n Cross Section Relative Errors Summary Plots



From Theoretical Potentials to Theoretical Cross Sections

**How are the theoretical cross sections
determined from an NN potential ?**



D(e,e'p)n Reduced Cross Sections Linear Fit Results

Interpreting the Statistical Significance Test

p-value definition:

The p -value is the probability of getting the observed value of the test statistic, or a value with even greater evidence against H_0 , if the null hypothesis is true

$$H_0 : \mu = \mu_0 \quad (\text{null hypothesis})$$

$$H_a : \mu > \mu_0 \quad (\text{alternative hypothesis})$$

Z-test statistic

$$Z = \frac{\bar{X} - \mu_0}{\sigma / \sqrt{n}}$$

\bar{X} : measured variable

μ_0 : population mean of H_0

σ : population standard deviation of H_0

n : number of trials or experiments

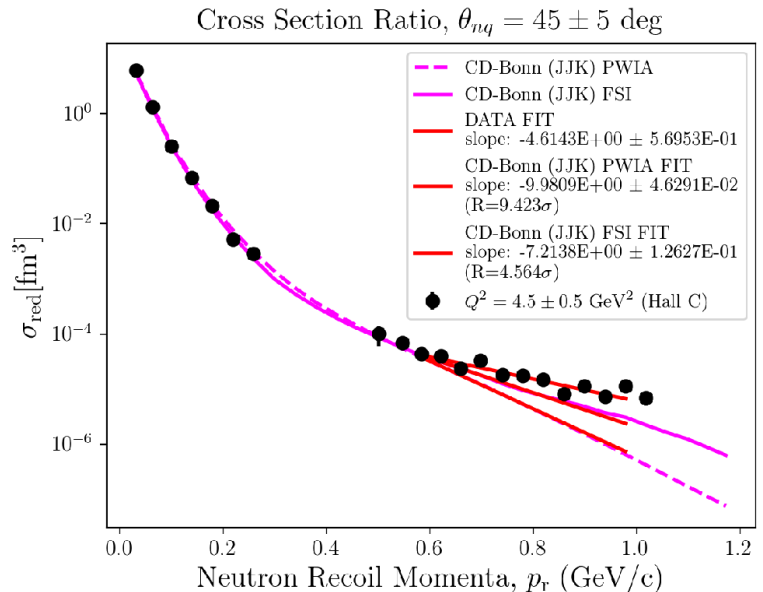
For the E12-10-003:

$$\bar{X} \equiv \mu_{\text{data}} - \mu_{\text{theory}} \quad (\text{Slope difference})$$

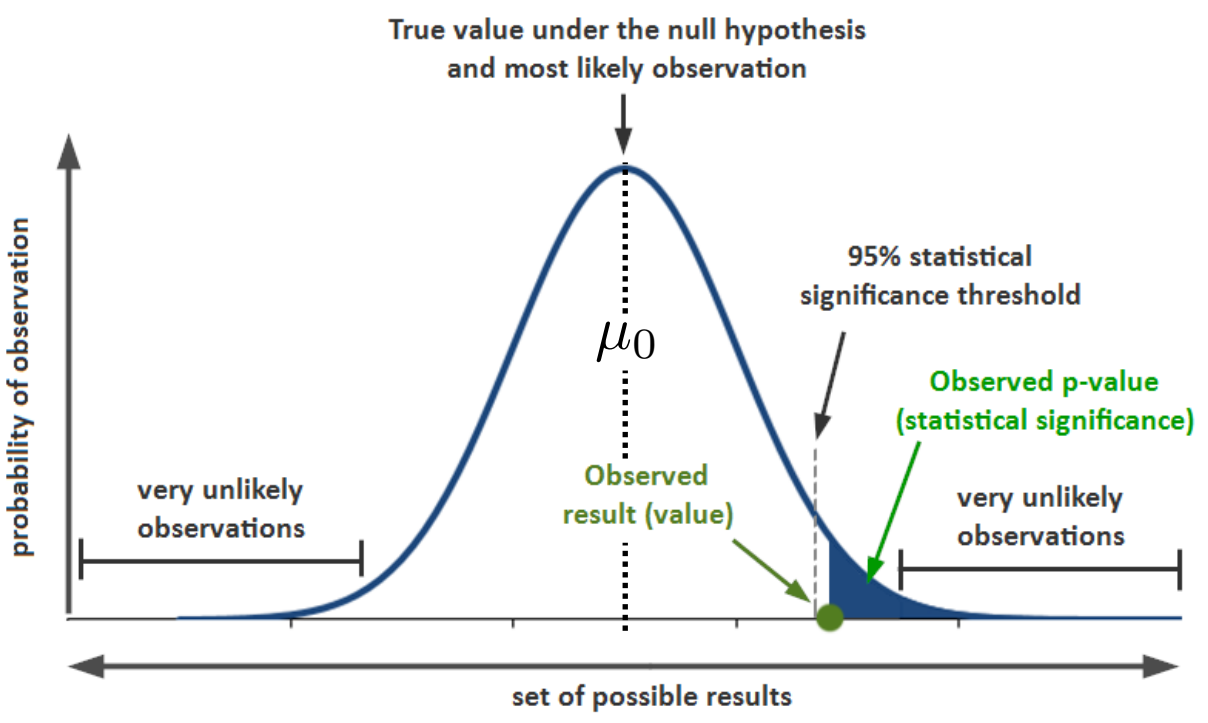
$$\mu_0 = 0 \quad n = 1$$

$$\sigma \equiv \sigma_{\mu_{\text{data}}}$$

null hypothesis: if the E12-10-003 were to be repeated n times, the difference between the data and theory slopes would follow a standard normal distribution with a mean of zero. That is, the difference in the slopes would only be due to statistical fluctuations.



Distribution of Z if H_0 is true:



$$Z$$

$$p\text{-value} = p(Z \geq Z_0)$$

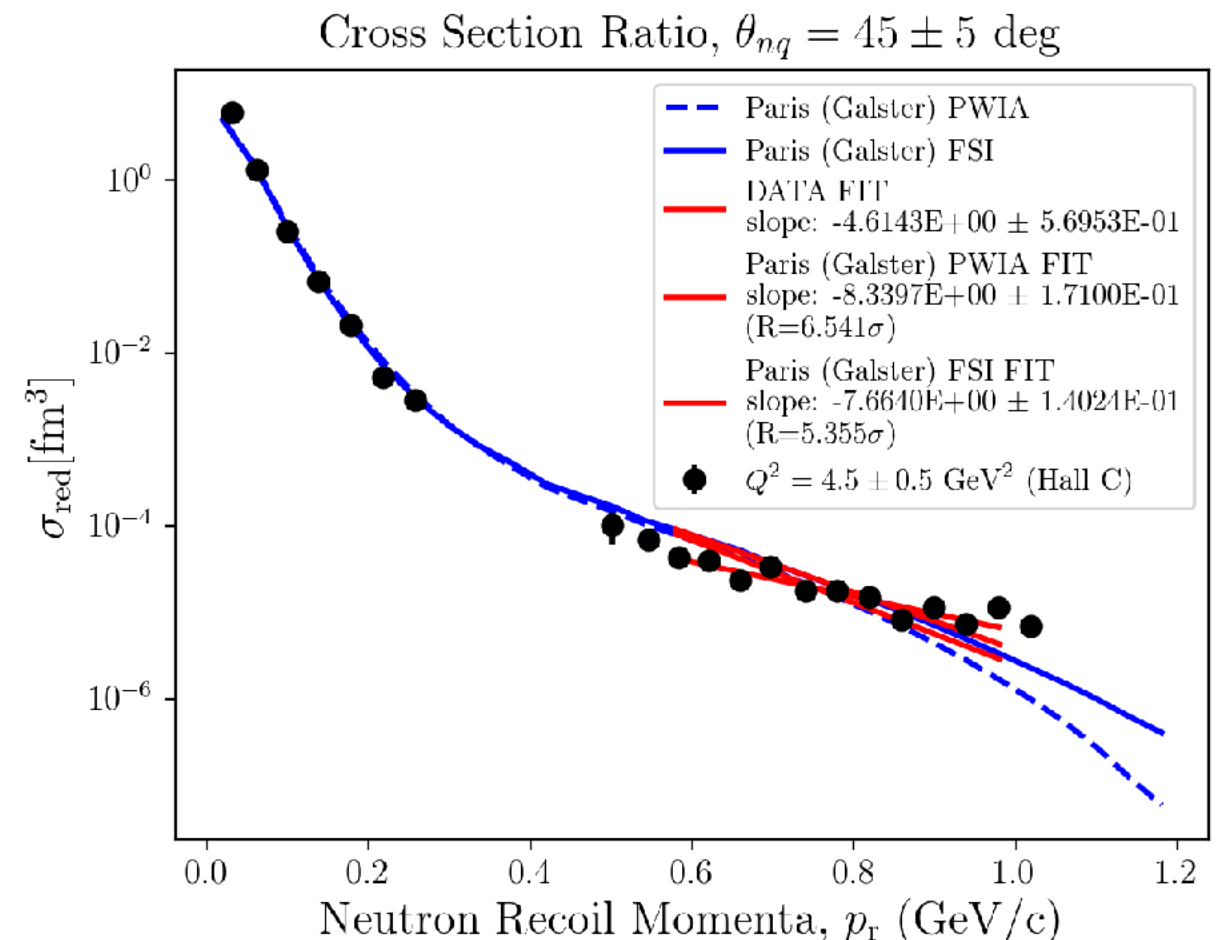
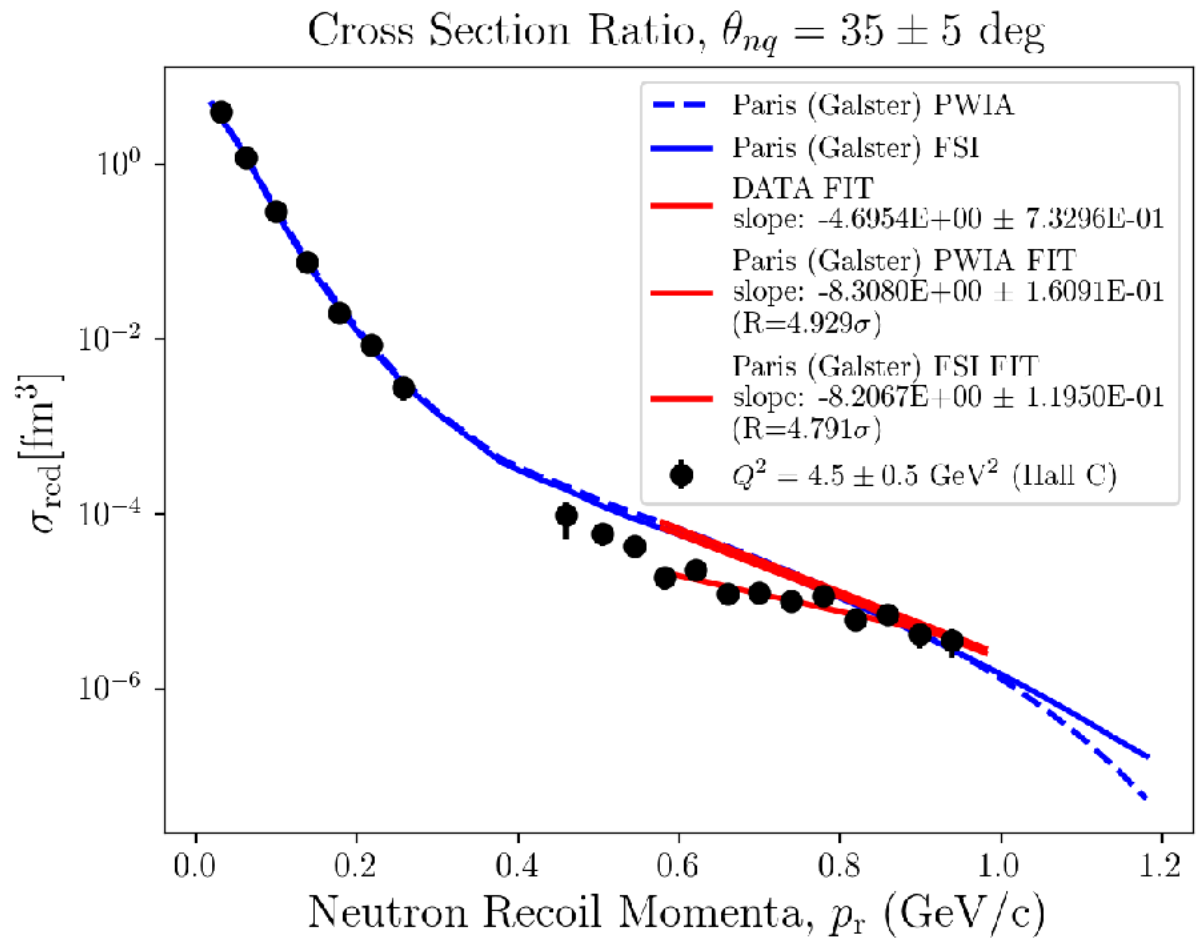
Statistical Significance Test: Z-score and p-values

- The p-values describe the probability that the observed difference in the measurements is due to a statistical fluctuation
- The data differs from the CD-Bonn slopes by ~ 4 - 9 standard deviations (statistical fluctuations extremely unlikely)

Theoretical Model	PWIA (35 deg) Z-score	p-value	PWIA (45 deg) Z-score	p-value	FSI (35 deg) Z-score	p-value	FSI (45 deg) Z-score	p-value
Paris (Galster)	4.929	4.1E-07	6.541	3.0E-11	4.791	8.2E-07	5.355	4.2E-08
AV18 (JJK)	4.373	6.1E-06	5.632	8.9E-09	5.184	1.0E-07	4.721	1.1E-06
AV18 (GKex05)	4.623	1.9E-06	6.079	6.0E-10	5.616	9.7E-09	5.889	1.9E-09
AV18 (AMT)	4.598	2.1E-06	6.066	6.5E-10	5.597	1.0E-08	5.976	1.1E-09
CD-Bonn (JJK)	7.321	1.2E-13	9.423	2.1E-21	6.648	1.4E-11	4.564	2.5E-06
CD-Bonn (GKex05)	7.611	1.3E-14	9.895	2.1E-23	7.484	3.6E-14	5.383	3.6E-08
CD-Bonn (AMT)	7.586	1.6E-14	9.882	2.4E-23	7.460	4.3E-14	5.516	1.7E-08
WJC2 (GKex05)	4.241	1.1E-05	5.575	1.2E-08	5.133	1.4E-07	5.519	1.7E-08
WJC2 (AMT)	4.217	1.2E-05	5.561	1.3E-08	5.110	1.6E-07	5.598	1.0E-08

D(e,e'p)n Linear Fit Plots

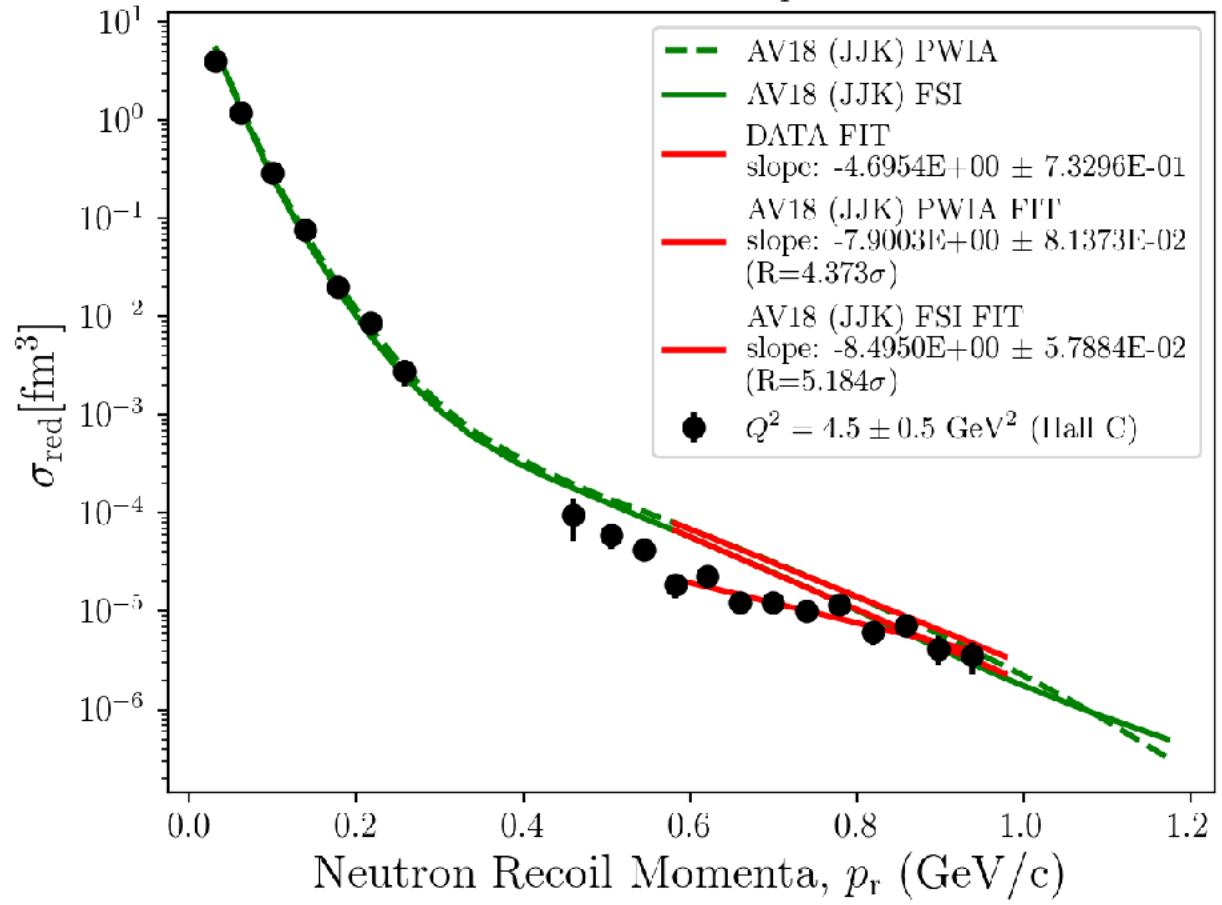
Paris Potential (Galster parametrization)



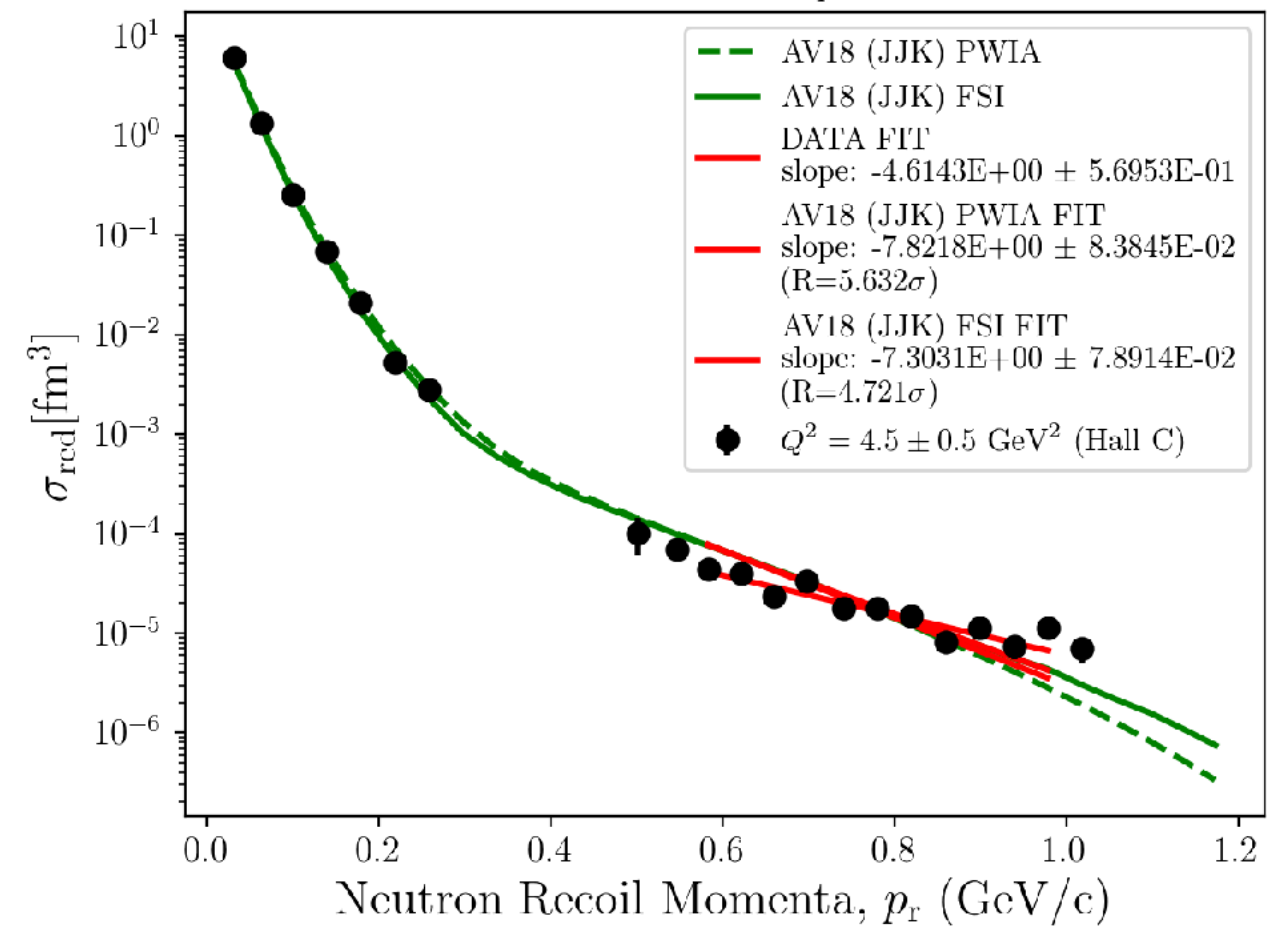
D(e,e'p)n Linear Fit Plots

AV18 (JJK parametrization)

Cross Section Ratio, $\theta_{nq} = 35 \pm 5$ deg



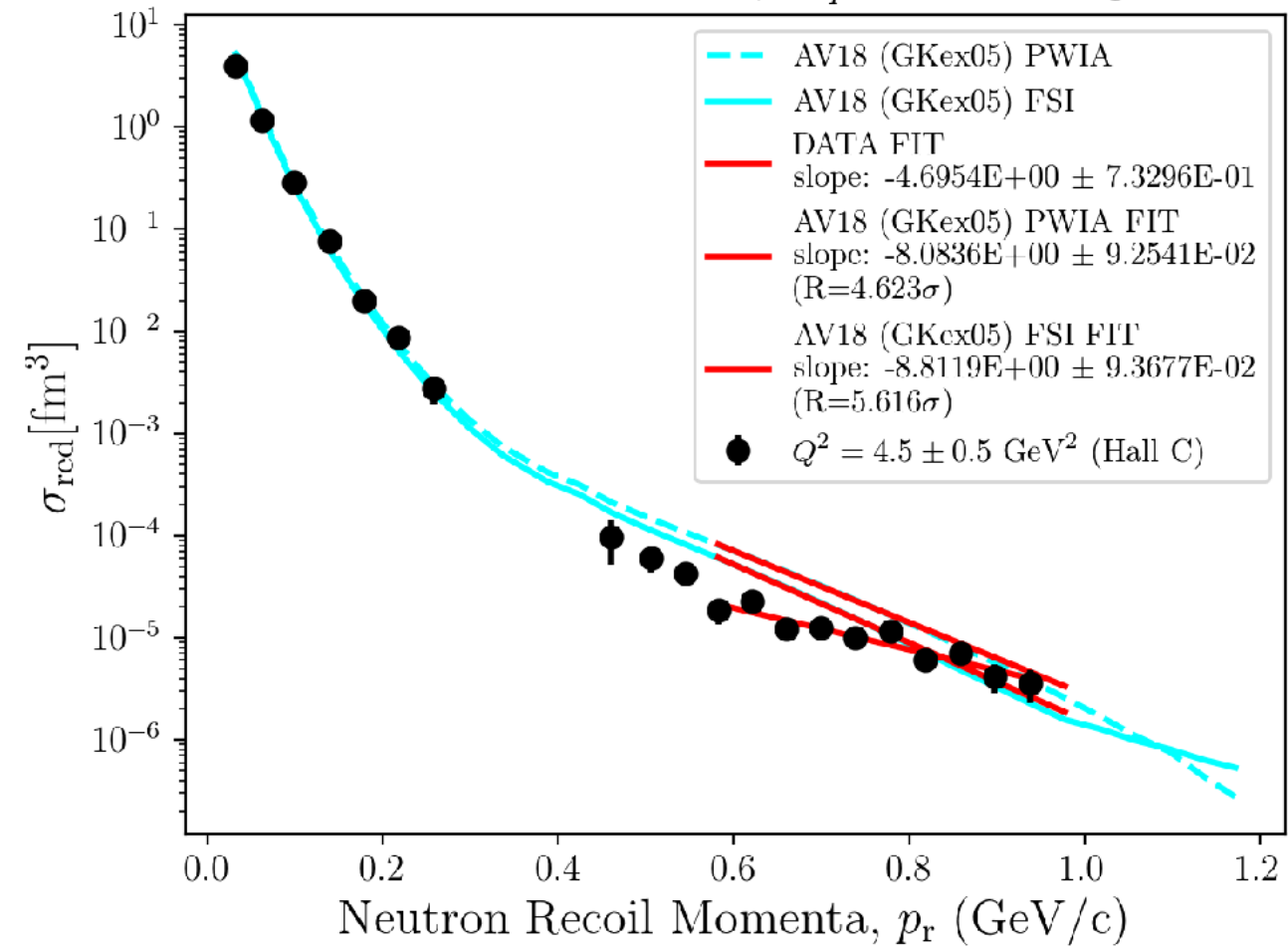
Cross Section Ratio, $\theta_{nq} = 45 \pm 5$ deg



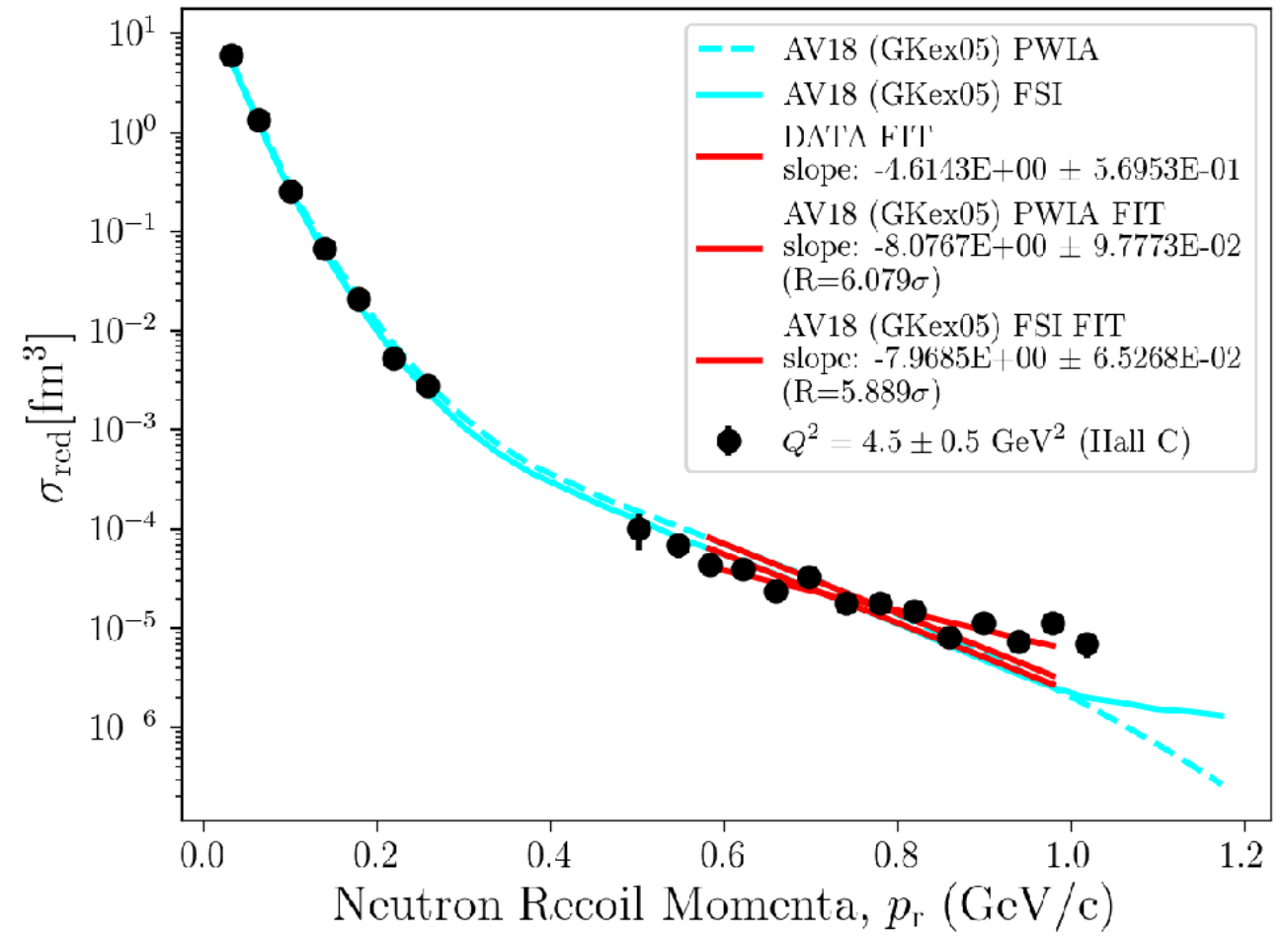
D(e,e'p)n Linear Fit Plots

AV18 (GKex05 parametrization)

Cross Section Ratio, $\theta_{nq} = 35 \pm 5$ deg



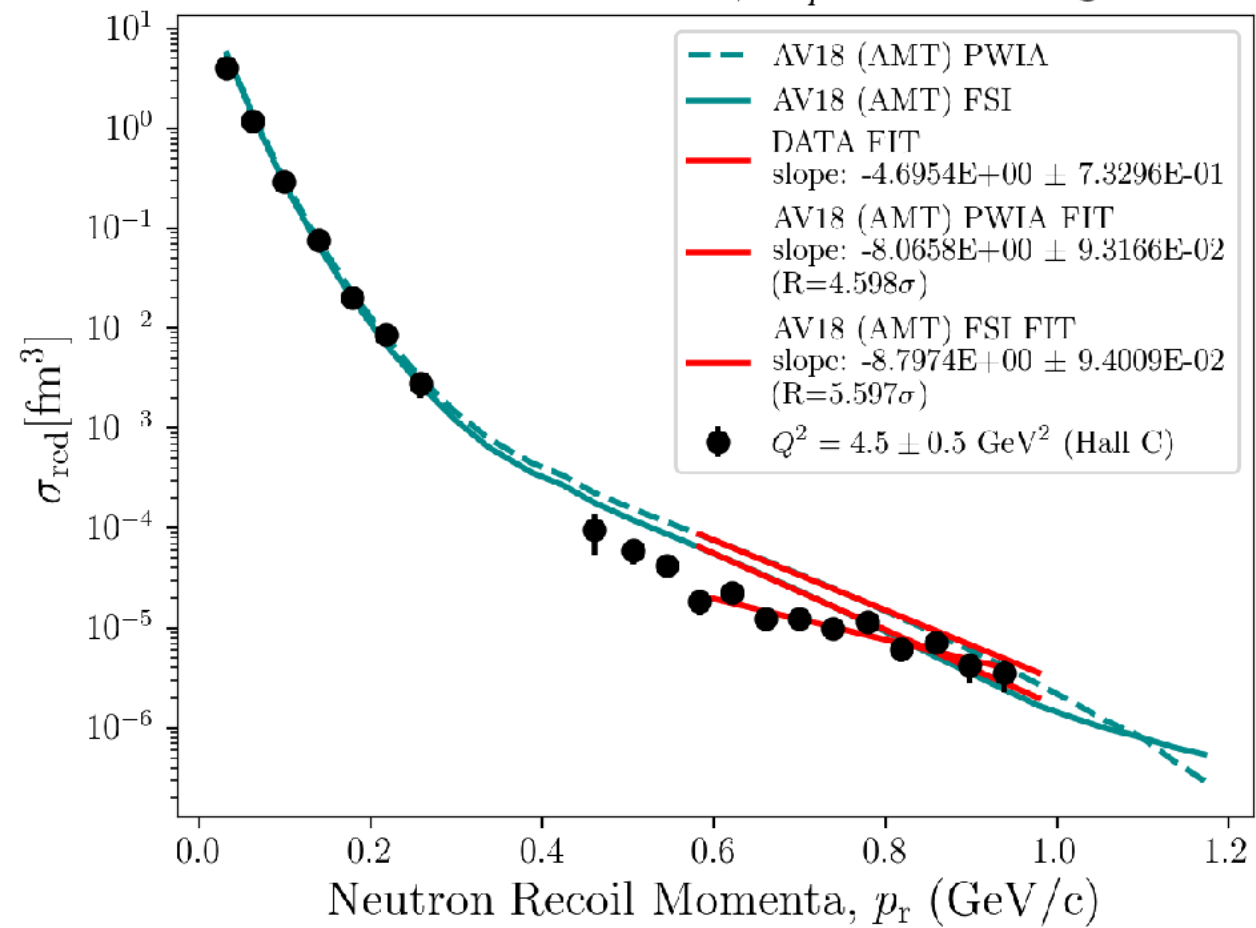
Cross Section Ratio, $\theta_{nq} = 45 \pm 5$ deg



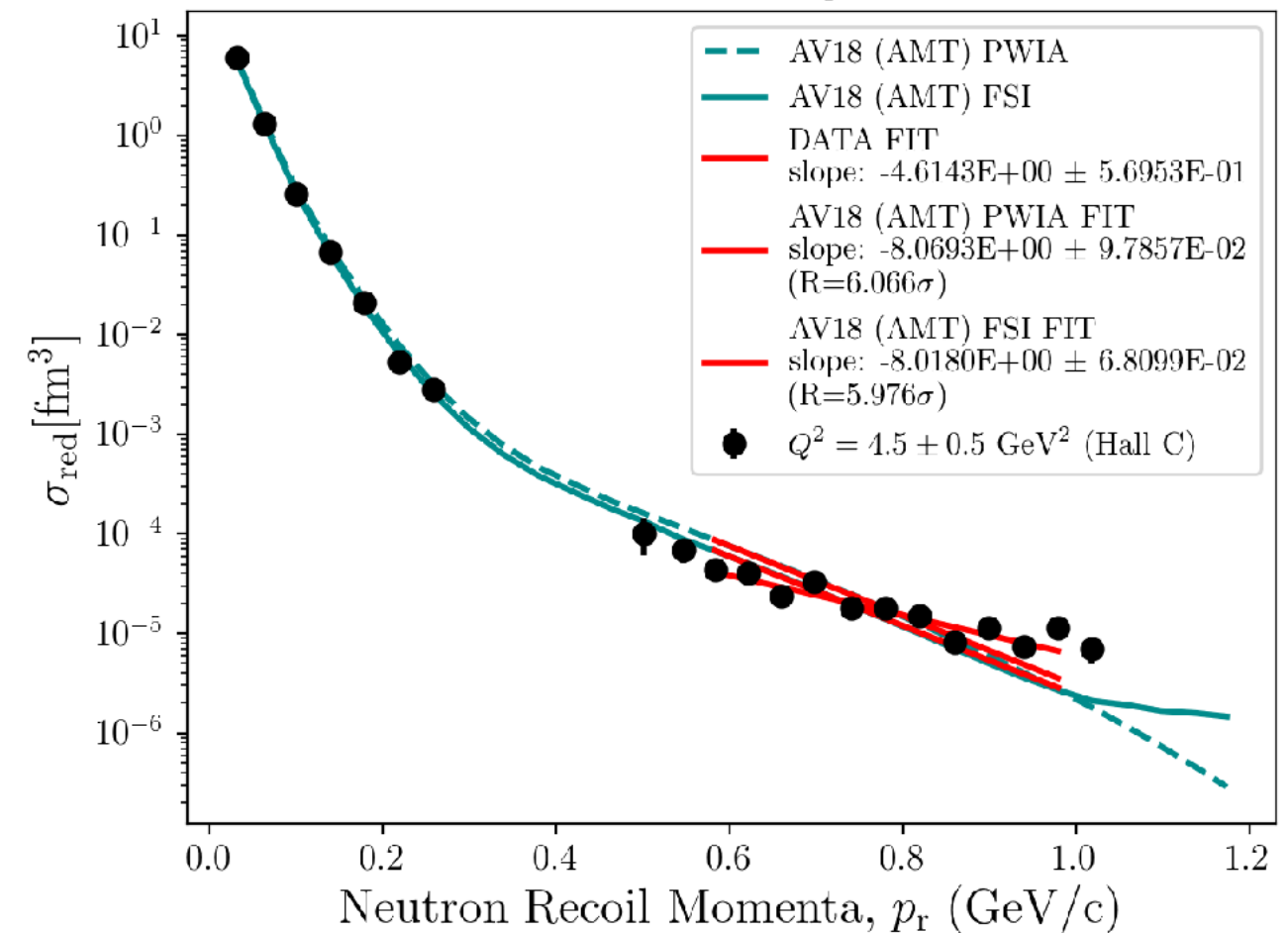
D(e,e'p)n Linear Fit Plots

AV18 (AMT parametrization)

Cross Section Ratio, $\theta_{nq} = 35 \pm 5$ deg



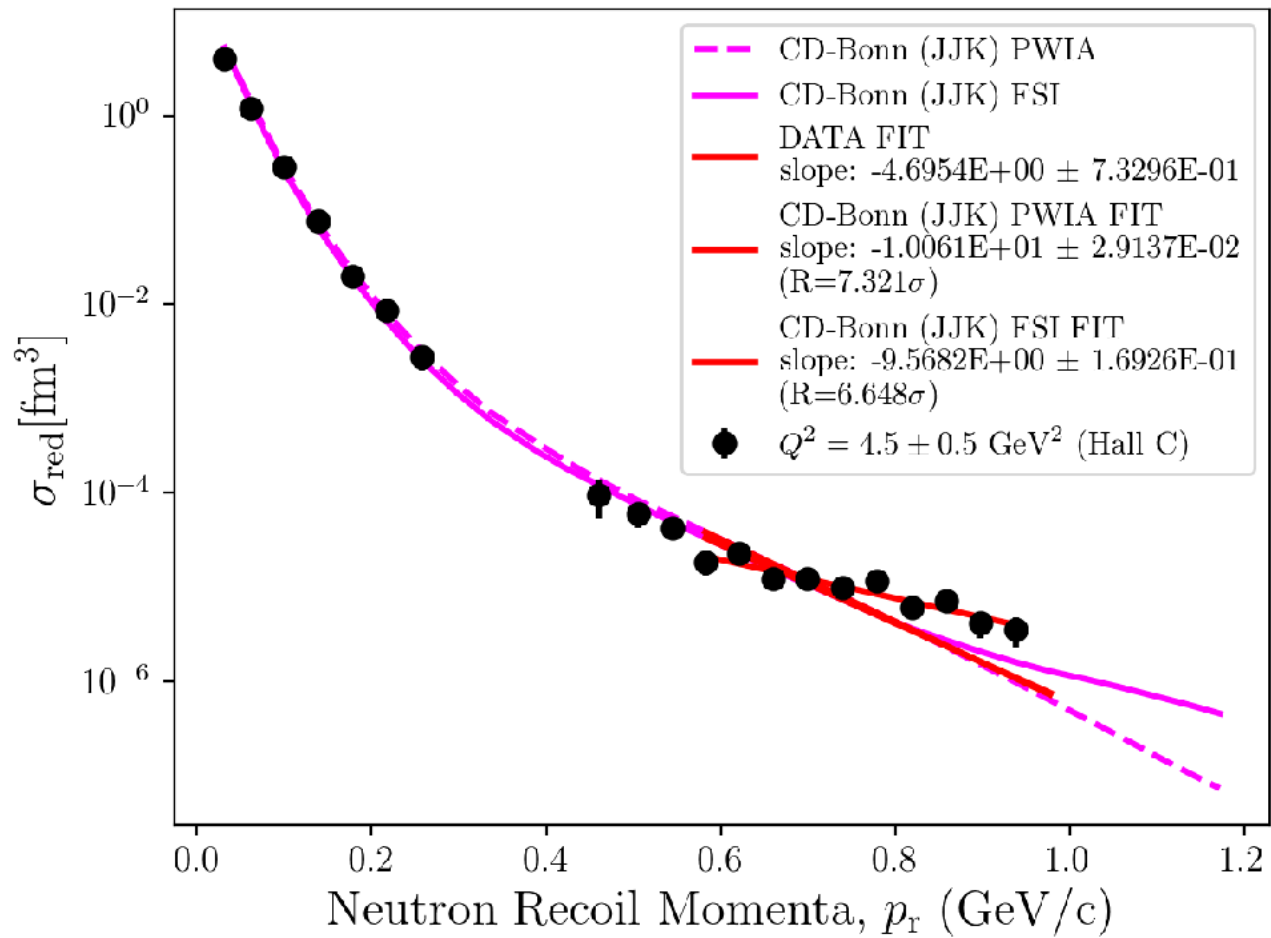
Cross Section Ratio, $\theta_{nq} = 45 \pm 5$ deg



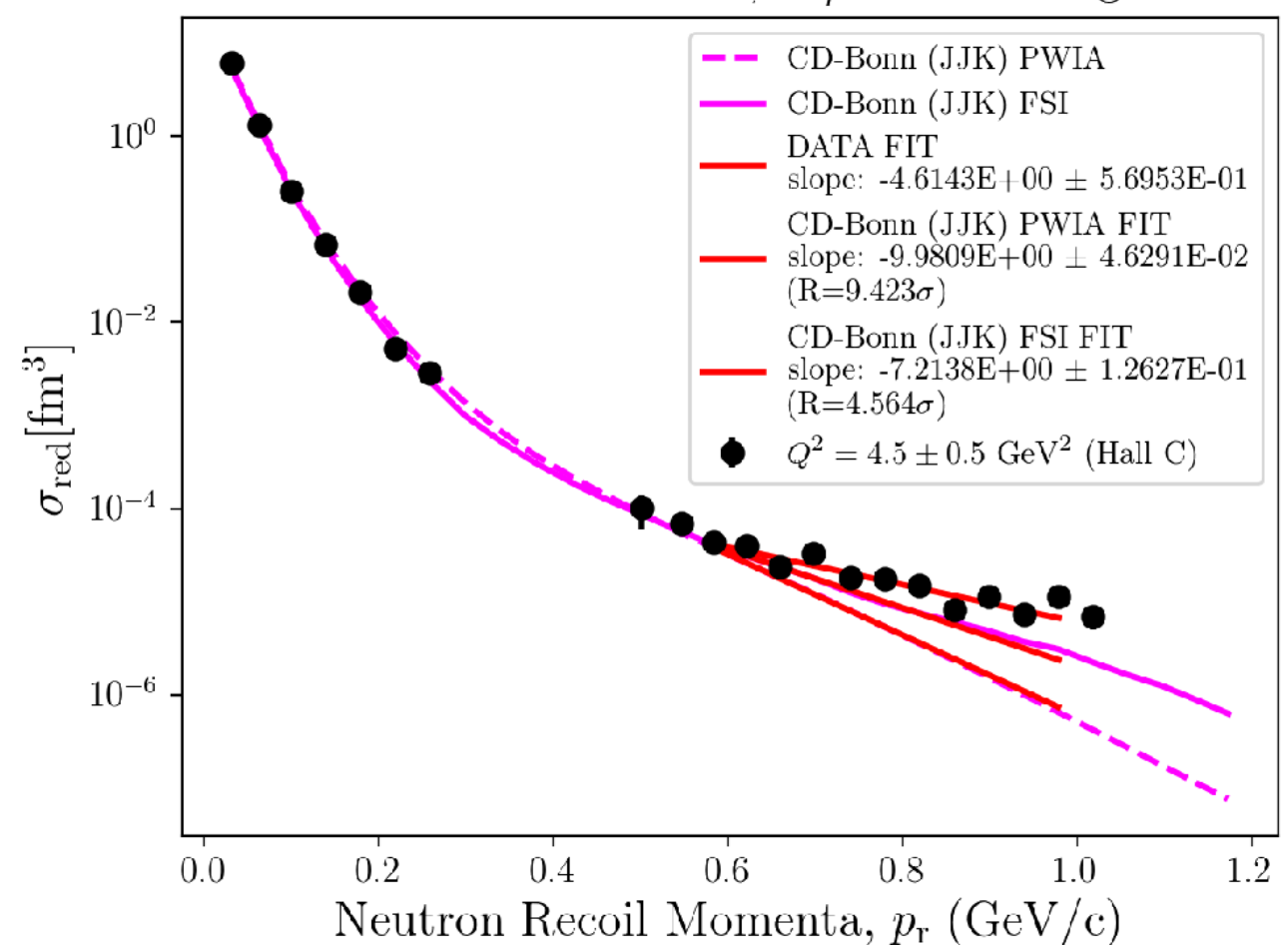
D(e,e'p)n Linear Fit Plots

CD-Bonn (JJK parametrization)

Cross Section Ratio, $\theta_{nq} = 35 \pm 5$ deg



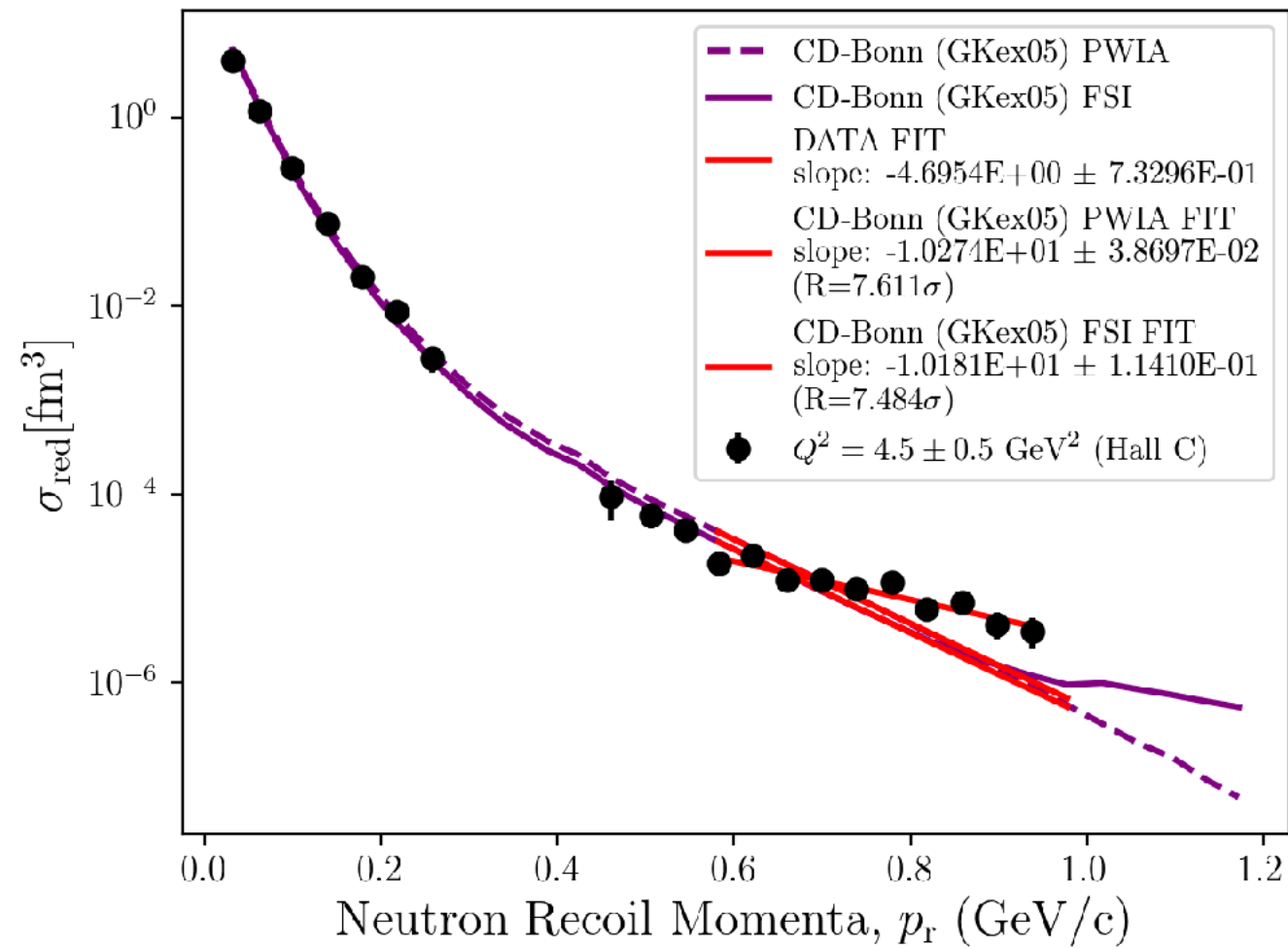
Cross Section Ratio, $\theta_{nq} = 45 \pm 5$ deg



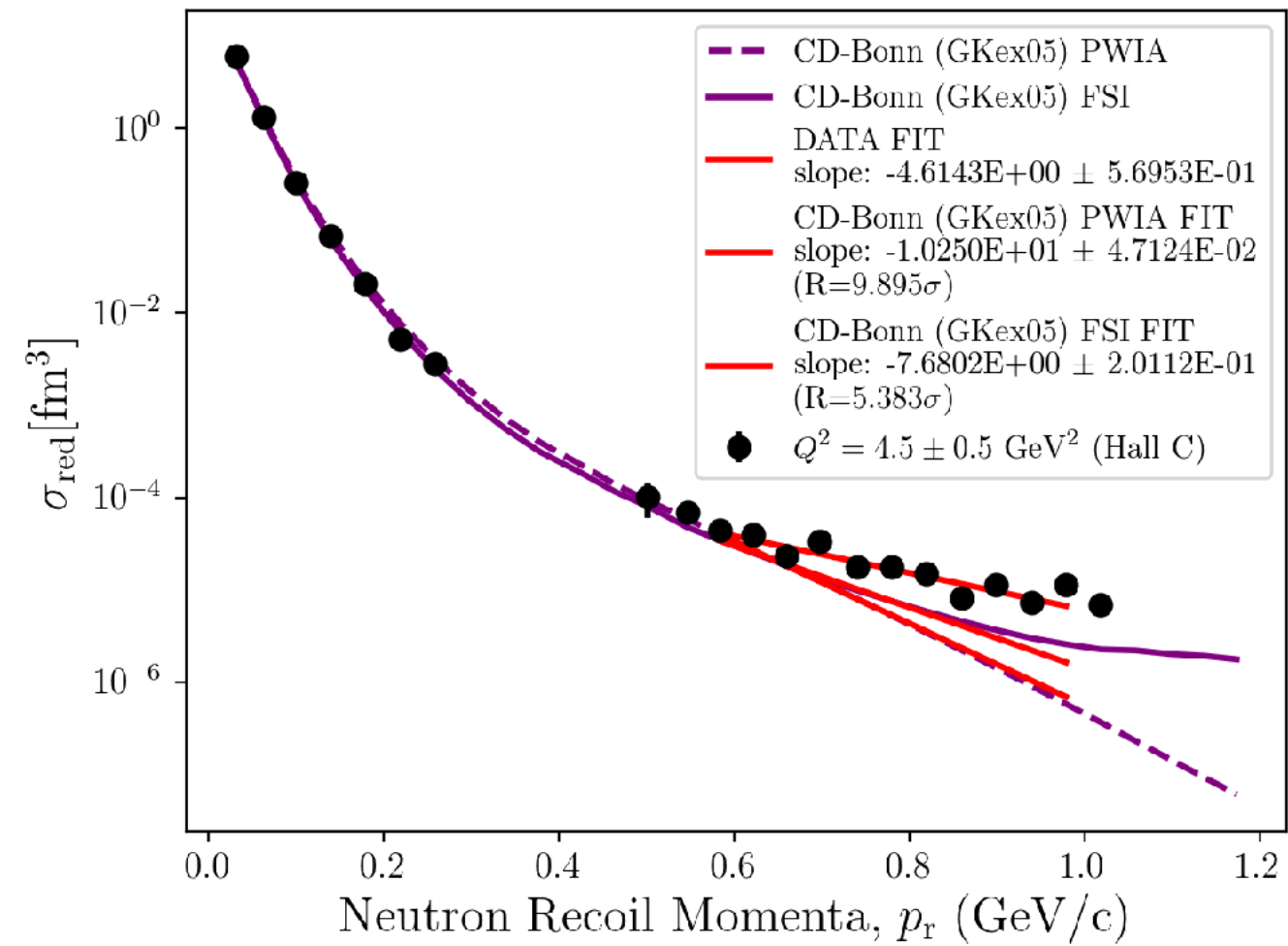
D(e,e'p)n Linear Fit Plots

CD-Bonn (GKex05 parametrization)

Cross Section Ratio, $\theta_{nq} = 35 \pm 5$ deg



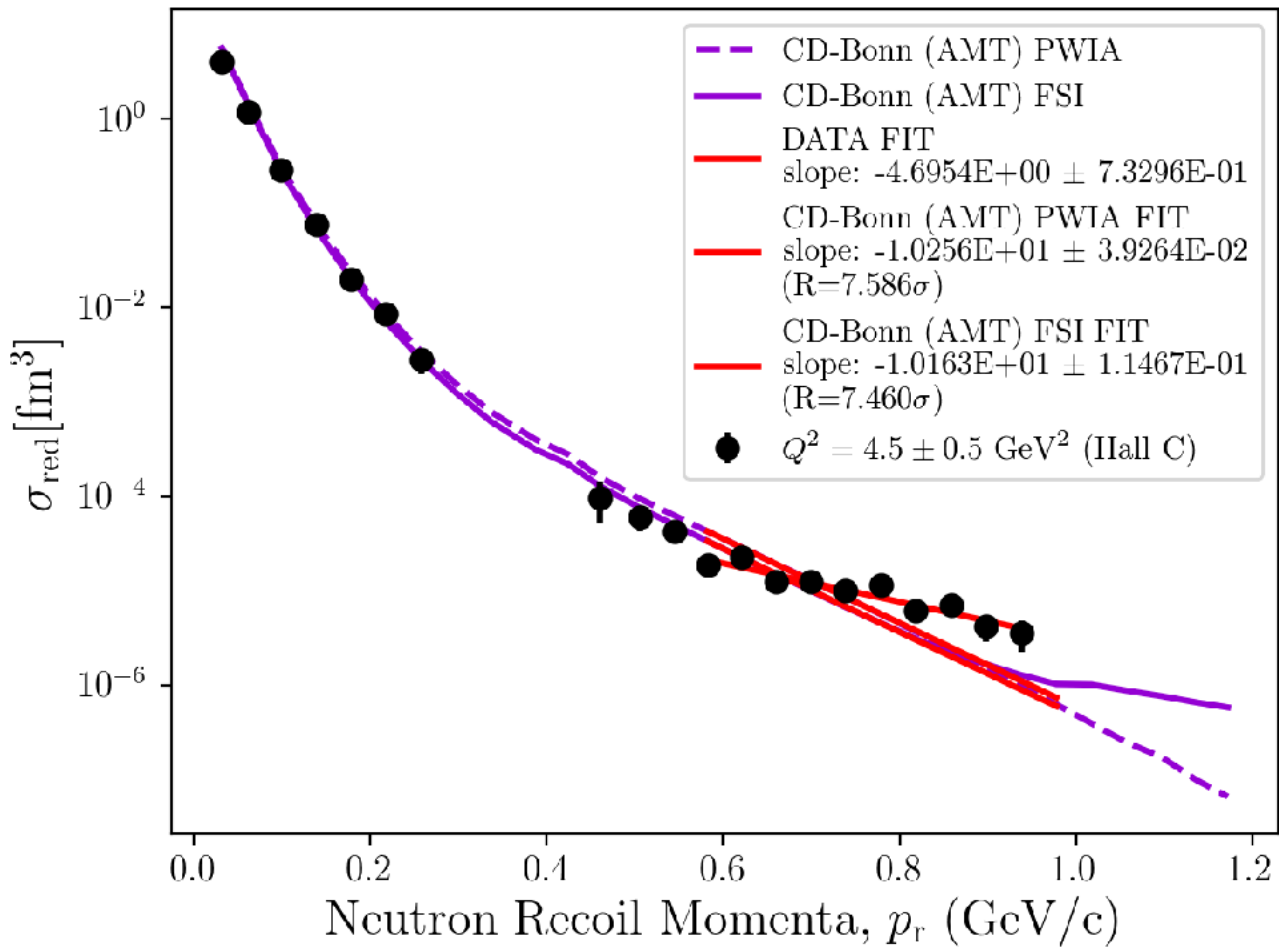
Cross Section Ratio, $\theta_{nq} = 45 \pm 5$ deg



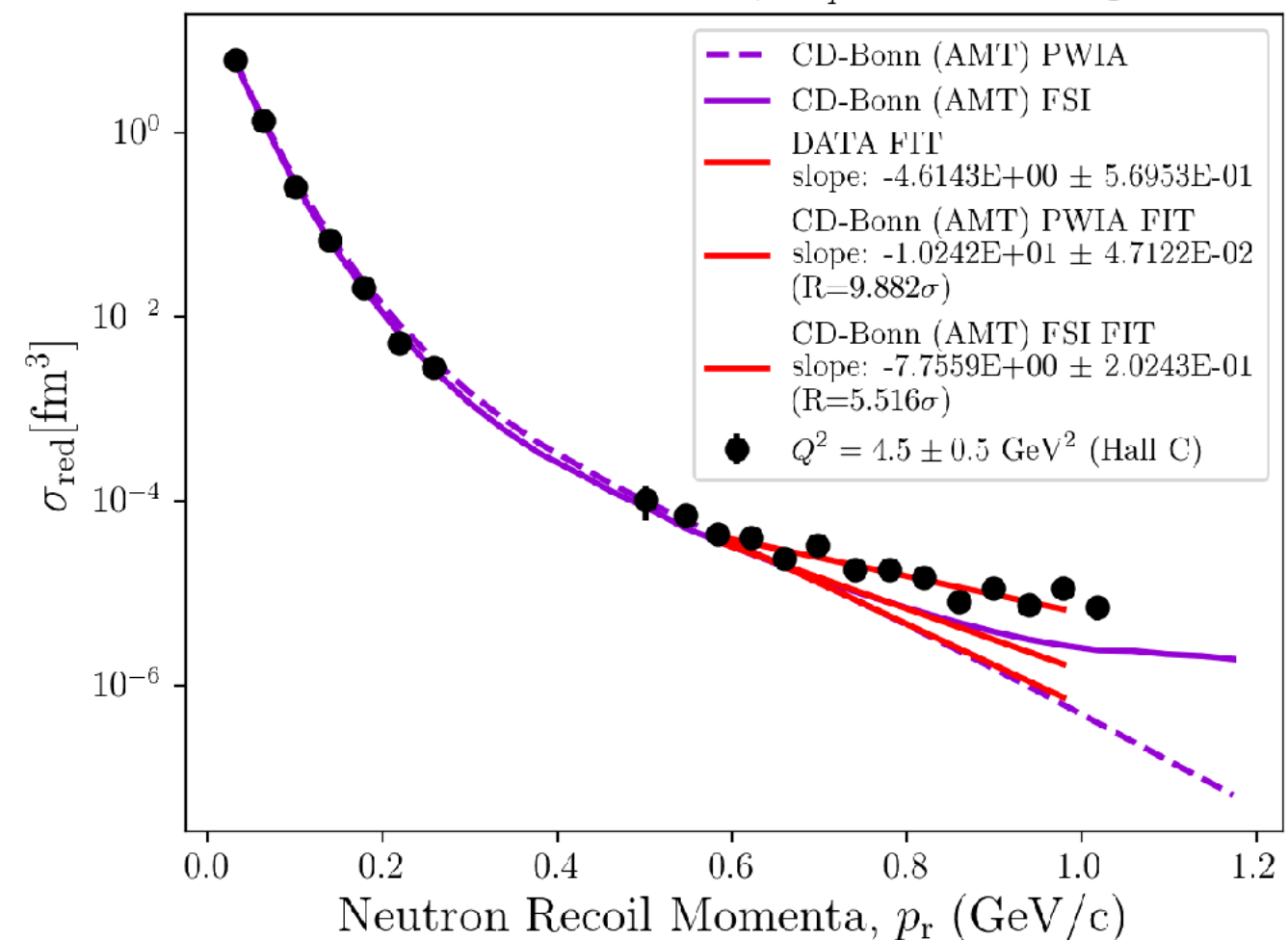
D(e,e'p)n Linear Fit Plots

CD-Bonn (AMT parametrization)

Cross Section Ratio, $\theta_{nq} = 35 \pm 5$ deg



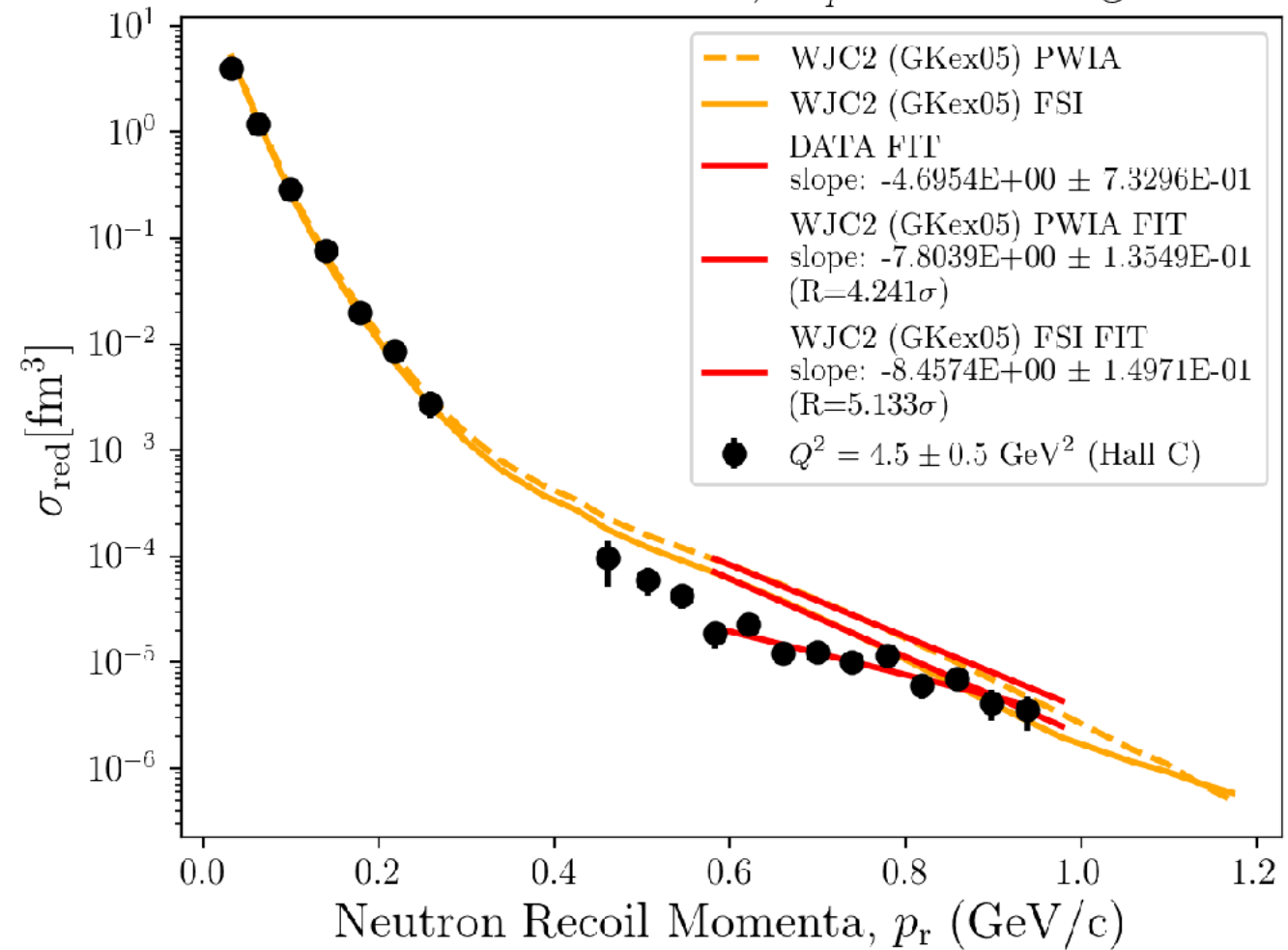
Cross Section Ratio, $\theta_{nq} = 45 \pm 5$ deg



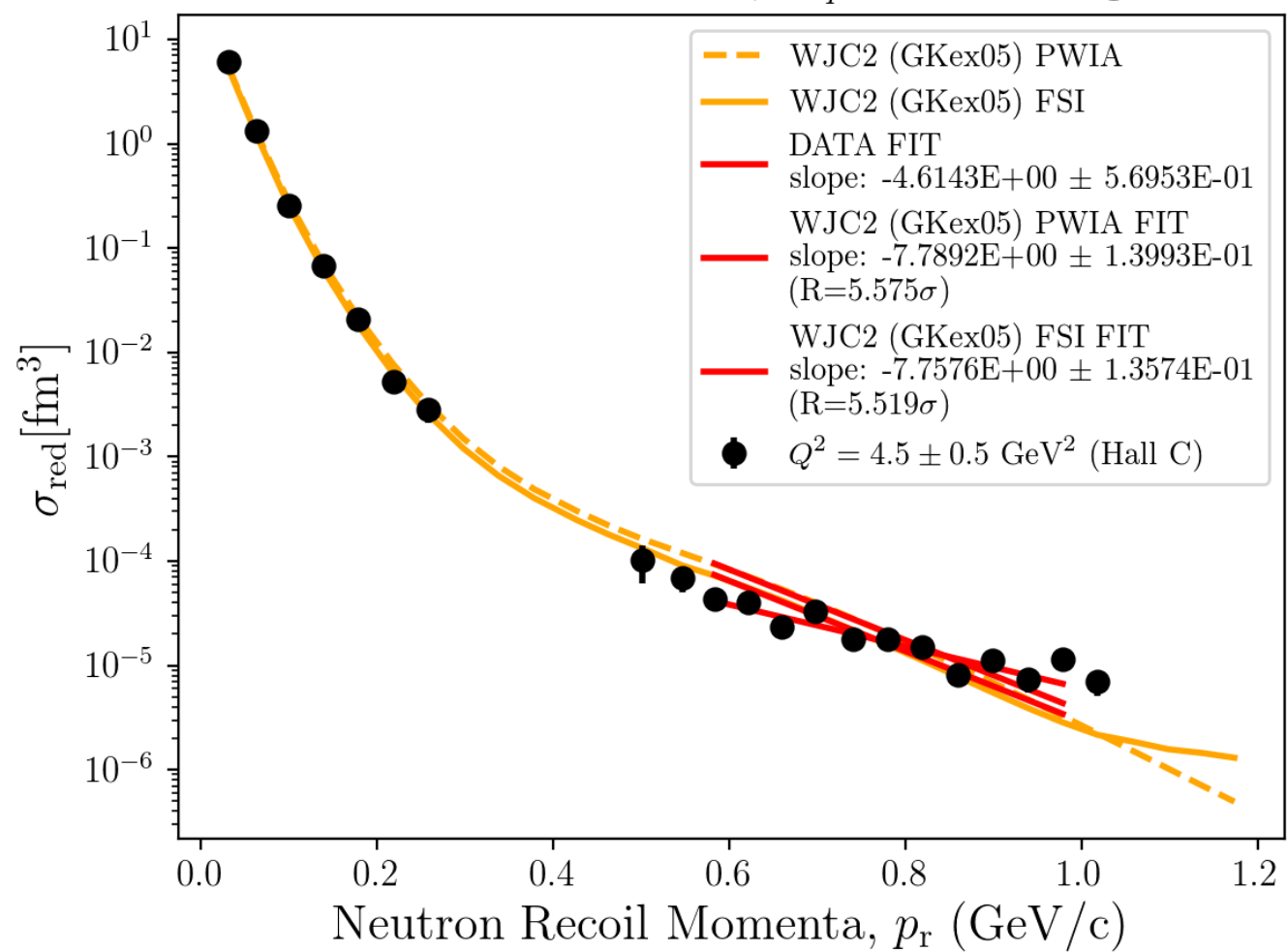
D(e,e'p)n Linear Fit Plots

WJC2 (GKex05 parametrization)

Cross Section Ratio, $\theta_{nq} = 35 \pm 5$ deg



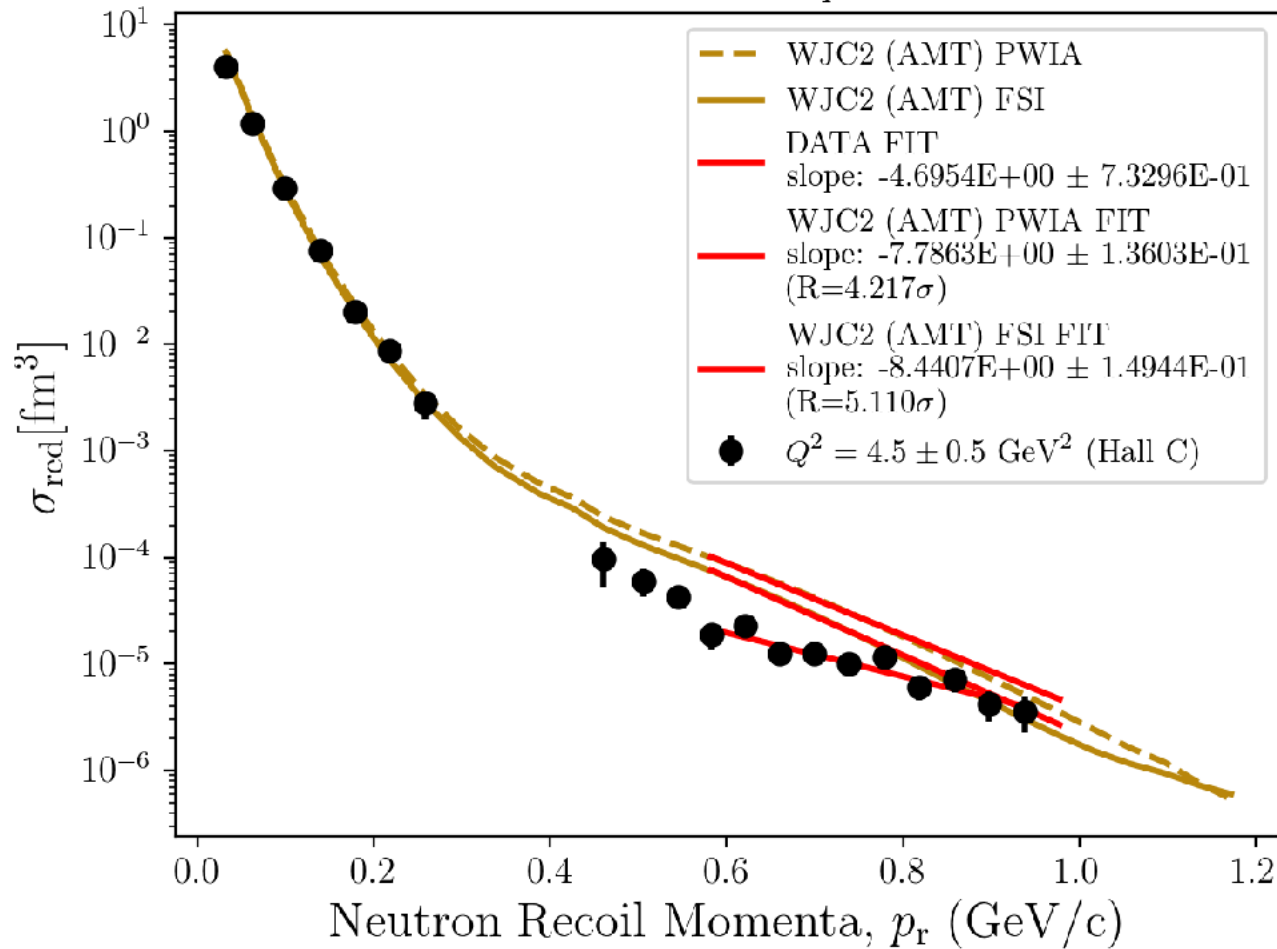
Cross Section Ratio, $\theta_{nq} = 45 \pm 5$ deg



D(e,e'p)n Linear Fit Plots

WJC2 (AMT parametrization)

Cross Section Ratio, $\theta_{nq} = 35 \pm 5$ deg



Cross Section Ratio, $\theta_{nq} = 45 \pm 5$ deg

